

## **UC Merced**

### **UC Merced Electronic Theses and Dissertations**

#### **Title**

On the implications of incompressibility of the quantum mechanical wavefunction in the presence of tidal gravitational fields

#### **Permalink**

<https://escholarship.org/uc/item/6bq0q0wh>

#### **Author**

Minter, Stephen

#### **Publication Date**

2010-05-14

Peer reviewed|Thesis/dissertation

UNIVERSITY OF CALIFORNIA, MERCED

On the Implications of Incompressibility  
of the Quantum Mechanical Wavefunction  
in the Presence of Tidal Gravitational Fields

A dissertation submitted in the partial satisfaction  
of the requirements for the degree of

Doctor of Philosophy

in

Applied Mathematics

by

Stephen Minter

Committee in Charge

Professor Raymond Chiao, Chair

Professor Boaz Ilan

Professor Arnold Kim

Professor Kevin Mitchell

Professor Jay Sharping

2010

Copyright

Stephen Minter, 2010

All rights reserved.

Dedicated, in endless appreciation and love,  
to James and Terry McGuffin

# Contents

<b>Contents</b>	<b>v</b>
<b>List of Figures</b>	<b>viii</b>
<b>List of Tables</b>	<b>x</b>
<b>1 Acknowledgements</b>	<b>11</b>
<b>2 Curriculum Vitae</b>	<b>13</b>
<b>3 Abstract</b>	<b>18</b>
<b>4 Introduction</b>	<b>19</b>
<b>5 Quantum Incompressibility of the Hydrogen Atom Electron Wavefunction</b>	<b>21</b>
5.1 Introduction . . . . .	21
5.2 Wavefunctions and Circular States of the Hydrogen Atom . . . . .	23
5.3 Free Fall of Classical Matter: Point Masses and Extended Objects in Tidal Gravitational Fields . . . . .	25
5.4 Free Fall of the Hydrogen Atom through Vacuum in Tidal Gravitational Fields . . . . .	30
5.5 The DeWitt Interaction Hamiltonian Operator . . . . .	38
5.5.1 Quantum Incompressibility of the Rydberg Atom in a Weak Magnetic Field . . . . .	40
5.5.2 Quantum Incompressibility of the Rydberg Atom in a Weak Tidal Gravitational Field . . . . .	45
5.5.3 Gauge Invariance of Energy Shifts . . . . .	53
5.6 Down the Rabbit Hole: Free Fall Through a Massive Gravitational Source . . . . .	58
5.6.1 Free Fall of Classical Systems Within the Rabbit Hole . . . . .	58
5.6.2 Free Fall of the Hydrogen Atom Within the Rabbit Hole . . . . .	63
5.7 Classical Objects and Circular Rydberg Atoms in Free Fall . . . . .	68

5.7.1	Classical Objects and Circular Rydberg Atoms in Free Fall Through the Rabbit Hole . . . . .	68
5.7.2	Classical Objects and Circular Rydberg Atoms in Free Fall in the Field of a Point Mass . . . . .	70
5.8	Gravitational Potential Inside and Outside the Rabbit Hole . . . . .	72
5.9	Conclusions . . . . .	75
<b>6</b>	<b>Reflection of Gravitational Microwaves from Thin Superconducting Films</b>	<b>77</b>
6.1	Abstract . . . . .	77
6.2	Introduction . . . . .	78
6.3	The Uncertainty Principle Limits the Applicability of the Equivalence Principle . . . . .	84
6.4	The Interaction of an EM Wave with a Thin Metallic Film . . . . .	91
6.5	A Criterion for the Specular Reflection of EM Waves from Superconducting Films . . . . .	97
6.6	The Gravitational Characteristic Impedance of Free Space . . . . .	103
6.7	A Criterion for the Specular Reflection of GR Waves from Superconducting Films . . . . .	106
6.8	The Specular Reflection of GR Waves . . . . .	110
6.9	The Negligibility of Single-Bounce Transduction . . . . .	124
6.10	Conservation of Energy in the Reflection Process . . . . .	132
6.11	Experimental and Theoretical Implications . . . . .	138
6.12	Appendix 6A: The Magnetic and Kinetic Inductances of a Thin Metallic Film . . . . .	143
6.13	Appendix 6B: The Kinetic Inductance Length Scale in a Collisionless Plasma Model . . . . .	145
6.14	Appendix 6C: Impedance and Scattering Cross-Section . . . . .	148
<b>7</b>	<b>Gravitationally-Induced Charge Separation in Finite Superconductors</b>	<b>152</b>
7.1	Charge Separation During Free Fall in the Earth's Tidal Gravitational Field . . . . .	152
7.2	Experimental Detection of Charge Separation in the Earth's Tidal Gravitational Field . . . . .	158
7.3	Charge Separation Induced by External Source Masses . . . . .	159
7.4	Beyond First Order: Exploring the Zero-Momentum Approximation . . . . .	166

7.5	Experimental Detection of Charge Separation Induced by External Source Masses . . . . .	170
7.6	Experimental Results and Conclusions . . . . .	172
<b>8</b>	<b>Gravitational Wave Transducer Experiment</b>	<b>174</b>
8.1	Brief Outline of Proposed Experiment . . . . .	174
8.2	Levitation of Gravitational Wave Scatterers . . . . .	177
8.2.1	Electrostatic Levitation Using a Charged Ring, and Extending Earnshaw's Theorem to Include Neutral, Polarizable Particles . . . . .	179
	Introduction . . . . .	179
	Calculation of the Electric Potential and Field of a Charged Ring . . . . .	181
	Earnshaw's Theorem Revisited . . . . .	185
	Charged Particle Case . . . . .	185
	Adding a Uniform Gravitational Field Such as the Earth's, in the Case of a Charged Object . . . . .	188
	Generalization to the Case of a Neutral, Polarizable Particle . . . . .	189
	Adding a Uniform Gravitational Field Such as the Earth's, in the Case of a Neutral, Polarizable Object . . . . .	192
	The Electric Field Distributions of a Charged Ring and a Focused Laser Beam	193
8.2.2	Ways to Evade Earnshaw's Theorem . . . . .	194
	Magnetostatic Levitation . . . . .	195
<b>9</b>	<b>Conclusions</b>	<b>199</b>
	<b>References</b>	<b>199</b>

## List of Figures

1	Radial converging geodesics . . . . .	25
2	A point mass and a rigid ring undergoing free fall in the inhomogeneous gravitational field of a point object . . . . .	26
3	Quotient of sine integrals as a function of principal quantum number $n$ . . . . .	36
4	A system of test masses undergoing free fall through the rabbit hole . . . . .	58
5	Spatial diagram of freely-falling test masses within the rabbit hole . . . . .	63
6	Dimensionless relationships between gravitational acceleration and potential and the distance from the center of the Earth . . . . .	74
7	Snapshot of tidal forces from high-frequency gravitational radiation acting on a thin superconducting sheet. . . . .	85
8	Interaction between electromagnetic radiation and a thin conducting film . . . . .	91
9	Point charge distribution model in the charge separation experiment . . . . .	154
10	Converging geodesics in tidal gravitational fields . . . . .	156
11	Drawing of the dual-pendulum system used in the charge separation experiment . . . . .	159
12	Tidal gravitational forces acting on the dual-pendulum system in the charge separation experiment . . . . .	160
13	Free body diagram of a single pendulum acted upon by tidal gravitational forces . . . . .	162
14	Electrically-polarized superconducting pendula . . . . .	163
15	Plot of complex order parameters for semi-infinite superconductors, and an approximation for a finite superconductor . . . . .	167
16	Experimental setup for the charge separation experiment . . . . .	170
17	Charge vs. time in the charge separation experiment. . . . .	171
18	Electric field of a uniformly charged ring . . . . .	179
19	Comparison of the electric fields of a charged ring and a focused laser beam . . . . .	193



20	A thin, current-carrying ring creates a magnetic field at an arbitrary field point given by the Biot-Savart law. . . . .	195
21	Contour plot of potential energy density in a DC homogeneous gravitational field and a inhomogeneous magnetostatic field for perfect diamagnets . . . . .	197

## List of Tables

1	Energy shifts for various wavefunction states . . . . .	76
2	Charge and voltage potential as a function of length for charged sheet model . . . .	153
3	Charge and voltage potential as a function of length for point-charge model . . . . .	155

# 1 Acknowledgements

First and foremost, I thank my mentor and friend Dr. Raymond Chiao for his support as my advisor and committee chair. I am forever indebted to him for his guidance and encouragement over the years, in research and on life in general.

I also thank our collaborator Dr. Kirk Wegter-McNelly of Boston University for his invaluable insights and contributions. Drs. Chiao and Wegter-McNelly co-authored a portion of the material presented here.

I thank my committee members Dr. Boaz Ilan, Dr. Arnold Kim, Dr. Kevin Mitchell, and Dr. Jay Sharping for their advice and guidance on this effort, as well as throughout my graduate career.

My sincere appreciation goes to Dr. Michael Sprague for his influence that initially brought me to the applied mathematics program as a pioneering student. In addition, I also thank Dr. Mitchell, Dr. Bruce Birkett, Dr. Christopher Viney, Dr. Maria Pallavicini, Tammy Johnson, Nicholetta Sarsen, and Marna Cooper in this regard.

I also thank Dr. Mayya Tokman, Dr. Francois Blanchette, and Dr. Roland Winston for teaching me innumerable helpful concepts in math and physics, many of them used in this work.

I thank my fellow student researchers, especially Luis Martinez, for his help in the lab on the charge separation experiments as well as his keen ability to interpret our results better than any of us, also Bong-Soo Kang, Philip Jensen, Spencer DeSanto, and Jolie McLane. I thank our local collaborator Dr. Michael Scheibner for his theoretical and financial contributions to the charge separation experiments. The idea for the basic design of the experiment described in Section 7.5 was his.

I appreciate the extensive assistance I received on both theory and practical matters from faculty and staff at the University of California, Berkeley, namely Walt Fitelson, Richard Packard, Dick Plambeck, Ken Tatebe, Paul Thompson, and Ed Wishnow. The expertise they shared with me made the experimental process much more streamlined.

I thank Sir Roger Penrose of Oxford University, Dr. Carlton Caves of the University of New

Mexico, and Dr. Douglas Singleton of California State University, Fresno, for giving me a personal audience, and for their valuable input on my research.

In loving memory of Robert Minter Sr., Albert Fidalgo Jr., and Bill Rocha. While they cannot be here to share this with me, I know that they are forever here in spirit.

Last but not least, I thank my family and friends for their support and encouragement. More than words can express, I appreciate their understanding and patience in regards to the fact that over much of my graduate career, my presence in their lives was scarce at best. I promise that will change now.

Some of the material presented in Section 5 is from a manuscript being prepared for publication, co-authored by Dr. Raymond Chiao and Dr. Kirk Wegter-McNelly. The dissertation author is the first author of this manuscript.

Section 6, in its entirety, is presented as it is published in *Physica E* [1], co-authored by Drs. Chiao and Wegter-McNelly.

Some of the material presented in Section 7.1 is from a publication in the American Institute of Physics Conference Proceedings, from the International Conference on Numerical Analysis and Applied Mathematics (ICNAAM), Crete, Greece, 2009 [2], co-authored by Drs. Chiao and Wegter-McNelly. The dissertation author is the first author of this publication.

Section 8.1.1, in its entirety, is presented as it is published in *Laser Physics* [3], co-authored by Dr. Chiao. The dissertation author is the first author of this publication.

## 2 Curriculum Vitae

**Stephen J. Minter**

Ph.D. candidate, Graduate Student Representative, Applied Mathematics

University of California, Merced, Department of Natural Sciences

5200 N. Lake Rd.

Merced, CA 95344

Advisor: Dr. Raymond Chiao, Depts. of Natural Sciences and Engineering

sminter2@ucmerced.edu

### EDUCATION

Ph.D. Candidacy, Applied Mathematics, University of California, Merced, 2008.

BS, Physics, with a minor in mathematics, California State University, Stanislaus, 2005.

AS, Physics, Modesto Junior College, 2003.

AA, Political Science, Modesto Junior College, 1999.

### PUBLICATIONS

- Minter, S.J., K. Wegter-McNelly, R.Y. Chiao. Charge Separation Within Superconductors in the Presence of Tidal Gravitational Fields. AIP Conf. Proc. 1168, 1084 (2009).
- Minter, S.J., K. Wetger-McNelly, and R.Y. Chiao. Do Mirrors for Gravitational Radiation Exist? Physica E 42, 234 (2010).

- Minter, S.J. and R.Y. Chiao. Can a Charged Ring Levitate a Neutral, Polarizable Object? Can Earnshaw's Theorem be Extended to Such Objects? *Laser Physics* **17** (7), 942, (2007).
- Minter, S.J. and R.Y. Chiao. Multiple-Equilibria Traps for Diamagnetic Objects. In preparation.
- Minter, S.J., R.Y.Chiao, K.Wegter-McNelly. Quantum Incompressibility of a Hydrogen Atom in a Circular Rydberg State during Free Fall in Tidal Gravitational Fields. In preparation.

**RESEARCH EXPERIENCE:**

**Laboratory Manager, Senior Research Assistant**, January 2006 to present.

PI: Dr. Raymond Chiao, UC Merced. Experimental and theoretical research in

- Production and detection of gravitational radiation
- Field coupling between gravitation and electromagnetism
- Interaction between tidal gravitational fields and quantum-coherent matter
- New methods of particle and ion trapping
- Numerical scattering and field simulations

**Research Assistant**, 12/2004 to 5/2005. PI: Dr. Rose Zhang, CSU Stanislaus. Theoretical and experimental research in Type II superconductivity.

**Research Assistant**, 9/2005 to 12/2005. PI: Dr. Susan Mokhtari, CSU Stanislaus. Theoretical research in general relativity.

**TEACHING EXPERIENCE:**

**Instructor**, UC Merced, Math 24 (Linear Algebra and Differential Equations)

**Instructor**, UC Merced, Math 22 (Advanced single-variable calculus)

**Teaching Assistant**, UC Merced, Math 32 (Probability and Statistics)

**Teaching Assistant**, UC Merced, Math 23 (Multivariable calculus)

**Instructor**, UC Merced, Math 21 (Beginning single-variable calculus)

**Instructor**, UC Merced, Phys 8 (Calculus-based Newtonian mechanics)

**Teaching Assistant**, CSU Stanislaus. College algebra

**Teaching Assistant**, CSU Stanislaus. Calculus-based electricity and magnetism

**Teaching Assistant**, CSU Stanislaus. Algebra-based Newtonian mechanics

**Teaching Assistant**, CSU Stanislaus. Algebra-based electricity and magnetism

**AVID Tutor (volunteer)**, Escalon High School. In-class assistance in multiple subjects to high school students at all levels.

**Math Doctor (volunteer)**, Drexel University, Philadelphia, PA. Online assistance in all sciences and mathematics at all levels to all ages.

## **AWARDS, HONORS, AND PRESENTATIONS:**

Recipient of Legacy Award, University of California, Merced, 2010.

Recipient of President's Dissertation Year Fellowship, University of California Office of the President, Academic Year 2009-2010.

### **Invited Colloquia:**

**April 2010, University of New Mexico.** "Quantum Incompressibility of the Superconducting Electron Wavefunction in the Presence of Tidal Gravitational Fields"

**March 2010, California State University, Fresno.** "Charge Separation Within Superconductors in the Presence of Tidal Gravitational Fields"

**September 2009, University of California, Merced.** "Charge Separation Within Superconductors in the Presence of Tidal Gravitational Fields"

**April 2009, California State University, Fresno.** "Do Mirrors for Gravitational Waves Exist?"

**February 2008, California State University, Fresno.** "Production and Detection of Gravitational Radiation by Means of a Two-Body Superconducting System."

**February 2008, University of California, Merced.** "Production and Detection of Gravitational Radiation by Means of a Two-Body Superconducting System."

**April 2007, University of California, Merced.** "Multiple-Equilibria Traps for Charged and Neutral Dielectrics."



**Contributed talks:**

**October 2008, California Section of American Physical Society, California State University, Dominguez Hills.** “Do Mirrors for Gravitational Radiation Exist?”

**March 2008, Pacific Coast Gravity Meeting, UC Santa Barbara.** “Production and Detection of Gravitational Radiation by Means of a Two-Body Superconducting System.”

**October 2007, California Section of American Physical Society, Lawrence Berkeley National Laboratory.** “Production and Detection of Gravitational Radiation by Means of a Two-Body Superconducting System.” **Awarded first-place Margaret Burbidge award for best experimental research talk by a graduate student.**

**Posters:**

April 2009, University of California, Merced. “Laboratory-Scale Superconducting Mirrors for Gravitational Microwaves.”

March 2008, University of California, Merced. “Production and Detection of Gravitational Radiation by Means of a Two-Body Superconducting System.”

March 2007, University of California, Merced. “At the Interface of Quantum Mechanics and General Relativity.”

**PROFESSIONAL SOCIETIES:**

American Physical Society, since 2006.

American Institute of Physics, since 2004.

### **3 Abstract**

The quantum mechanical wavefunction of a freely falling hydrogen atom will remain unchanged to first order in the presence of sufficiently weak tidal gravitational fields, giving rise to a form of incompressibility not seen in classical systems. The fact that the electron is in a bound state and that only discrete energy level transitions can occur causes the atom to behave differently than a classical object in an inhomogeneous gravitational field under certain circumstances. A time-dependent energy shift that is overlooked in a widely-used gauge choice will be explored, and shown to be a real physical effect through gauge invariance. Quantum incompressibility of the wavefunction governing the electron superfluid of a Type-I superconductor will also lead to non-classical behavior in the presence of tidal gravitational fields, via coupling between gravitational and electromagnetic fields. Theoretical and experimental implications will be discussed.

## 4 Introduction

The notion of the incompressibility of a quantum-mechanical wavefunction was introduced by Laughlin [4] in connection with the fractional quantum Hall effect. Here, the mathematical formalism that leads to wavefunction incompressibility is discussed in detail. Multiple theoretical and experimental implications of the ensuing relative motion between classical objects and quantum-mechanically coherent systems in the presence of inhomogeneous, tidal gravitational fields are explored.

This work begins in Section 5, where a tidal gravitational field is treated as a perturbation to the energy levels of a hydrogen atom. A natural “quantum of size” exists for the orbit of an electron in a hydrogen atom, due to the quantization of nuclear charge, whereas no “quantum of size” exists for classical objects. Since the orbital radius of the electron can only take on discrete values, a quantum form of rigidity can arise in this system between Bohr’s “quantum jumps.” This will cause the atom to behave differently than a point-like object during free fall in inhomogeneous, tidal gravitational fields. This problem has been previously considered, but only as measured by the local frame of the center of mass of the hydrogen atom, resulting in a time-independent shift of the energy states of the electron wavefunction. A novel result is obtained when global measurements are made from the frame of a distant inertial observer, namely that a time-dependent energy shift arises due to the effects of the curvature of space.

The behavior of a hydrogen atom in the presence of a weak tidal gravitational field is relevant to the development of a unified gravito-electrodynamical theory for weak, but quantized, gravitational and electromagnetic fields interacting with non-relativistic quantum mechanical matter. Such a theory would fall short of the ultimate goal of unifying all known forces of nature into a “theory of everything,” but it would nonetheless be a very useful theory to have in order to compare with experiments. Here, a need for such a theory is discussed by solving a simple hydrogen-atom problem that reveals the “quantum incompressibility” of a spatially-extended quantum object in the presence of an inhomogeneous gravitational field. In particular, the response of a hydrogen atom to the tidal gravitational field of the Earth is considered. Using first-order perturbation theory, it is found

that under certain circumstances, an incompressible, extended quantum mechanical system such as this atom will behave differently than both point-like and extended classical objects in the Earth's inhomogeneous gravitational field. The main objective of this section is to demonstrate the existence of a time-dependent shift in the hydrogen atom energy spectrum due to the curvature of space when measurements are made by a distant inertial observer in asymptotically flat spacetime.

Section 6, as mentioned, is presented as published in *Physica E*, apart from modifications to the format, and the equation, figure, and reference numbers, for the purposes of continuity within this dissertation. This section addresses the possibility of reflection of high-frequency gravitational radiation from the surface of a thin superconducting film. The electron superfluid of a Type-I superconductor is also governed by a quantum-mechanical wavefunction which also exhibits a form of incompressibility. Detailed analysis is performed showing the reaction of a superconductor to high- and low-frequency gravitational perturbations, leading to multiple experimental possibilities.

Sections 7 and 8 are analyses of two of those experimental possibilities, including a brief description of some preliminary data. Section 7 addresses electrostatic charge separation within a bulk superconductor in the presence of a low-frequency perturbing gravitational field. Section 8.1 briefly addresses the possibility of conversion between electromagnetic wave power and gravitational wave power by means of two sets of superconducting systems, while Section 8.2 deals with practical, experimental concepts that are helpful to the implementation of the experiment that is described in Section 8.1. Specifically, stable levitation of two spatially-separated superconducting samples is considered. Some of these experiments have been performed, and an experiment on the transduction between electromagnetic and gravitational radiation (first discussed in Section 6) is on-going and fully funded.

# 5 Quantum Incompressibility of the Hydrogen Atom Electron Wavefunction

## 5.1 Introduction

The nature of the quantum mechanical wavefunction of the electron in a hydrogen atom will cause it to behave differently than any classical matter in certain types of inhomogeneous gravitational fields. A time-independent shift of the atom's energy spectrum has been studied extensively by many, several of them mentioned in the main body of this section, but here it is proposed that there is also a novel time-dependent energy shift when the atom is viewed by a distant inertial observer in asymptotically flat spacetime.

Section 5.2 briefly introduces the quantum mechanical wavefunction of the hydrogen atom, and defines certain parameters and variables.

Section 5.3 analyzes the free-fall behavior of classical matter in tidal gravitational fields. This section was written to point out the fact that classical point masses behave differently than classical extended masses in tidal gravitational fields, though no violation of the Equivalence Principle occurs.

An explicit derivation of the interaction Hamiltonian operator that leads to a time-independent shift in the atom's energy spectrum due to the curvature of space is performed in Section 5.4, which has been previously considered. This operator arises from the potential energy term in the full Hamiltonian. In Section 5.5, it is argued that there is a time-dependent energy shift that arises from an interaction Hamiltonian that has not been previously considered. This operator arises from the kinetic energy term in the full Hamiltonian. It is suggested that this time-dependent energy shift is generally overlooked when performing an allowed local gauge transformation which sets the contributions of the vector potentials to the kinetic energy to be identically zero everywhere. However, this does not take into account holonomic effects seen in global measurements. An analogy is made, in that there are experimentally-verified holonomic effects in electromagnetism which arise in the same form as the interaction Hamiltonian that leads to the time-dependent energy shift due

to the curvature of space. Gauge invariance of these time-dependent energy shifts are shown in Section 5.6.

While exploring this gauge invariance, it is shown that the Riemann curvature tensor one often encounters in general relativity has a different form when free fall occurs outside of a spherically-symmetric object, as compared to free fall *through* a spherically-symmetric object, such as a hole dug through the diameter of the Earth. This serves as motivation to evaluate the energy shift problem when the atom is freely falling through the Earth, as opposed to freely falling above the Earth's surface. It is found that the interaction Hamiltonian terms have different forms in each case. For example, though there are additional differences, the kinetic energy shift above the surface of the Earth is positive-definite for all quantum states of the hydrogen atom, whereas this energy shift is negative-definite for all states when free fall occurs within the Earth.

Section 5.7 directly compares the free fall behavior of the hydrogen atom to that of classical objects, both point-like and extended.

Section 5.8 discusses a discontinuity in the gravitational potential that occurs at the surface of the Earth in the expressions for the potential within the Earth, and above the surface. A gravitational potential that is valid in both cases is derived. It is noted that the previous results remain unaffected, since physical effects arise only from changes in potential, not absolute potential.

Section 5.9 contains concluding remarks.

## 5.2 Wavefunctions and Circular States of the Hydrogen Atom

A relatively simple quantum-coherent system is the hydrogen atom. The wavefunction for a hydrogen atom is uniquely defined by three quantum numbers:  $n$ , the principal quantum number;  $l$ , the angular momentum quantum number; and  $m_l$ , the magnetic quantum number. When  $n \gg 1$ , the system is commonly called a ‘‘Rydberg atom.’’

The normalized wavefunction of the hydrogen atom is given in spherical polar coordinates by [5]

$$\psi_{nlm_l}(r, \theta, \phi) = -\sqrt{\left(\frac{2}{na_0}\right)^3 \frac{(n-l-1)!}{2n(n+l)!}} \exp\left(-\frac{r}{na_0}\right) \left(\frac{2r}{na_0}\right)^l L_{n+l}^{2l+1}\left(\frac{2r}{na_0}\right) Y_{lm}(\theta, \phi), \quad (1)$$

where  $a_0$  is the Bohr radius,  $L_{n+l}^{2l+1}$  are associated Laguerre polynomials of degree  $n+l$  and order  $2l+1$ , and  $Y_{lm}$  are spherical harmonics. Particular attention will be focused on ‘‘circular states’’ of the Rydberg atom, where  $l$  and  $|m|$  are equal to their maximum values of  $n-1$ . These states are called ‘‘circular’’ due to the fact that the electron probability distribution is strongly peaked in a ring-like shape, and thus Rydberg atoms in these states make good examples of quantum-coherent ‘‘rings’’ when  $n$  is large. The unnormalized wavefunction for circular states is given by [6]

$$\psi_{n,n-1,n-1}(r, \theta, \phi) = [r \sin \theta \exp(i\phi)]^{n-1} \exp\left(-\frac{r}{na_0}\right). \quad (2)$$

The wavefunction for the center of mass of the system is a plane-wave state given by

$$\psi'(\mathbf{r}_{\text{cm}}) = \exp(i\mathbf{k}_{\text{cm}} \cdot \mathbf{r}_{\text{cm}}), \quad (3)$$

where  $\mathbf{k}_{\text{cm}}$  is the wave vector, and  $\mathbf{r}_{\text{cm}} = \langle x_{\text{cm}}, y_{\text{cm}}, z_{\text{cm}} \rangle$  is the position, of the center of mass. Since the center of mass of atom is undergoing free fall in Earth’s gravity,

$$\mathbf{k}_{\text{cm}} = -\frac{Mg_{\text{eff}}t}{\hbar} \mathbf{e}_z = k_{\text{cm}} \mathbf{e}_z, \quad (4)$$

where  $g_{\text{eff}}$  is the effective acceleration due to Earth's gravity, defined later in (15),  $\mathbf{e}_z$  is the unit vector parallel to the local vertical axis, and  $\hbar$  is the reduced Planck's constant.

The total wavefunction for the system is given by the product of the wavefunctions in (2) and (3), and is thus

$$\Psi_{n,n-1,n-1} = \psi_{n,n-1,n-1} \psi' = (r \sin \theta e^{i\phi})^{n-1} \exp\left(ik_{\text{cm}} z_{\text{cm}} - \frac{r}{na_0}\right). \quad (5)$$

The associated probability density of the electron has the form of a strongly peaked, ring-like distribution lying in the  $(x, y)$  plane with a maximum located at a radius of

$$a_n = n^2 \frac{\hbar^2}{m_e e^2} = n^2 a_0, \quad (6)$$

where  $a_0$  is the Bohr radius, and  $m_e$  and  $e$  are the mass and charge of the electron, respectively. Such an atom, unlike a freely falling rubber ring, will resist any change in its size during free fall until it can make a discontinuous quantum jump out of its initial state into a different quantum state. In this sense, a hydrogen atom in a circular Rydberg state is “quantum incompressible” in its response to tidal gravitational forces – apart from possible quantum transitions. However, as it will be shown that appreciable quantum transition probability amplitudes are only present for highly curved space and/or values of  $n$  that preclude the atom from being stable against ionizing effects, such transitions are beyond the scope of this work, and only the gravitational field of the Earth and realistic values of  $n$  will be considered.



### 5.3 Free Fall of Classical Matter: Point Masses and Extended Objects in Tidal Gravitational Fields

Consider the free fall of two nearby, point-like objects dropped from the same height above the surface of the Earth (see Figure 1). These two objects, whose trajectories radially converge towards the center of the Earth, each apparently undergo a small horizontal component of acceleration  $\mathbf{g}'$  of the radial acceleration  $\mathbf{g}$  due to the Earth's mass, according to a distant inertial observer, where  $g'_i = \frac{g}{R_E} x_i$  for  $i = 1, 2$ . These horizontal components of acceleration are equivalent to a tidal gravitational force that, in a Newtonian picture, causes the two objects to converge toward each other during free fall.

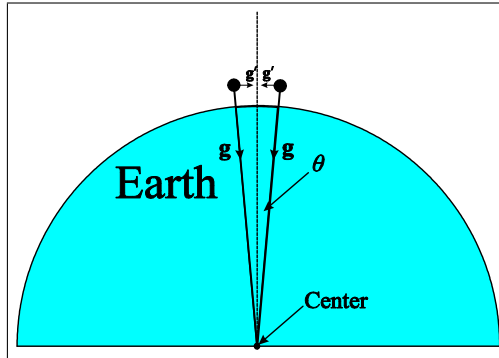


Figure 1: Two nearby, freely falling, point-like classical objects dropped from the same height above the Earth's surface follow converging geodesics that are inclined at a slight angle with respect to the vertical plumb line equidistant between them. The two objects, whose trajectories radially converge towards the center of the Earth, each apparently undergo a small horizontal component of acceleration  $\mathbf{g}'$  of the radial acceleration  $\mathbf{g}$  due to the Earth's mass, according to a distant inertial observer. These horizontal components of acceleration are equivalent to a tidal gravitational force that, in a Newtonian picture, causes the two objects to converge toward each other during free fall.

Now replace these two objects by a ring made of classical, compressible matter, such as a rubber ring. Let this ring be oriented in a horizontal plane when it is initially dropped. Over short time scales, the ring will undergo *continuous* compression into a ring of smaller radius during free fall under the adiabatic, slowly time-varying, squeezing action of the tidal gravitational field of the Earth, whose action is isotropic in the two transverse directions perpendicular to the local vertical plumb line indicated in Figure 1. Since the ring continuously changes its dimensions as it falls, no

natural “quantum of size” exists for such a ring.

Now consider two classical objects, one point-like mass, and one spatially-extended mass, in the presence of the inhomogeneous, tidal gravitational field of a point-like object with mass  $M'$  (e.g., a point-like Earth). Both objects are released from rest at a vertical distance  $h$  from mass  $M'$ . Once released, the objects are allowed to undergo free fall. One object consists of an infinitely rigid ring of radius  $a$  and mass  $m_{\text{ext}}$ . The other is a point-like test mass  $m_{\text{pt}}$  which is located at the center of mass of the ring, and is free to fall independently. Both the ring and the test mass are simultaneously released from rest into free fall at time  $t = 0$ . Let  $M' \gg m_{\text{ext}}, m_{\text{pt}}$  so that the position of mass  $M'$  stays fixed. See Figure 2.

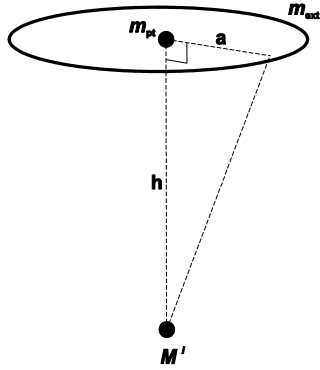


Figure 2: A point mass  $m_{\text{pt}}$  and a rigid ring of mass  $m_{\text{ext}}$  undergoing free fall in the inhomogeneous gravitational field of a point object with much greater mass  $M'$ .

The total energy of the freely falling, point-like test particle, with mass  $m_{\text{pt}}$ , is a conserved quantity equal to its initial potential energy, and is thus given by

$$E_{\text{pt}} = -\frac{GM'm_{\text{pt}}}{h}, \quad (7)$$

where  $G$  is Newton’s gravitational constant. The gravitational potential energy of the point-like test mass  $m$  is given by

$$V_{\text{pt}} = -\frac{GM'm_{\text{pt}}}{h-y}, \quad (8)$$

where  $y$  is the distance fallen.

A differential volume element  $dm$  of the rigid ring has a total energy

$$dE_{\text{ext}} = -\frac{GM'dm}{\sqrt{h^2 + a^2}} = -\frac{GM'\rho_\ell a d\phi}{\sqrt{h^2 + a^2}}, \quad (9)$$

where  $\rho_\ell = \frac{m_{\text{ext}}}{2\pi a}$  is the uniform, linear mass density of the thin ring, and  $d\phi$  is a differential angle element along the ring. Substituting this expression for the mass density and integrating, the conserved total energy of the ring is given by

$$E_{\text{ext}} = -\frac{GM'm_{\text{ext}}}{\sqrt{h^2 + a^2}}. \quad (10)$$

Similarly, the potential energy of the ring is given by

$$V_{\text{ext}} = -\frac{GM'm_{\text{ext}}}{\sqrt{(h-y)^2 + a^2}}. \quad (11)$$

By the principle of conservation of energy, the total energy of both objects satisfies  $E = T + V$ , where  $T$  is the kinetic energy, and thus the kinetic energies of each object are

$$T_{\text{pt}} = \frac{GM'm_{\text{pt}}}{h} \frac{Y}{1-Y} \quad (12)$$

$$T_{\text{ext}} = \frac{GM'm_{\text{ext}}}{h} \left[ \frac{1}{\sqrt{(1-Y)^2 + D^2}} - \frac{1}{\sqrt{1+D^2}} \right], \quad (13)$$

where  $Y \equiv y/h$  is the dimensionless free-fall distance, and  $D \equiv a/h$  is the dimensionless radius of the rigid ring. Note that  $T_{\text{ext}} \rightarrow T_{\text{pt}}$  as  $D \rightarrow 0$ , as would be expected. Although this non-geodesic effect may be too small to measure using realistic dimensions for Earth-based experiments (since  $D$  would be small due to the large radius of the Earth), (12) and (13) can be used, via  $T = \frac{1}{2}mv^2$ , to show that everywhere on the open interval  $Y = (0, 1)$ , the velocity of the ring is less than the velocity of the test mass, showing that an extended, rigid system will behave differently than a point-like object during free fall in the inhomogeneous, tidal gravitational field of point mass  $M'$ .

The gravitational acceleration of the extended object over short free fall distances, where the

acceleration is approximately constant, can be derived from (10) by noting that

$$E_{\text{ext}} = -\frac{GM'm_{\text{ext}}}{\sqrt{h^2 + a^2}} \equiv -\frac{GM'm_{\text{ext}}}{R} = -m_{\text{ext}}g_{\text{ext}}R, \quad (14)$$

where  $g_{\text{ext}}$  is an effective gravitational acceleration given by

$$g_{\text{ext}} = \frac{GM'}{R^2} = \frac{GM'}{h^2 + a^2}. \quad (15)$$

For free fall in the Earth's tidal gravitational field,  $g_{\text{ext}}$  differs from the gravitational acceleration of a point mass at the surface of the Earth  $g_{\text{E}} = 9.8 \frac{\text{m}}{\text{s}^2}$  by a very small amount for realistic lengths  $a$ .

The fractional difference between the two is given by

$$\frac{g_{\text{ext}}}{g_{\text{E}}} = \frac{1}{1 + \left(\frac{a}{R_{\text{E}}}\right)^2} \approx 1 - \left(\frac{a}{R_{\text{E}}}\right)^2, \quad (16)$$

where  $R_{\text{E}}$  is the Earth's radius, when the extended object is dropped near the Earth's surface. Note that the subscript in  $g_{\text{E}}$  is present to remind the reader that this value is the magnitude of gravitational acceleration at the surface of the Earth, which is a constant that does not vary with distance from the center of Earth, reserving the symbol  $g$  for the magnitude of the gravitational acceleration that is inversely proportional to that distance when free fall occurs above the Earth's surface.

Initially, it seems that this result challenges a major aspect of the equivalence principle (EP), namely that all objects in free fall undergo the same acceleration. However, this is not the case, since the EP is applicable only to point-like objects in free fall. The EP does not apply, except in approximation, to the spatially extended ring in an *inhomogeneous* gravitational field.

Since the two objects have different velocities in a tidal gravitational field, the question can be raised, what if the two objects are bound together, so that their velocities must be the same? Consider a single object that consists of the extended ring and the point-like mass that are rigidly

bound together during free fall. The total kinetic energy of this system is given by the sum of the individual kinetic energies defined in (12) and (13), and thus

$$T_{\text{tot}} = T_{\text{pt}} + T_{\text{ext}} = \frac{GM'}{h} \left[ m_{\text{pt}} \left( \frac{Y}{1-Y} \right) + \frac{m_{\text{ext}}}{\sqrt{(1-Y)^2 + D^2}} - \frac{m_{\text{ext}}}{\sqrt{1+D^2}} \right] = \frac{1}{2} m_{\text{tot}} v_{\text{tot}}^2, \quad (17)$$

where  $m_{\text{tot}} = m_{\text{pt}} + m_{\text{ext}}$ , and  $v$  is the velocity of the entire system. The velocity satisfies

$$v_{\text{tot}}^2 = \frac{2GM'}{h} \left\{ u \left( \frac{Y}{1-Y} \right) + (1-u) \left[ \frac{1}{\sqrt{(1-Y)^2 + D^2}} - \frac{1}{\sqrt{1+D^2}} \right] \right\}, \quad (18)$$

where  $u$  is the dimensionless ratio satisfying

$$u \equiv \frac{m_{\text{pt}}}{m_{\text{tot}}} = 1 - \frac{m_{\text{ext}}}{m_{\text{tot}}}. \quad (19)$$

Therefore, the velocity of the system is dependent on the masses of the ring and the point mass. As one would expect,  $v_{\text{tot}}$  approaches the velocity of the point mass when  $u \rightarrow 1$  and that of the ring as  $u \rightarrow 0$ .

Again, a mass-dependent free-fall velocity seems to be a contradiction to the EP. However, again, the EP does not apply to this system because the point mass and the ring are rigidly bound, and therefore are not individually free particles. The EP can only be applied rigorously to freely-falling point masses. The rigid binding of the two masses precludes them from falling as free particles.

## 5.4 Free Fall of the Hydrogen Atom through Vacuum in Tidal Gravitational Fields

The Hamiltonian operator for the hydrogen atom in a perturbing field is given by

$$H = H_0 + H_1, \quad (20)$$

where  $H_0$  is the unperturbed Hamiltonian, and  $H_1$  is the interaction Hamiltonian due to the field perturbation.

An interaction Hamiltonian for the hydrogen atom in a gravitational field, moving with non-relativistic velocity, has been previously considered by Parker [7] and shown to be

$$H_P = \frac{1}{2} m_e R_{0l0m} x^l x^m \quad (21)$$

where  $m_e$  is the mass of the electron,  $R_{0l0m}$  are components of the Riemann curvature tensor, and  $x^l$  and  $x^m$  are components of the position operator of the electron. Equation (21) is obtained by taking the nonrelativistic limit of the Dirac equation embedded into curved spacetime [8][9]. The subscript  $P$  is used for Parker, the author of the papers referenced here, and his index notation is adopted as well. Superscripts  $l$  and  $m$  are contravariant indices satisfying  $l, m = 1, 2, 3$ , and should not be confused with quantum number  $l$  or mass  $m$ . The index 0 refers to the time components. Greek indices are spacetime indices, and Latin indices are space indices only. The Einstein summation convention is used here as well, in which repeated indices are summed over all possible values.

The physical meaning of (21) can be seen by going to the Newtonian limit of general relativity, where [10]

$$R_{0j0}^i = \delta^{ik} \frac{\partial^2 \Phi}{\partial x^k \partial x^j}, \quad (22)$$

where  $\Phi$  is the Newtonian gravitational potential that satisfies

$$-\nabla\Phi = \mathbf{g}. \quad (23)$$

Lowering the index  $i$  in (22) by means of multiplying by the metric tensor  $g_{li}$ , one gets

$$R_{l0j0} = g_{li}R_{0j0}^i = g_{li}\delta^{ik}\frac{\partial^2\Phi}{\partial x^k\partial x^j} = g_{lk}\frac{\partial^2\Phi}{\partial x^k\partial x^j}. \quad (24)$$

For weak gravitational fields, spacetime is almost flat, so that to a good approximation

$$g_{lk} \approx \eta_{lk} = \delta_{lk} \quad (25)$$

where  $\eta_{\mu\nu} = \text{diag}(-1, +1, +1, +1)$  is the Minkowski metric for flat spacetime. Thus one arrives at the expression relating the Riemann curvature tensor to derivatives of the Newtonian gravitational potential

$$R_{l0j0} = \delta_{lk}\frac{\partial^2\Phi}{\partial x^k\partial x^j} = \frac{\partial^2\Phi}{\partial x^l\partial x^j}. \quad (26)$$

The covariant indices of the Riemann curvature tensor obey the following identities:

$$R_{\kappa\lambda\mu\nu} = -R_{\lambda\kappa\mu\nu} = -R_{\kappa\lambda\nu\mu}. \quad (27)$$

It therefore follows that

$$R_{l0j0} = R_{0l0j}. \quad (28)$$

Using this identity and (26), we can rewrite (21) as follows:

$$H_P = \frac{1}{2}m_e R_{0l0m}x^l x^m = \frac{1}{2}m_e \frac{\partial^2\Phi}{\partial x^l\partial x^m}x^l x^m. \quad (29)$$

Since the 3-by-3 matrix

$$\begin{bmatrix} \frac{\partial^2 \Phi}{\partial x^1 \partial x^1} & \frac{\partial^2 \Phi}{\partial x^1 \partial x^2} & \frac{\partial^2 \Phi}{\partial x^1 \partial x^3} \\ \frac{\partial^2 \Phi}{\partial x^2 \partial x^1} & \frac{\partial^2 \Phi}{\partial x^2 \partial x^2} & \frac{\partial^2 \Phi}{\partial x^2 \partial x^3} \\ \frac{\partial^2 \Phi}{\partial x^3 \partial x^1} & \frac{\partial^2 \Phi}{\partial x^3 \partial x^2} & \frac{\partial^2 \Phi}{\partial x^3 \partial x^3} \end{bmatrix} \quad (30)$$

is Hermitian, one can solve for its eigenvalues and their corresponding eigenvectors, and thereby define the principal axes of the ellipsoid obtained by setting the quadratic form (29) equal to a constant. Using a principal-axis coordinate system  $(x, y, z)$  which is centered on the center of mass of the atom, we obtain

$$H_P = \frac{1}{2} m_e \left( \frac{\partial^2 \Phi}{\partial x^2} x^2 + \frac{\partial^2 \Phi}{\partial y^2} y^2 + \frac{\partial^2 \Phi}{\partial z^2} z^2 \right), \quad (31)$$

i.e., that the interaction Hamiltonian (21) can be cast into a principal-axis quadratic form.

By Taylor's theorem, one can expand  $\Phi$  around the origin, located at the center of mass of the atom, as follows:

$$\Phi(x, y, z) = \Phi_0 + \left( \frac{\partial \Phi}{\partial x} \Big|_{x=0} x + \frac{\partial \Phi}{\partial y} \Big|_{y=0} y + \frac{\partial \Phi}{\partial z} \Big|_{z=0} z \right) \quad (32)$$

$$+ \frac{1}{2} \left( \frac{\partial^2 \Phi}{\partial x^2} \Big|_{x=0} x^2 + \frac{\partial^2 \Phi}{\partial y^2} \Big|_{y=0} y^2 + \frac{\partial^2 \Phi}{\partial z^2} \Big|_{z=0} z^2 \right) + \dots \quad (33)$$

where  $\Phi_0 = \Phi(0, 0, 0)$ . Since there are no tidal forces at the origin,

$$\frac{\partial \Phi}{\partial x} \Big|_{x=0} = \frac{\partial \Phi}{\partial y} \Big|_{y=0} = \frac{\partial \Phi}{\partial z} \Big|_{z=0} = 0. \quad (34)$$

Furthermore, one is free to choose  $\Phi_0 = 0$ .

Thus, one can see from (31) that the physical significance of  $H_P$  is that

$$H_P = m_e \Phi(x, y, z). \quad (35)$$

In other words, Parker's interaction Hamiltonian (21) has the physical significance of being the tidal gravitational potential energy operator, viewed as a perturbation on the electronic wavefunction



of the hydrogen atom in the principal-axis coordinate system centered on the center of mass of the atom.

If one further chooses the  $z$  axis to be the vertical axis of the freely falling system, the potential  $\Phi$  must then be rotationally symmetric in the  $(x, y)$  plane, so that expanding the potential around the origin by Taylor's theorem implies that  $\Phi$  must have the form

$$\Phi = A(x^2 + y^2) + Bz^2, \quad (36)$$

recalling that  $\Phi_0$  was chosen to be zero at the origin. Since the atom is falling through vacuum, the potential must satisfy Laplace's equation

$$\nabla^2 \Phi = 0. \quad (37)$$

Substituting (36) into (37) yields

$$B = -2A, \quad (38)$$

and thus

$$\Phi = A(x^2 + y^2 - 2z^2). \quad (39)$$

To determine  $A$ , one can consider the tidal forces on the electron, which satisfy

$$\mathbf{F} = -m_e \nabla \Phi = -2m_e A \langle x, y, -2z \rangle = m_e \mathbf{g}'. \quad (40)$$

For sufficiently short free fall distances, over which the gravitational acceleration can be considered constant, the velocity of the particle is given by

$$\mathbf{v} = \mathbf{g}'t = -2At \langle x, y, -2z \rangle. \quad (41)$$

Considering specifically the  $x$ -component of the velocity,

$$v_x = g'_x t = -g \frac{x}{R_E} t = -2Atx, \quad (42)$$

and therefore

$$A = \frac{g}{2R_E}. \quad (43)$$

The full expression for the potential is thus

$$\Phi = \frac{g}{2R_E} (x^2 + y^2 - 2z^2), \quad (44)$$

and the interaction Hamiltonian is given by substituting this expression into (35), yielding

$$H_P = \frac{m_e g}{2R_E} (x^2 + y^2 - 2z^2). \quad (45)$$

When calculating the shifts to the unperturbed energy levels resulting from the expectation value of this interaction Hamiltonian, it is convenient to express this operator in spherical coordinates by

$$H_P = \frac{m_e g}{2R_E} [r^2 (3 \sin^2 \theta - 2)] = -4 \sqrt{\frac{\pi}{5}} \frac{m_e g}{2R_E} Y_2^0, \quad (46)$$

where  $Y_2^0$  is the second degree, zero-order spherical harmonic. Thus, this interaction Hamiltonian represents a rank-2 angular momentum operator, since its angular dependence is quadrupolar [11]. One immediate consequence is that, by the Wigner-Eckart theorem, there will be no effect on a hydrogen atom in a state with zero angular momentum (i.e. where  $l = 0$ ), to first order, through this interaction Hamiltonian.

The energy shift of the atom in a highly-excited, stretched Rydberg state due to this interaction Hamiltonian is given by

$$\Delta E_P = \frac{\langle \Psi | H_P | \Psi \rangle}{\langle \Psi | \Psi \rangle}. \quad (47)$$

Beginning with the normalizing element,

$$\begin{aligned}\langle \Psi | \Psi \rangle &= \int_0^{2\pi} \int_0^\pi \int_0^\infty r^{2n} \exp\left(-\frac{2r}{na_0}\right) \sin^{2n-1} \theta \, dr \, d\theta \, d\phi \\ &= 2\pi (2n)! \left(\frac{na_0}{2}\right)^{2n+1} S(2n-1),\end{aligned}\tag{48}$$

where

$$S(\alpha) \equiv \int_0^\pi \sin^\alpha \theta \, d\theta.\tag{49}$$

Evaluating the expectation value for the Parker interaction Hamiltonian yields

$$\langle \Psi | H_P | \Psi \rangle = \frac{m_e g}{2R_E} 2\pi (2n+2)! \left(\frac{na_0}{2}\right)^{2n+3} [3S(2n+1) - 2S(2n-1)],\tag{50}$$

and thus the energy shift is equal to

$$\Delta E_P = \frac{m_e g}{2R_E} (2n+2)(2n+1) \left(\frac{na_0}{2}\right)^2 [3I(2n+1, 2n-1) - 2],\tag{51}$$

where

$$I(\alpha, \beta) \equiv \frac{S(\alpha)}{S(\beta)} = \frac{\int_0^\pi \sin^\alpha \theta \, d\theta}{\int_0^\pi \sin^\beta \theta \, d\theta}.\tag{52}$$

A plot of this integral quotient appearing in (51) as a function of  $n$  is shown in Figure 3, indicating that  $I$  approaches unity as  $n$  becomes large. The integrals were calculated numerically using an adaptive Simpson quadrature method with an error tolerance of  $10^{-6}$ .

Thus, for large values of principal quantum number  $n$ ,

$$\Delta E_P \approx \frac{m_e g}{2R_E} (n^2 a_0)^2 = \frac{m_e g}{2R_E} a_n^2.\tag{53}$$

This expression defines a shift in the energy spectrum of the hydrogen due to the curvature of space.

In light of the fact that the energy shift grows as  $n^4$ , one might ask, for what values of  $n$  does this energy shift become comparable to the unperturbed energy level spacings? Recall that the

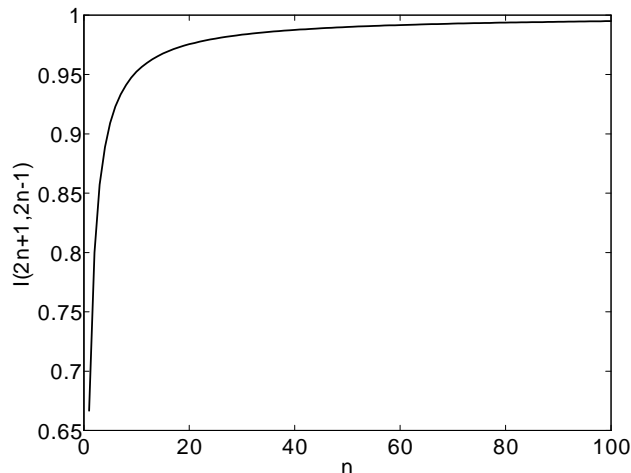


Figure 3: Quotient of sine integrals that appears in (51) as a function of  $n$ .

energy of the  $n$ th state is given by

$$E_n = \frac{E_0}{n^2}, \quad (54)$$

where  $E_0 = -13.6$  eV, the energy of the ground state. Thus, for the energy shift to be comparable to the spacing,

$$E_n + \Delta E_P \sim E_{n+1}. \quad (55)$$

For the gravitational field of Earth, this occurs when  $n \sim 10^5$ . Rydberg atoms with this excitation energy would be extremely short-lived [12], not due to spontaneous emission, but to ionizing effects. Atoms in these energy states have not been prepared in a laboratory setting. Note that the atomic radius would be on the order of tens of centimeters.

Alternatively, one could ask, for realistic values of  $n$ , what value of  $\frac{g}{R}$  is required for the energy shift to become comparable to the unperturbed level spacing? To satisfy (55),  $\frac{g}{R}$  would have to be on the order of  $10^{12}$  Hz<sup>2</sup> for  $n \sim 10^3$ . Note that gravitational fields near a black hole are required, since this value is on the order of  $10^{-5}$  Hz<sup>2</sup> on Earth,  $10^{-1}$  Hz<sup>2</sup> for a white dwarf, and  $10^9$  Hz<sup>2</sup> for a neutron star. Furthermore, for this curvature, the gravitational field may become too strong to be considered a perturbing field, which will be discussed in more detail in the following sections.

Up to this point, the analysis matches that which was previously considered extensively. See, for example, [7][8][9][13][14]. While no claims are made here that the energy shift in (53) is incorrect, it does not constitute a complete analysis for the energy shifts of the circular Rydberg atom in curved spacetime. In Section 5.5.2, it will be shown that an additional, time-dependent energy shift arises when one considers the interaction Hamiltonian that arises from the DeWitt minimal coupling rule.

## 5.5 The DeWitt Interaction Hamiltonian Operator

Generally, in nonrelativistic quantum mechanics when weak electromagnetic and gravitational fields are present, one must make the substitution according to DeWitt's minimal coupling rule [15]

$$\mathbf{p} \rightarrow \mathbf{p} - q\mathbf{A} - m\mathbf{h} , \quad (56)$$

where  $\mathbf{p}$  is the canonical momentum operator,  $q$  and  $m$  are the electrical charge and mass of the object being considered, respectively, and  $\mathbf{A}$  and  $\mathbf{h}$  are the electromagnetic and DeWitt gravitational vector potentials, respectively. Applying this minimal coupling rule to the Hamiltonian for a freely falling hydrogen atom in presence of weak electromagnetic and gravitational fields yields

$$H = \frac{1}{2m_p} (\mathbf{p}_p - q_p\mathbf{A}_p - m_p\mathbf{h}_p)^2 + \frac{1}{2m_e} (\mathbf{p}_e - q_e\mathbf{A}_e - m_e\mathbf{h}_e)^2 + V(\mathbf{r}_p, \mathbf{r}_e) , \quad (57)$$

where  $m_p$  and  $m_e$  are the proton and electron masses, respectively,  $\mathbf{A}_p$  and  $\mathbf{A}_e$  are the electromagnetic vector potentials evaluated at the position coordinates of the proton and electron, respectively,  $\mathbf{h}_p$  and  $\mathbf{h}_e$  are the corresponding gravitational vector potentials, and  $V$  is the potential energy. The coordinate system being used here is that of the distant inertial observer.

Expanding the Hamiltonian in (57), yields

$$\begin{aligned} H = & \left[ \frac{p_p^2}{2m_p} + \frac{p_e^2}{2m_e} + V(\mathbf{r}_p, \mathbf{r}_e) \right] \\ & + \left( \frac{q_p^2}{2m_p} \mathbf{A}_p \cdot \mathbf{A}_p + \frac{1}{2} m_p \mathbf{h}_p \cdot \mathbf{h}_p - \frac{q_p}{m_p} \mathbf{A}_p \cdot \mathbf{p}_p - \frac{1}{2} \{ \mathbf{h}_p, \mathbf{p}_p \} + q_p \mathbf{A}_p \cdot \mathbf{h}_p \right) \\ & + \left( \frac{q_e^2}{2m_e} \mathbf{A}_e \cdot \mathbf{A}_e + \frac{1}{2} m_e \mathbf{h}_e \cdot \mathbf{h}_e - \frac{q_e}{m_e} \mathbf{A}_e \cdot \mathbf{p}_e - \frac{1}{2} \{ \mathbf{h}_e, \mathbf{p}_e \} + q_e \mathbf{A}_e \cdot \mathbf{h}_e \right) , \end{aligned} \quad (58)$$

where the commutation relation  $[\mathbf{p}, \mathbf{A}] = \mathbf{0}$  was used, since the electromagnetic vector potential is solenoidal, and  $\{ \mathbf{h}, \mathbf{p} \} = \mathbf{h} \cdot \mathbf{p} + \mathbf{p} \cdot \mathbf{h}$  is the anti-commutator. It is desirable to transform to relative and center-of-mass coordinate systems. Since an analytic expression for the DeWitt Hamiltonian

corresponding to an object in the presence of electromagnetic and gravitational fields does not exist in the transformed coordinate system [13][16], the transformation will be applied only to the terms in the square brackets in (58), treating the additional terms in the parentheses as perturbations to the system. This can be justified by comparing the energy shifts one calculates for these terms to the much larger Coulomb potential. Applying the coordinate transformation

$$\mathbf{r}_{\text{cm}} = \frac{m_p \mathbf{r}_p + m_e \mathbf{r}_e}{m_p + m_e} \quad (59)$$

$$r = |\mathbf{r}_e - \mathbf{r}_p| \quad (60)$$

only to the terms in the square brackets of the above Hamiltonian yields

$$\begin{aligned} H \approx & \left[ \frac{p_{\text{cm}}^2}{2M} + \frac{p^2}{2\mu} + V(\mathbf{r}) \right] \\ & + \left( \frac{q_p^2}{2m_p} \mathbf{A}_p \cdot \mathbf{A}_p + \frac{1}{2} m_p \mathbf{h}_p \cdot \mathbf{h}_p - \frac{q_p}{m_p} \mathbf{A}_p \cdot \mathbf{p}_p - \frac{1}{2} \{ \mathbf{h}_p, \mathbf{p}_p \} + q_p \mathbf{A}_p \cdot \mathbf{h}_p \right) \\ & + \left( \frac{q_e^2}{2m_e} \mathbf{A}_e \cdot \mathbf{A}_e + \frac{1}{2} m_e \mathbf{h}_e \cdot \mathbf{h}_e - \frac{q_e}{m_e} \mathbf{A}_e \cdot \mathbf{p}_e - \frac{1}{2} \{ \mathbf{h}_e, \mathbf{p}_e \} + q_e \mathbf{A}_e \cdot \mathbf{h}_e \right), \end{aligned} \quad (61)$$

where  $p_{\text{cm}}$  and  $p$  are the magnitudes of the canonical momentum of the center of mass of the atom and the canonical relative momentum, respectively,  $M$  is the total mass of the atom, and  $\mu = m_p m_e / (m_p + m_e)$  is the reduced mass of the electron.

### 5.5.1 Quantum Incompressibility of the Rydberg Atom in a Weak Magnetic Field

In the DeWitt minimal coupling rule defined in (56), it is clear that the gravitational vector potential  $\mathbf{h}$  enters the kinetic momentum operator in a similar manner to the electromagnetic vector potential  $\mathbf{A}$ . Analysis of the energy shifts that arise from considering non-zero external electromagnetic vector potentials  $\mathbf{A}$  yields experimentally-verified results, which is shown below. The intention here is to demonstrate the necessity of a non-zero energy shift arising from the DeWitt Hamiltonian by considering an electromagnetic analogy that yields experimentally-verified results.

Thus, before examining the gravitational case, consider the effect of a homogeneous, DC magnetic field upon a system with Hamiltonian given by (61), in the situation that  $\mathbf{h} = \mathbf{0}$  but  $\mathbf{A} \neq \mathbf{0}$ .

In the symmetric gauge, the electromagnetic vector potentials for the proton and electron are given by

$$\mathbf{A}_p = \frac{1}{2}\mathbf{B} \times \mathbf{r}_p = -\frac{1}{2}B \langle y_p, -x_p, 0 \rangle, \quad (62)$$

and

$$\mathbf{A}_e = \frac{1}{2}\mathbf{B} \times \mathbf{r}_e = -\frac{1}{2}B \langle y_e, -x_e, 0 \rangle, \quad (63)$$

in the Cartesian coordinate system, respectively, for  $\mathbf{B} = B\mathbf{e}_z$ , where  $\mathbf{e}_z$  is the unit vector parallel to the local vertical axis. As before, the energy shifts due to the presence of the perturbing fields are found by taking the expectation value of the corresponding interaction Hamiltonian terms.

The interaction Hamiltonian for the  $\mathbf{A} \cdot \mathbf{A}$  term, commonly referred to as the ‘‘Landau diamagnetism term’’ [17], is given by

$$\begin{aligned} H_{\mathbf{A} \cdot \mathbf{A}} &= \frac{e^2}{2m_p} \mathbf{A}_p \cdot \mathbf{A}_p + \frac{e^2}{2m_e} \mathbf{A}_e \cdot \mathbf{A}_e \\ &= \frac{e^2 B^2}{8m_p} (x_p^2 + y_p^2) + \frac{e^2 B^2}{8m_e} (x_e^2 + y_e^2) \\ &\approx \frac{e^2 B^2}{8m_e} (x_e^2 + y_e^2), \end{aligned} \quad (64)$$

where the approximation has been made due to relative sizes of the proton and electron terms [18].



The corresponding normalized matrix element is given by

$$\frac{\langle \Psi | \mathbf{A}_e \cdot \mathbf{A}_e | \Psi \rangle}{\langle \Psi | \Psi \rangle} = \frac{B^2}{4} \frac{\langle \Psi | x_e^2 + y_e^2 | \Psi \rangle}{\langle \Psi | \Psi \rangle}. \quad (65)$$

Henceforth, the subscripts will be suppressed as understood. Transforming to spherical polar coordinates and performing the integration, the matrix element that appears in the numerator on the right hand side of (65) becomes

$$\begin{aligned} \langle \Psi | x^2 + y^2 | \Psi \rangle &= \langle \Psi | r^2 \sin^2 \theta | \Psi \rangle \\ &= \int_0^{2\pi} \int_0^\pi \int_0^\infty r^{2n+2} \exp\left(-\frac{2r_e}{na_0}\right) \sin^{2n+1} \theta \, dr \, d\theta \, d\phi \\ &= 2\pi (2n+2)! \left(\frac{na_0}{2}\right)^{2n+3} S(2n+1). \end{aligned} \quad (66)$$

Dividing this by (48), the normalized element becomes

$$\frac{\langle \Psi | x^2 + y^2 | \Psi \rangle}{\langle \Psi | \Psi \rangle} = (2n+2)(2n+1) \left(\frac{na_0}{2}\right)^2 I(2n+1, 2n-1). \quad (67)$$

Thus, for large values of the principal quantum number  $n$ ,

$$\frac{\langle \Psi | x^2 + y^2 | \Psi \rangle}{\langle \Psi | \Psi \rangle} \approx (n^2 a_0)^2 = a_n^2. \quad (68)$$

The resulting energy shift thus satisfies

$$(\Delta E_{\mathbf{A} \cdot \mathbf{A}})_n = \langle H_{\mathbf{A} \cdot \mathbf{A}} \rangle \approx \frac{e^2 B^2}{8m_e} a_n^2, \quad (69)$$

in first-order perturbation theory. Comparing this to the Coulomb potential, it is noted that for sufficiently weak magnetic fields and realistic values of  $n$  (where  $n^3 B \ll 7 \times 10^5 T$ ), the  $\mathbf{A} \cdot \mathbf{A}$  term can be treated as a perturbation in (61). The energy shift given by (69) causes the atom to become

a low-field seeker in inhomogeneous magnetic fields through the relationship

$$(\mathbf{F}_{\mathbf{A}\cdot\mathbf{A}})_n = -\nabla (\Delta E_{\mathbf{A}\cdot\mathbf{A}})_n \approx -\frac{e^2 a_n^2}{8m_e} \nabla (B^2), \quad (70)$$

where  $(\mathbf{F}_{\mathbf{A}\cdot\mathbf{A}})_n$  is the force on the atom in the ring-like state (2) in the presence of an inhomogeneous magnetic field.

According to first-order perturbation theory, the result given in (69) implies that the size of the atom does not change in the presence of an externally applied DC magnetic field, in the sense that the root-mean-square transverse size of the atom, which is given by

$$a_n|_{\text{rms}} = \sqrt{\langle \Psi_{n,n-1,n-1} | x_e^2 + y_e^2 | \Psi_{n,n-1,n-1} \rangle} = a_n, \quad (71)$$

does not change with time during the application of the field.

For the  $\mathbf{A} \cdot \mathbf{p}$  term, we start with

$$\mathbf{A} \cdot \mathbf{p} = \frac{B}{2} \langle -y, x, 0 \rangle \cdot -i\hbar \left\langle \frac{\partial}{\partial x}, \frac{\partial}{\partial y}, \frac{\partial}{\partial z} \right\rangle = -i\hbar \frac{B}{2} \left( x \frac{\partial}{\partial y} - y \frac{\partial}{\partial x} \right). \quad (72)$$

Converting this to spherical polar coordinates, we have

$$\mathbf{A} \cdot \mathbf{p} = -i\hbar \frac{B}{2} \frac{\partial}{\partial \phi} = \frac{B}{2} L_z, \quad (73)$$

where  $L_z$  is the  $z$ -component of the quantum-mechanical angular momentum operator  $\mathbf{L}$ . The corresponding matrix element is given by

$$\langle \Psi | \mathbf{A} \cdot \mathbf{p} | \Psi \rangle = \frac{1}{2} \hbar B (n-1) \int_0^{2\pi} \int_0^\pi \int_0^\infty r^{2n} \exp\left(-\frac{2r}{na_0}\right) \sin^{2n-1} \theta \, dr d\theta d\phi. \quad (74)$$

Evaluating the radial part of the integral analytically leads to

$$\langle \Psi | \mathbf{A} \cdot \mathbf{p} | \Psi \rangle = \pi \hbar B (n-1) (2n)! \left( \frac{na_0}{2} \right)^{2n+1} S(2n-1). \quad (75)$$

Dividing the above by (48) gives

$$\frac{\langle \Psi | \mathbf{A} \cdot \mathbf{p} | \Psi \rangle}{\langle \Psi | \Psi \rangle} = \frac{\hbar}{2} B (n-1), \quad (76)$$

and thus the energy shift is given by

$$(\Delta E_{\mathbf{A} \cdot \mathbf{p}})_n \approx \frac{\hbar}{2m_e} q_e (n-1) B = \frac{\hbar}{2m_e} q_e m_\ell B, \quad (77)$$

which is the linear Zeeman level-splitting term. The expression in (77) is valid for all values of  $n$ , and the approximation arises from again neglecting the proton contribution, since its charge-to-mass ratio is much smaller. This energy shift is significantly smaller than the Coulomb potential for realistic values of  $m_\ell$  and  $B$ .

Since the  $\mathbf{A} \cdot \mathbf{p}$  term is linear in the electromagnetic vector potential, and the  $\mathbf{A} \cdot \mathbf{A}$  term is quadratic, one must calculate the second-order perturbation term in  $\mathbf{A} \cdot \mathbf{p}$ , since any contribution from this term will be of the same order as that in (69). The full energy expression corresponding to the  $\mathbf{A} \cdot \mathbf{p}$  interaction Hamiltonian, out to second order, is given by

$$E_n \approx E_n^{(0)} + (\Delta E_{\mathbf{A} \cdot \mathbf{p}})_n + \sum_{n' \neq n, l', m'} \frac{|\langle \Psi_{nlm} | \mathbf{A} \cdot \mathbf{p} | \Psi_{n'l'm'} \rangle|^2}{E_n^{(0)} - E_{n'}^{(0)}}. \quad (78)$$

Applying the  $\mathbf{A} \cdot \mathbf{p}$  operator to the wavefunction eigenstate, one obtains

$$\mathbf{A} \cdot \mathbf{p} | \Psi_{n'l'm'} \rangle = \hbar \frac{B}{2} m' | \Psi_{n'l'm'} \rangle, \quad (79)$$

and thus

$$\langle \Psi_{nlm} | \mathbf{A} \cdot \mathbf{p} | \Psi_{n'l'm'} \rangle = \hbar \frac{B}{2} m' \langle \Psi_{nlm} | \Psi_{n'l'm'} \rangle. \quad (80)$$

Since the matrix element on the right side of (80) is proportional to  $\delta_{nn'}$ , all terms in the sum in (78) are zero, and thus there are no contributions from second-order terms in  $\mathbf{A} \cdot \mathbf{p}$ .

As with the  $\mathbf{A} \cdot \mathbf{A}$  term, the result given in (77) also implies that the size of the atom is unchanged to first order by the  $\mathbf{A} \cdot \mathbf{p}$  interaction Hamiltonian, since the wavefunction state did not change with the application of this operator. In fact, none of the moments of the atomic probability distribution can change, since the wavefunction  $\Psi_{n,n-1,n-1}$  must remain unaltered in first-order perturbation theory in the presence of a weak applied magnetic field. This will also be true when the applied field varies slowly in time, as long as the characteristic frequency of its variation is sufficiently low to render quantum transitions out of the initial state  $\Psi_{n,n-1,n-1}$  highly improbable. The electronic wavefunction of the circular Rydberg atom is thus “quantum incompressible” not only in the presence of DC magnetic fields but also in the presence of sufficiently weak, and sufficiently slowly varying, magnetic fields that do not cause quantum transitions.

For the general case of external perturbations arising from changes in potential energy, such as those that would arise from continuous variation of the nuclear charge, a corresponding continuous variation of the size of the quantum system would be possible. However, due to the discreteness of the charge of the nucleus and of the electron, the Coulomb potential energy of a circular Rydberg atom governed by (61) is fixed, and cannot be continuously altered to first order. Continuous variation of the size of the atom in this particular case is therefore impossible via any process which arises from changes in an external perturbing electromagnetic field, and thus it is not meaningful to perform an analysis using the quantum adiabatic theorem. The quantum adiabatic theorem is only appropriate when dominant contributions to the Hamiltonian operator can be varied slowly and continuously, which is not the case here.

### 5.5.2 Quantum Incompressibility of the Rydberg Atom in a Weak Tidal Gravitational Field

Now consider the case in which a weak tidal gravitational field is present without any accompanying electromagnetic field, i.e., when  $\mathbf{A} = \mathbf{0}$  but  $\mathbf{h} \neq \mathbf{0}$ , such as when a hydrogen atom in a circular Rydberg state freely falls in the Earth's tidal field in the absence of any electromagnetic field. As before, the atom is initially prepared in the state given by (5). It is oriented such that its  $z$ -axis, which goes through its center of mass, coincides with the local vertical axis of the Earth's gravitational field. The horizontal tidal gravitational field of the Earth experienced by the atom during free fall, as observed in the coordinate system of a distant inertial observer, where the  $(x, y)$  plane is the local horizontal plane, is given by

$$\mathbf{h}(x, y, z, t) = \mathbf{v}(x, y, z, t) = \mathbf{g}'t = \frac{gt}{R_E} \langle x, y, -2z \rangle, \quad (81)$$

where, in accordance with Figure 1,  $\mathbf{v}(x, y, z, t)$  is the velocity of a freely falling test particle located at  $(x, y, z)$  and observed at time  $t$  by the distant inertial observer [1, which is Section 6 of this work],  $\mathbf{g}'$  is the horizontal component of Earth's gravitational acceleration arising from the radial convergence of free-fall trajectories towards the center of the Earth as seen by this observer, and  $R_E$  is the radius of the Earth. Such freely falling test particles located at the origin of the spacetime coordinate system establish the local inertial frame that is being used here. It is assumed in (81) that the excursions of the electron from the center of mass of the atom are much smaller than  $R_E$ .

The interaction Hamiltonian for the  $\mathbf{h} \cdot \mathbf{h}$  terms in (61) is then given by

$$H_{\mathbf{h} \cdot \mathbf{h}} = \frac{m_p}{2} \mathbf{h}_p \cdot \mathbf{h}_p + \frac{m_e}{2} \mathbf{h}_e \cdot \mathbf{h}_e \approx \frac{m_e}{2} \mathbf{h}_e \cdot \mathbf{h}_e = \frac{m_e g^2 t^2}{2R_E^2} (x_e^2 + y_e^2 + 4z^2), \quad (82)$$

where a similar approximation [18] to that appearing in (64) has been used. This leads to an energy level shift of the atom in the circular Rydberg wavefunction state (5), due to the Earth's tidal field

in (81), given by

$$(\Delta E_{\mathbf{h}\cdot\mathbf{h}})_n \approx \frac{m_e g^2 t^2}{2R_E^2} \langle \Psi_{n,n-1,n-1} | r^2 (4 - 3 \sin^2 \theta) | \Psi_{n,n-1,n-1} \rangle \approx \frac{m_e g^2 t^2}{2R_E^2} a_n^2 \quad (83)$$

in first-order perturbation theory, where the expectation value is expressed in spherical coordinates. This shows that the  $\mathbf{h}\cdot\mathbf{h}$  term can be treated as a perturbation in (61) because the Coulomb potential energy is much greater than the energy shift in (83) even for large values of  $n$ , when the system undergoes free fall in the Earth's tidal gravitational field. The Parker and DeWitt energy shifts in (53) and (83), respectively, are related by

$$\Delta E_{\mathbf{h}\cdot\mathbf{h}} = 2 \frac{y}{R_E} \Delta E_P, \quad (84)$$

where  $y = \frac{1}{2}gt^2$  is the distance fallen. It is noted here that  $\Delta E_P$ , unlike  $\Delta E_{\mathbf{h}\cdot\mathbf{h}}$ , is non-zero at time  $t = 0$ , where, for example, a laser-stimulated quantum transition occurs, and the atom is released into free fall. The explicit time-dependence of  $\Delta E_{\mathbf{h}\cdot\mathbf{h}}$  can be compared to the energy shift in a classical system consisting of two masses joined by a spring. When the system is released into free fall, there will be a time-dependent change in the potential energy of the spring as the two masses converge towards the center of the Earth.

Note that actual free fall is not strictly required, since the tidal gravitational fields that cause two massive objects to horizontally converge are present even in a system that has no local vertical motion. Consider two horizontally-separated masses connected by a spring. Over short time scales, when the gravitational acceleration and the distance from the center of Earth can be considered as constant, a time-dependent shift in the spring energy will be present, which will be the same for a freely-falling system, and a system that is placed on a flat, frictionless surface that is tangent to the surface of the Earth.

As before, since the expectation value in (83) is the mean-square transverse size of the atom, this size cannot change during free fall, according to first-order perturbation theory. In other words,

as was the case for the same atom in the presence of an applied DC magnetic field, the atom is “quantum incompressible” in the presence of the tidal gravitational field of the Earth, which tries to squeeze the atom radially so as to *continuously* change its energy state, as if it were a dropped rubber ring. Once again, one must make a distinction here between continuous compressions arising from changes in the total potential energy (e.g. compression of the walls containing a quantum object in an infinite square well), and the response of the system to a perturbing field. In the gravitational case, once again, just as in the magnetic case, the energy-level shift brought about in the atom by the Earth’s tidal gravitational field leads to a force on the atom in a Newtonian picture. This force causes the atom to become a low-field seeker in an inhomogeneous field – in this case an inhomogeneous gravitational field – through the relationship

$$(\mathbf{F}_{\mathbf{h}\cdot\mathbf{h}})_n = -\nabla (\Delta E_{\mathbf{h}\cdot\mathbf{h}})_n \approx -\frac{1}{2}m_e a_n^2 t^2 \nabla \left( \frac{g^2}{R_E^2} \right). \quad (85)$$

This force will cause the atom to fall slightly more slowly in an inhomogeneous gravitational field when its motion is compared to that of a freely falling, point-like, classical test particle located near the center of mass of the atom.

For the  $\mathbf{h} \cdot \mathbf{p}$  terms in (61), one can start by defining the anti-unitary time-reversal operator  $\Theta$ , which is unitary (i.e.  $\Theta\Theta^\dagger = \Theta^\dagger\Theta = \mathbf{1}$ ), and anti-linear (i.e.  $\Theta c|\Psi\rangle = c^*\Theta|\Psi\rangle$ , where  $c$  is a constant, and  $c^*$  is its complex conjugate). This operator has eigenvalues  $e = \pm 1$ , which satisfy

$$\Theta|\Psi\rangle = e|\Psi\rangle. \quad (86)$$

The value of  $e$  depends on the time-reversal symmetry of the wavefunction  $\Psi$ , where  $e = 1$  for even-symmetry wavefunctions and  $e = -1$  for odd-symmetry wavefunctions. The time-reversal symmetry of an operator  $\mathbf{a}$  is determined by  $\Theta\mathbf{a}\Theta^\dagger = \pm\mathbf{a}$ , where, again, the result is dependent upon the time-reversal symmetry of the operator. The expectation value for the  $\mathbf{h} \cdot \mathbf{p}$  operator

satisfies

$$\begin{aligned}
\langle \Psi | \mathbf{h} \cdot \mathbf{p} | \Psi \rangle &= \langle \Psi | (\Theta^\dagger \Theta \mathbf{h} \Theta^\dagger \cdot \Theta \mathbf{p} \Theta^\dagger \Theta | \Psi \rangle) \\
&= [(\langle \Psi | \Theta^\dagger) \Theta \mathbf{h} \Theta^\dagger \cdot \Theta \mathbf{p} \Theta^\dagger \Theta | \Psi \rangle]^*,
\end{aligned} \tag{87}$$

where the complex conjugate was taken so that the first  $\Theta^\dagger$  operates on the bra  $\langle \Psi |$ . The Hermitian conjugate of  $\langle \Psi | \Theta^\dagger$  is  $\Theta | \Psi \rangle$ , and thus the expression becomes

$$\langle \Psi | \mathbf{h} \cdot \mathbf{p} | \Psi \rangle = [(\Theta | \Psi \rangle)^\dagger \Theta \mathbf{h} \Theta^\dagger \cdot \Theta \mathbf{p} \Theta^\dagger \Theta | \Psi \rangle]^*. \tag{88}$$

Substituting (86) into this expression yields

$$\begin{aligned}
\langle \Psi | \mathbf{h} \cdot \mathbf{p} | \Psi \rangle &= [(e | \Psi \rangle)^\dagger \Theta \mathbf{h} \Theta^\dagger \cdot \Theta \mathbf{p} \Theta^\dagger e | \Psi \rangle]^* \\
&= \langle \Psi | e^* \Theta \mathbf{h} \Theta^\dagger \cdot \Theta \mathbf{p} \Theta^\dagger e | \Psi \rangle^* \\
&= \langle \Psi | |e|^2 \Theta \mathbf{h} \Theta^\dagger \cdot \Theta \mathbf{p} \Theta^\dagger | \Psi \rangle^* \\
&= \langle \Psi | \Theta \mathbf{h} \Theta^\dagger \cdot \Theta \mathbf{p} \Theta^\dagger | \Psi \rangle^*.
\end{aligned} \tag{89}$$

The operator  $\mathbf{h}$  has even time-reversal symmetry, so that  $\Theta \mathbf{h} \Theta^\dagger = \mathbf{h}$ , though one might be tempted to say otherwise, since  $\mathbf{h}$  is a velocity field. However, one can see from (81) that

$$\Theta \mathbf{h} \Theta^\dagger = \Theta \frac{gt}{R_E} \Theta^\dagger \Theta \langle x, y, -2z \rangle \Theta^\dagger. \tag{90}$$

The time-reversal operator only acts on quantum-mechanical observables as a complex conjugate operator, and not on classical values, so  $\Theta \frac{gt}{R_E} \Theta^\dagger = \frac{gt}{R_E}$ . Since the position vector also has even time-reversal symmetry, it is clear that  $\mathbf{h}$  itself has even time-reversal symmetry. The momentum operator, being an imaginary operator, has odd time-reversal symmetry under the complex



conjugation operation, since the gradient operator has even symmetry. Thus,

$$\langle \Psi | \mathbf{h} \cdot \mathbf{p} | \Psi \rangle = \langle \Psi | \Theta \mathbf{h} \Theta^\dagger \cdot \Theta \mathbf{p} \Theta^\dagger | \Psi \rangle^* = \langle \Psi | \mathbf{h} \cdot (-\mathbf{p}) | \Psi \rangle^* = -\langle \Psi | \mathbf{h} \cdot \mathbf{p} | \Psi \rangle^*. \quad (91)$$

Since the expectation value is equal to the additive inverse of its own complex conjugate, the matrix element is a purely imaginary quantity, and therefore the  $\mathbf{h} \cdot \mathbf{p}$  operator is non-Hermitian. However, it is clear that the operator  $\mathbf{h}$  by itself is Hermitian, since each of its components contains only real-valued scalar functions. Also, it is well-known that the momentum operator is Hermitian.

In general, it can be shown that for any two quantum operators  $\mathbf{a}$  and  $\mathbf{b}$  that operate on a wavefunction  $\Psi'$ ,

$$\langle \Psi' | \mathbf{a} \cdot \mathbf{b} | \Psi' \rangle = \langle \Psi' | \mathbf{b}^\dagger \cdot \mathbf{a}^\dagger | \Psi' \rangle^*, \quad (92)$$

and in the special case that both  $\mathbf{a}$  and  $\mathbf{b}$  are Hermitian operators, i.e.  $\mathbf{a}^\dagger = \mathbf{a}$  and  $\mathbf{b}^\dagger = \mathbf{b}$ ,

$$\langle \Psi' | \mathbf{a} \cdot \mathbf{b} | \Psi' \rangle = \langle \Psi' | \mathbf{b} \cdot \mathbf{a} | \Psi' \rangle^*.$$

Thus,

$$\langle \Psi | \{\mathbf{h}, \mathbf{p}\} | \Psi \rangle = \langle \Psi | \mathbf{h} \cdot \mathbf{p} | \Psi \rangle + \langle \Psi | \mathbf{p} \cdot \mathbf{h} | \Psi \rangle = \langle \Psi | \mathbf{h} \cdot \mathbf{p} | \Psi \rangle + \langle \Psi | \mathbf{h} \cdot \mathbf{p} | \Psi \rangle^* = 2 \operatorname{Re} \langle \Psi | \mathbf{h} \cdot \mathbf{p} | \Psi \rangle = 0, \quad (93)$$

and one sees that the operator  $\{\mathbf{h}, \mathbf{p}\}$  is Hermitian, with eigenvalue zero. Thus, the energy shifts due to the interaction Hamiltonians that are proportional to  $\{\mathbf{h}, \mathbf{p}\}$  are zero for all states.

As with the  $\mathbf{A} \cdot \mathbf{A}$  and  $\mathbf{A} \cdot \mathbf{p}$  terms, for completeness, one must calculate the second-order perturbation term in  $\{\mathbf{h}, \mathbf{p}\}$  in addition to the first-order perturbation term in  $\mathbf{h} \cdot \mathbf{h}$ . Similar to that in (78), the full energy expression for an  $\{\mathbf{h}, \mathbf{p}\}$  perturbation is given by

$$E_n \approx E_n^{(0)} + \sum_{n' \neq n, l', m'} \frac{|\langle \Psi_{nlm} | \{\mathbf{h}, \mathbf{p}\} | \Psi_{n'l'm'} \rangle|^2}{E_n^{(0)} - E_{n'}^{(0)}}, \quad (94)$$

where the first-order term is omitted, since it was previously shown to be zero.

Since  $\{\mathbf{h}, \mathbf{p}\}$  represents a tensor of rank-2 and order-0, symbolized by  $T_0^{(2)}$  following the notation in Sakurai [5, p. 235], the Wigner-Eckart theorem says that the matrix element

$$\langle \Psi_{nlm} | \{\mathbf{h}, \mathbf{p}\} | \Psi_{n'l'm'} \rangle = \left\langle \Psi_{nlm} \left| T_0^{(2)} \right| \Psi_{n'l'm'} \right\rangle \quad (95)$$

will be non-zero only in the case that  $m' = m$ .

It has been shown that the  $\{\mathbf{h}, \mathbf{p}\}$  operator has odd time-reversal symmetry, so for the expectation value of this operator to be non-zero, the initial and final states must have opposite time-reversal symmetry (i.e. one must have even symmetry and the other odd). However, any initial and final states  $|\Psi_{n'l'm'}\rangle$  and  $|\Psi_{nlm}\rangle$  such that  $m' = m$  must have the same time-reversal symmetry (i.e. both even or both odd), and thus *all* matrix elements corresponding to the  $\{\mathbf{h}, \mathbf{p}\}$  operator are zero for any initial and final wavefunction states. This result can also be obtained by replacing the matrix element  $\langle \Psi | \mathbf{h} \cdot \mathbf{p} | \Psi \rangle$  in (87) by the more general element  $\langle \Psi_{nlm} | \mathbf{h} \cdot \mathbf{p} | \Psi_{n'l'm'} \rangle$  and carrying out the same analysis.

Unlike the  $\{\mathbf{h}, \mathbf{p}\}$  operator, the  $\mathbf{A} \cdot \mathbf{p}$  operator has a non-zero expectation value, since the electromagnetic vector potential  $\mathbf{A}$  has odd time-reversal symmetry due to its dependence on the magnetic field, which itself has odd symmetry. Since the momentum operator also has odd symmetry, the  $\mathbf{A} \cdot \mathbf{p}$  operator has even symmetry, This operator is Hermitian, and leads to non-zero expectation values.

Quantum incompressibility will hold as long as transitions out of the initial quantum state  $\Psi_{n,n-1,n-1}$  cannot occur. It will also hold more generally for a time-varying tidal gravitational field, as long as the characteristic frequency of this field is much less than the energy gap corresponding to a quantum transition of the atom from the  $n$ th state to the nearest allowed adjacent states divided by Planck's constant, i.e., when the field is sufficiently weak to render any *discontinuous* quantum jump out of the initial state  $\Psi_{n,n-1,n-1}$  highly improbable. The same consideration also implies

that the duration of free fall  $t$  must be sufficiently short for the energy level shift given in (83) to remain a small perturbation.

The time-dependence of the interaction Hamiltonian in (82) can be explained when one considers the following thought experiment. If, at time  $t = 0$ , a quantum transition is made (e.g. excited by laser stimulation), the wavefunction for the new state, which, to first order, has an energy given by the sum of the unperturbed energy level and the expectation value of the interaction Hamiltonian in (46), represents the initial state. For short time scales, the DeWitt energy shift, found by taking the expectation value of the interaction Hamiltonian in (82), further perturbs the energy levels, as measured by the distant inertial observer. This energy shift would cause a time-dependent change in the transition frequency between two adjacent states, though this effect would be extremely difficult to measure in the Earth's gravitational field.

If a Rydberg atom with principal quantum number  $n \sim 10^3$  were suspended at the surface of the Earth, one could expect the possibility of a quantum transition to occur over a time scale on the order of  $10^4$  years due to the DeWitt energy shift. For a Chandrasekhar-limit gravitational source, the time scale is reduced to tens of days, and at the surface of a typical neutron star, the time scale is reduced to milliseconds.

In the transverse-traceless gauge, the gravitational vector potential  $\mathbf{h}$  is identically set to zero everywhere, akin to performing a gauge transformation that sets the electromagnetic vector potential  $\mathbf{A}$  identically equal to zero everywhere. Recall that since the magnetic field  $\mathbf{B}$  is equal to the curl of  $\mathbf{A}$ , one can arbitrarily add a term that can be expressed as the gradient of a scalar function to  $\mathbf{A}$  without changing the value of the magnetic field, since the curl of any gradient is equal to the zero vector. Thus, one can locally define a gauge where the electromagnetic vector potential is zero at each point in space by choosing the scalar function such that its gradient is equal to the additive inverse of  $\mathbf{A}$  at that point. However, physical effects that depend on  $\mathbf{A}$ , such as the Aharonov-Bohm effect, are overlooked. In general relativity, one can describe the transverse-traceless gauge as the coordinate system which is “locked-on” to freely-falling test particles in the gravitational field,

i.e. a coordinate grid whose intersections are defined in such a way as to co-move along with the freely falling particles located at these intersections, as seen by the distant inertial observer. Thus, the coordinate system itself is distorted by the gravitational field, and therefore no relative motion between the coordinate system and the freely falling particles is measured. Therefore, there can never be any non-zero kinetic energy of the test particles as measured by the observer in this frame, and thus the velocity field  $\mathbf{h}$  is zero everywhere. In the DeWitt gauge, where measurements are made by a distant inertial observer in asymptotically flat spacetime, global, holonomic effects can be measured due to the presence of the gravitational vector potential [19]. Though the measurements made from these two gauge choices are different, gauge invariance is still preserved, since the two represent more than a simple gauge choice. The transverse-traceless gauge assumes that the local spacetime coordinate grid is curved in such a way that the spacetime at infinity need not be asymptotically flat, whereas the DeWitt gauge requires that spacetime be asymptotically flat at infinity. Thus, a distant inertial observer situated in asymptotically flat space using the DeWitt gauge measures relative motion between the freely-falling particles and his/her coordinate system, and concludes that  $\mathbf{h}$  is non-zero. Thus, these two gauges use a different model for spacetime itself, with different boundary conditions at infinity, whereas gauge invariance only applies to different coordinate systems within the same space. Further analysis of gauge invariance of the energy shifts derived above is presented in the next section.

### 5.5.3 Gauge Invariance of Energy Shifts

The energy shift in (83) cannot be transformed away by any particular gauge choice, just as (69) cannot be transformed away either, since both can be expressed in terms of the square of the covariant Riemann curvature tensor components  $R_{0i0}^i$  of the Earth's gravitational field, where  $i = \{1, 2\}$ , recalling that the Earth's tidal field is isotropic in the  $x$  and  $y$  directions. The fact that the force in (85) cannot be transformed away by gauge choice can be demonstrated by recasting this result in terms of the Riemann curvature tensor arising from Earth's gravity.

The two objects in Figure 1 obey the geodesic deviation equation of motion (EOM) [10]

$$\frac{d^2 \xi^i}{dt^2} = -R_{0j0}^i \xi^j, \quad (96)$$

where  $\xi^i$  is the distance vector from one object to the other object (here  $i = 1, 2$  and  $j = 1, 2$  correspond to the horizontal  $x$  and  $y$  axes of the tangent plane to the midpoint between the two objects; the  $z$  axis, which is the vertical axis with  $i = j = 3$ , will be omitted throughout this calculation),  $t$  is the free-fall time, and  $R_{0j0}^i$  are certain components of the Riemann curvature tensor (the zero index corresponds to the time index, and repeated indices are summed in accordance with the Einstein summation convention.) This EOM is valid assuming that the objects are nonrelativistic, i.e., that they are moving slowly compared to the speed of light. Also, in the Newtonian limit (which is valid for Earth's weak gravitational field), recall from (26) that [10]

$$R_{0j0}^i = \delta^{ik} \frac{\partial^2 \Phi}{\partial x^k \partial x^j}, \quad (97)$$

where  $\Phi$  is the gravitational potential of Earth's field. Thus the two objects experience tidal gravitational fields according to the Newtonian viewpoint. Since the second partial derivatives of  $\Phi$  are nonvanishing for Earth's gravitational field, the Riemann curvature tensor from (97) is also nonvanishing. Hence no coordinate transformation can cause this tensor, or any quantity that depends on it, to vanish identically.

Since the two objects in Figure 1 are being dropped from the same height above the Earth's surface, and since the tidal fields are isotropic in the  $x$  and  $y$  directions, the Riemann curvature tensor is diagonal in the indices  $i$  and  $j$ , i.e.,

$$R_{0j0}^i = \frac{1}{2} \delta_j^i R'_{00} \text{ for } \{i, j\} = \{1, 2\} , \quad (98)$$

where the prime denotes a partial contraction over the isotropic, horizontal spatial indices only, i.e., explicitly,

$$R'_{00} \equiv \sum_{i=1}^2 R_{0i0}^i, \quad (99)$$

which are components of the Ricci tensor. From a general relativistic viewpoint, this means that the two objects are being squeezed horizontally along with space as they fall, so that they approach the midpoint in between them. Therefore they converge towards each other during free fall.

For the case of two identical objects with mass  $m$ , the geodesic deviation EOM reduces to the following Newton's EOM for each object:

$$F_i = mg'_i = m \frac{d^2 x_i}{dt^2} = -k_{\text{eff}} x_i , \quad (100)$$

where  $k_{\text{eff}}$  is an effective Hooke's constant. In this case, the horizontal components of the acceleration  $g'_i$  of the two objects is related to the relative acceleration between them as follows:

$$2g'_i = 2 \frac{d^2 x_i}{dt^2} = \frac{d^2 \xi^i}{dt^2} = -R_{0j0}^i \xi^j .$$

Now consider the free fall of the two objects through a hole which is dug across an entire diameter of the Earth. It shall be shown that in this case the Riemann curvature tensor is a constant, and that the motion of the two objects reduces to that of a simple harmonic oscillator, assuming that the mass density of the Earth is a constant. Recall that Newton's theorem of spheres (or equivalently, Gauss's theorem) implies that only the mass interior to the two objects as they fall is effective in

contributing to the gravitational force, i.e.,

$$|F| = \frac{GM_{\text{enc}}m}{r^2} = \frac{4\pi\rho r^3}{3} \frac{Gm}{r^2} = \frac{4\pi G\rho m}{3} r = k_{\text{eff}} r . \quad (101)$$

Thus the effective Hooke's constant is

$$k_{\text{eff}} = \frac{4\pi G\rho m}{3} , \quad (102)$$

where the mass density  $\rho$  of the Earth has been assumed to be constant. This implies that freely falling masses undergo simple harmonic motion with a period of

$$T = \frac{2\pi}{\omega} = \sqrt{\frac{3\pi}{G\rho}} = 2\pi\sqrt{\frac{R_E^3}{GM_E}} = 2\pi\sqrt{\frac{R_E}{g_E}} , \quad (103)$$

where  $R_E$  is the radius of the Earth, and  $M_E$  is its mass. Note that in accordance with the equivalence principle,  $T$  is independent of the mass  $m$ .

The free-fall trajectories are directed radially towards the center of the Earth, and so the inclination angle does not change during free fall, using the approximation that the gravitational force between the two falling objects is negligible. Therefore, by a similar-triangles argument to be given below, the geodesic deviation EOM becomes the simple harmonic oscillator EOM with the same period of motion as that of a single object falling down the hole.

Since the right triangles in Figure 1 remain similar during the free fall of these objects down the hole, the distance between them scales proportionally to the radial distance to the center of the Earth at all times. Therefore the geodesic deviation EOM has the form of that of a simple harmonic oscillator with a frequency  $\omega$ , i.e.,

$$\frac{d^2x}{dt^2} = -R_{010}^1 x = -\omega^2 x = -\frac{4\pi^2}{T^2} x , \quad (104)$$

where the period  $T$  of simple harmonic motion is the same for both the radial and the horizontal

motions of the two objects. It is therefore concluded that the Riemann curvature tensor is a constant within the interior of the Earth, and is given by

$$R_{010}^1 = R_{020}^2 = \frac{1}{2}R'_{00} = \frac{4\pi^2}{T^2} = \frac{GM_E}{R_E^3} = \frac{g_E}{R_E} , \quad (105)$$

where  $g_E$  is the acceleration due to Earth's gravity at the surface of the Earth, which is a constant that does not depend on the distance from the center of Earth, reserving the symbol  $g$  for the gravitational acceleration that varies with the distance from the center of Earth, and  $M_E$  is the mass of the Earth.

DeWitt's vector potential in this case can be expressed as

$$\mathbf{h}(x, y, t) = \mathbf{v}(x, y, t) = \mathbf{g}'t = \frac{g_E t}{R_E} \langle x, y, -2z \rangle = \frac{1}{2}R'_{00}t \langle x, y, -2z \rangle , \quad (106)$$

which is analogous to the expression for the electromagnetic vector potential in the symmetric gauge choice

$$\mathbf{A} = \frac{1}{2}\mathbf{B} \times \mathbf{r} = -\frac{1}{2}B \langle y, -x, 0 \rangle , \quad (107)$$

where the EM vector potential has been expressed in terms of the magnetic field  $B$ , which is a homogeneous field, just as (106) expresses the gravitational vector potential in terms of the covariant Riemann curvature field  $R'_{00}$ , which is also a homogeneous field within the interior of the Earth.

The energy level shift expressed in terms of the Riemann curvature  $R'_{00}$  is given by

$$(\Delta E_{\mathbf{h}\cdot\mathbf{h}})_n = \frac{mg^2t^2}{2R^2} \langle \Psi_{n,n-1,n-1} | x^2 + y^2 | \Psi_{n,n-1,n-1} \rangle \approx \frac{ma_n^2g^2t^2}{2R^2} = \frac{ma_n^2R_{00}^2t^2}{8} , \quad (108)$$

which cannot vanish identically under any coordinate transformation.

The force on the Rydberg atom can also be expressed generally in terms of the Riemann curvature

$$(\mathbf{F}_{\mathbf{h}\cdot\mathbf{h}})_n = -\nabla (\Delta E_{\mathbf{h}\cdot\mathbf{h}})_n = -\frac{ma_n^2t^2}{2} \nabla \left( \frac{g^2}{R^2} \right) = -\frac{ma_n^2t^2}{8} \nabla (R_{00}^2) . \quad (109)$$



This force vanishes during the free fall down the hole dug through a diameter of the Earth, since the Riemann curvature tensor is a constant. However, it is nonvanishing when the circular Rydberg atom is above the surface of the Earth, leading to a time-dependent energy shift.

Though the energy shift in (108) is expressed in terms of the covariant Riemann curvature and thus cannot be made to vanish identically by any gauge choice, the value of the shift itself will be measured differently by observers in frames that have relative motion between them. This phenomenon occurs even in special relativity, where the total energy  $E$  of the atom satisfies

$$E^2 = p^2 c^2 + M^2 c^4. \tag{110}$$

This energy is minimized in the frame that is co-moving with the atom (where  $\mathbf{p} = \mathbf{0}$ ), yielding the rest energy  $E_{rest} = Mc^2$ . The rest energy is an invariant quantity which is agreed upon by all observers.

## 5.6 Down the Rabbit Hole: Free Fall Through a Massive Gravitational Source

It was noted in the previous section that the Riemann curvature tensor is constant within a hole drilled diametrically through the center of the Earth. This suggests that the behavior of a freely-falling system could be different when falling through this hole, as compared to free fall that occurs above the Earth's surface. This is indeed the case, and the problem of free fall through the hole, which will be henceforth dubbed as the “rabbit hole,” and abbreviated “RH,” will be explored further.

### 5.6.1 Free Fall of Classical Systems Within the Rabbit Hole

Consider a system of massive test particles free falling through the RH. It will be shown that the behavior of this system during free fall is quite different in the RH compared to free fall above the surface of the Earth. For simplicity, consider the RH to be sufficiently narrow as compared to the radius of the Earth, so that the Earth can be modeled as solid. Furthermore, the approximations that the Earth is non-rotating, spherical, and has a constant density are made as well. See Figure 4.

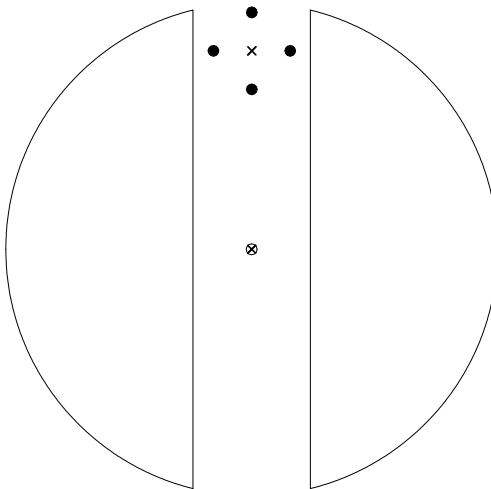


Figure 4: A system of test particles with center of mass labeled by  $\times$  freely falling through the RH.

The gravitational potential  $\Phi$  of an object in the RH can be found using Gauss' law for gravity, given by

$$\oint \mathbf{g} \cdot d\mathbf{a} = -4\pi GM_{\text{enc}}, \quad (111)$$

where  $d\mathbf{a}$  is a differential area element on the Gaussian surface,  $G$  is Newton's gravitational constant, and  $M_{\text{enc}}$  is the mass of the gravitational source that is enclosed by the Gaussian surface. By the divergence theorem, (111) can be expressed as

$$\int \nabla \cdot \mathbf{g} \, dV = -4\pi GM_{\text{enc}}. \quad (112)$$

Since the gravitational field is conservative, one can define a potential  $\Phi$  as

$$\mathbf{g} = -\nabla\Phi, \quad (113)$$

and thus (112) becomes

$$\int \nabla^2\Phi \, dV = 4\pi GM_{\text{enc}}. \quad (114)$$

Within the RH, one can consider a spherical Gaussian surface of radius  $r$ , over which  $\nabla^2\Phi$  is constant. Thus,

$$\nabla^2\Phi \left( \frac{4}{3}\pi r^3 \right) = 4\pi G \left( \frac{4}{3}\pi r^3 \rho \right), \quad (115)$$

where  $\rho$  is the mass density of the Earth, which is assumed constant. Thus, the potential is a solution to the Poisson equation

$$\nabla^2\Phi = \frac{\partial^2\Phi}{\partial r^2} + \frac{2}{r} \frac{\partial\Phi}{\partial r} = 4\pi\rho G, \quad (116)$$

which will be dependent only on the radius of the Gaussian sphere, due to the spherical symmetry of the Earth.

Substituting the ansatz

$$\Phi = C_1 r^2 + \Phi_0 \quad (117)$$

into (116) yields

$$\nabla^2 \Phi = 6C_1 = 4\pi\rho G, \quad (118)$$

and thus the potential is given by

$$\Phi = \frac{2}{3}\pi\rho G r^2 + \Phi_0, \quad (119)$$

where the constant  $\Phi_0$  is an arbitrary choice for the potential at the center of the sphere, where the gravitational field is zero since the potential is constant. This value will be set to zero for the moment, though this topic will be revisited in Section 5.8. By making a substitution for the mass density of the Earth, the potential can be rewritten as

$$\Phi = \frac{2}{3}\pi \left( \frac{M_E}{\frac{4}{3}\pi R_E^3} \right) G r^2 = \frac{g_E}{2R_E} r^2. \quad (120)$$

Thus, the gravitational potential energy is

$$V = m\Phi = \frac{mg_E}{2R_E} r^2, \quad (121)$$

where  $m$  is the mass of an object in the gravitational field. This gravitational field causes interesting behavior of a freely-falling system of particles. Gravitational acceleration increases linearly with increasing distance from the center of the Earth, as opposed to a  $1/r^2$  dependence outside the RH. If the hole is dug to the center of the Earth instead of diametrically across, two objects dropped from rest at different heights will strike the bottom of the hole at the same time, regardless of their initial positions, unlike free fall above the surface of the Earth, where the lower object will strike the ground first. If the hole is dug past the center of the Earth, it is the object dropped *further* from the center of the Earth which will strike the bottom of the hole first. Many of these results are counter-intuitive, but are the nature of the difference between gravitational potential solutions

to Laplace's equation above the surface of the Earth, and Poisson's equation within the RH.

Consider the same two objects that were freely falling in the gravitational field of a point mass, introduced in Section 5.3. Let these two objects, the ring and the point-like mass, now undergo free fall through the RH. For reasons that will become clear shortly, only the extended ring will be considered here. The gravitational potential energy of a differential element of the ring is given by

$$dV_{\text{ext}} = \frac{g_E r^2}{2R_E} dm = \frac{g_E r^2}{2R_E} \rho_\ell a d\theta, \quad (122)$$

where  $\rho_\ell$  is the linear mass density of the ring. Thus,

$$dV = \frac{g_E r^2}{2R_E} \left( \frac{m}{2\pi a} \right) a d\theta = \frac{g_E r^2}{2R_E} \frac{m}{2\pi} d\theta. \quad (123)$$

Integrating this expression, while noting that the prefactor of the differential angle element is independent of  $\theta$ , leads to

$$V = \frac{mg_E}{2R_E} r^2 = \frac{mg_E}{2R_E} \left[ (h - y)^2 + a^2 \right], \quad (124)$$

where  $y$  is the distance fallen. This expression is the same as that in (121), which is expected by symmetry, i.e. the distance from the center of the Earth is the same at each point in the ring.

The total energy of the ring, when dropped from rest at the opening of the RH, is

$$E = \frac{mg_E}{2R_E} (R_E^2 + a^2) = \frac{1}{2} mg_E R_E + \frac{mg_E a^2}{2R_E}. \quad (125)$$

The potential energy is

$$V = \frac{mg_E}{2R_E} \left[ (R_E - y)^2 + a^2 \right] \quad (126)$$

and thus the kinetic energy is

$$T = E - V = \frac{mg_E}{2R_E} (2R_E y - y^2). \quad (127)$$

It can be seen from this expression that the kinetic energy of the ring undergoing free fall through the RH is independent of  $a$ , and therefore will fall with the same velocity as the point-like object. Recall that this was not the case for free fall in the gravitational field of the point mass, which is the same gravitational field that the Earth produces (using the assumptions for the Earth described in the beginning of this section) when  $M' = M_E$ , when free fall occurs above the Earth's surface.

### 5.6.2 Free Fall of the Hydrogen Atom Within the Rabbit Hole

To analyze the behavior of the hydrogen atom in free fall within the RH, one can start by deriving the velocity field of a particle within the freely falling system as measured from the center of mass of the system. Consider the system shown in Figure 4, released from rest at time  $t = 0$ , freely falling down the RH. Let a single test particle within the freely falling system be at position  $\mathbf{r} = \langle x_1, x_2, x_3 \rangle$ . Without loss of generality, only the two-dimensional problem will be considered explicitly, since the Earth has axial symmetry, and thus the effects are isotropic along the  $x_1$  and  $x_2$  dimensions, which are transverse to the direction of motion of the center of mass of the test particle system during free fall. The accelerations of the center of mass, and an arbitrary particle at position  $\langle x_1, x_3 \rangle = \langle x, z \rangle$  are shown in Figure 5. The magnitude of the gravitational force of the Earth within the RH can

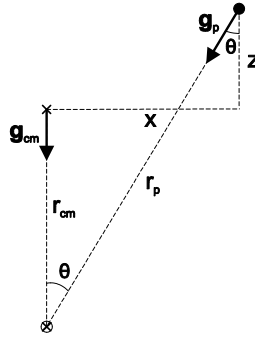


Figure 5: Diagram showing the acceleration of a particle within the freely falling system, and the acceleration of the center of mass of the system. Within the RH, the magnitude of the acceleration is no longer proportional to the inverse square of the distance between an object and the center of mass of the earth, but directly proportional to that distance.

be derived from Gauss' law for gravity

$$\oint \mathbf{g} \cdot d\mathbf{a} = -4\pi GM_{\text{enc}}, \quad (128)$$

where  $d\mathbf{a}$  is a differential area vector normal to the Gaussian-like spherical surface of radius  $r$ , and  $G$  is Newton's gravitational constant. Since  $\mathbf{g}$  is constant in magnitude and everywhere anti-parallel to  $d\mathbf{a}$  over the Gaussian-like surface, and mass is equal to the product of volume and density, (128)

becomes

$$g(4\pi r^2) = 4\pi G \left( \frac{4}{3} \pi \rho r^3 \right), \quad (129)$$

and thus

$$\mathbf{g} = -\omega^2 r \hat{\mathbf{r}}, \quad (130)$$

where

$$\omega \equiv \sqrt{\frac{4}{3} \pi \rho G} = \sqrt{\frac{g_E}{R_E}}. \quad (131)$$

This result, identical to that which was derived using the Riemann curvature tensor in Section 5.5.3, shows that the gravitational acceleration of an object freely falling through the RH is proportional to the radial distance from the center of the Earth. At the opening of the RH (i.e. the surface of the Earth),  $M_{\text{enc}}$  is equal to the mass of the Earth, and so one recovers Newton's inverse-square law for gravity, continuously, when the Gaussian-like surface is at the surface of the Earth.

Using (130), it can be seen that the accelerations of the particle and of the center of mass of the system are given by

$$\mathbf{g}_p = -\omega^2 r_p \langle \sin \theta, \cos \theta \rangle = -\omega^2 \langle x, z + r_{\text{cm}} \rangle \quad (132)$$

$$\mathbf{g}_{\text{cm}} = -\omega^2 \langle 0, r_{\text{cm}} \rangle, \quad (133)$$

and thus the acceleration of the particle with respect to the center of mass of the system is given by

$$\mathbf{g}_{\text{rel}} = \mathbf{g}_p - \mathbf{g}_{\text{cm}} = -\omega^2 \langle x, z \rangle. \quad (134)$$

The equations that describe the motion of the particle with respect to the center of mass are thus

$$\frac{d^2 x_i}{dt^2} = -\omega^2 x_i, \quad (135)$$



which has solutions

$$x_i = x_{0,i} \cos \omega t + \frac{h_{0,i}}{\omega} \sin \omega t, \quad (136)$$

where  $x_{0,i}$  and  $h_{0,i}$  are the initial position and velocity, respectively, of the particle with respect to the center of mass along the  $x_i$  axis, for  $i = 1, 2, 3$ .

Differentiating (136) with respect to  $t$  gives the components of the velocity field  $\mathbf{h}$  as

$$h_i = -\omega x_{0,i} \sin \omega t + h_{0,i} \cos \omega t = \omega \sqrt{x_{0,i}^2 + \frac{h_{0,i}^2}{\omega^2} - x_i^2}. \quad (137)$$

For a Rydberg atom released from rest and allowed to fall down the RH, this velocity field simplifies to

$$h_i = \omega \sqrt{a_n^2 - x_i^2}, \quad (138)$$

where  $a_n$  is the atomic radius of the atom in the  $n$ th energy eigenstate. This velocity field will become important when calculating gravitationally-induced energy shifts in the electron orbitals.

From (137), it is clear that the  $\mathbf{h} \cdot \mathbf{h}$  operator satisfies

$$\mathbf{h} \cdot \mathbf{h} = h_0^2 + \omega^2 (r_0^2 - r^2), \quad (139)$$

where  $r_0$  and  $h_0$  are the initial position and velocity of the particle with respect to the center of mass, satisfying

$$r_0^2 = \sum_i x_{i,0}^2 \quad (140)$$

$$h_0^2 = \sum_i h_{0,i}^2, \quad (141)$$

respectively.

Consider the energy shift in a hydrogen atom in which its constituent particles begin with zero

radial velocity with respect to the center of mass

$$\Delta E_{\mathbf{h}\cdot\mathbf{h}} = \frac{\omega^2}{2} \left( m_e \langle \Psi | a_n^2 - r_e^2 | \Psi \rangle + m_p \langle \Psi | a_p^2 - r_p^2 | \Psi \rangle \right), \quad (142)$$

where the second term in the parentheses is due to the proton contribution. Since the proton and electron move symmetrically about the center of mass of the atom, with the proton's deviation scaled down by a factor equal to the ratio of the masses of the electron and proton, and this deviation is squared in the energy shift,

$$m_p \langle \Psi | a_p^2 - r_p^2 | \Psi \rangle \propto m_p \left( \frac{m_e}{m_p} \right)^2 \langle \Psi | a_n^2 - r_e^2 | \Psi \rangle = \left( \frac{m_e}{m_p} \right) m_e \langle \Psi | a_n^2 - r_e^2 | \Psi \rangle, \quad (143)$$

and therefore the proton contribution will be three orders of magnitude smaller than that of the electron. Thus, the proton term will be neglected, and the expression for the energy shift that will be used for the hydrogen atom undergoing free fall in the RH is thus

$$\Delta E_{\mathbf{h}\cdot\mathbf{h}} \approx \frac{m_e \omega^2}{2} \langle \Psi | a_n^2 - r_e^2 | \Psi \rangle = \frac{m_e g_E}{2R_E} \langle \Psi | a_n^2 - r_e^2 | \Psi \rangle. \quad (144)$$

From this expression, it can be seen that the energy shifts with the largest magnitude will correspond to the states that have probability distributions that vary widely from the average atomic radius  $a_n$ , whereas the atom in states that have probability distributions that do not vary much from  $a_n$  will experience small energy shifts.

Since the electron probability distribution peaks at the center of the atom for states with zero angular momentum, and at  $a_n$  for the stretched states, it is expected that the largest magnitudes of this shift will correspond to large values of  $n$  and small values of  $l$ , and that the circular states will have small energy shifts which approach zero as  $n$  approaches infinity.

Explicitly evaluating the energy shifts for the stretched states yields

$$\begin{aligned}\Delta E_{\mathbf{h},\mathbf{h}} &\approx \frac{m_e g_E}{2R_E} \left[ a_n^2 - \frac{2\pi \int_0^\infty r^{2n+2} \exp\left(-\frac{2}{na_0}\right) dr \int_0^\pi \sin^{2n-1} \theta d\theta}{2\pi \int_0^\infty r^{2n} \exp\left(-\frac{2}{na_0}\right) dr \int_0^\pi \sin^{2n-1} \theta d\theta} \right] \\ &= \frac{m_e g_E}{2R_E} \left[ a_n^2 - (2n+2)(2n+1) \left(\frac{na_0}{2}\right)^2 \right].\end{aligned}\tag{145}$$

As  $n$  becomes large, this energy shift becomes

$$\Delta E_{\mathbf{h},\mathbf{h}} \approx \frac{m_e g_E}{2R_E} (a_n^2 - n^4 a_0^2) = \frac{m_e g_E}{2R_E} (a_n^2 - a_n^2) = 0,\tag{146}$$

as expected.

One can see by substitution of (120) into (35) that the Parker interaction Hamiltonian for a hydrogen atom that is freely falling through the RH is given by

$$H_P = \frac{m_e g_E}{2R_E} r^2,\tag{147}$$

and that the energy shift is given by

$$\Delta E_P = \langle \Psi | H_P | \Psi \rangle = \frac{m_e g_E}{2R_E} \langle \Psi | r^2 | \Psi \rangle.\tag{148}$$

Repeating the analysis presented in Section 5.5.2, one can see that the expectation values of the  $\{\mathbf{h}, \mathbf{p}\}$  operator will be zero for all states inside the RH, as they were outside.

## 5.7 Classical Objects and Circular Rydberg Atoms in Free Fall

### 5.7.1 Classical Objects and Circular Rydberg Atoms in Free Fall Through the Rabbit Hole

Inside the RH, it is clear from (121) that a point mass  $m$  has total energy

$$E_{\text{pt,inside}} = \frac{m_{\text{pt}}g_{\text{E}}h^2}{2R_{\text{E}}}, \quad (149)$$

and from (124) that a thin, classical, rigid ring with mass  $m$  and radius  $a$  has total energy

$$E_{\text{ext,inside}} = \frac{m_{\text{ext}}g_{\text{E}}(h^2 + a^2)}{2R_{\text{E}}} = \frac{m_{\text{ext}}g_{\text{E}}h^2}{2R_{\text{E}}} + \frac{m_{\text{ext}}g_{\text{E}}a^2}{2R_{\text{E}}} \equiv E'_{\text{pt,inside}} + \Delta E_{\text{ext}} \quad (150)$$

when released from rest a distance  $h$  from the center of Earth. Thus, the total energy of the ring consists of a term that considers the point-like energy of the system, plus an additional term that arises from its extended mass distribution.

Consider a Rydberg atom in the circular state, with a large value of  $n$ . The atom consists of a point-like proton with mass  $m_p$  and a ring-like electron with mass  $m_e$ . Thus, the proton contribution to the total energy is

$$E_{\text{p+,inside}} = \frac{m_p g_{\text{E}} h^2}{2R_{\text{E}}}, \quad (151)$$

and the electron contribution is

$$E_{\text{e-,inside}} = \frac{m_e g_{\text{E}} (h^2 + a_n^2)}{2R_{\text{E}}}, \quad (152)$$

and thus the total energy of the atom is

$$E_{\text{tot,inside}} = \frac{M g_{\text{E}} h^2}{2R_{\text{E}}} + \frac{m_e g_{\text{E}} a_n^2}{2R_{\text{E}}}, \quad (153)$$

where  $M = m_p + m_e$  is the total mass of the atom. This form is similar to (150) in that there is

a point mass energy for the atom, with an additional term for the electron orbital, which has an extended mass distribution.

Furthermore, recall that the energy shift for the hydrogen atom in a circular Rydberg state due to the Parker interaction Hamiltonian, shown in (53) is equal to the second term on the right side of (153). Thus, the potential energy shift resulting from this interaction Hamiltonian is the same energy shift due to an extended mass distribution of a classical system. Recall also that the energy shift for this atom due to the DeWitt interaction Hamiltonian was zero for free fall through the RH, suggesting that the highly excited Rydberg atom will behave like a thin, classical, rigid ring with radius  $a_n$  when the two systems undergo free fall through the RH.

### 5.7.2 Classical Objects and Circular Rydberg Atoms in Free Fall in the Field of a Point Mass

In Section 5.3, it was determined that a point mass  $m$  has total energy

$$E_{\text{pt,outside}} = -\frac{GM'm_{\text{pt}}}{h} = -m_{\text{pt}}gh, \quad (154)$$

and that a thin, classical, rigid ring with mass  $m$  and radius  $a$  has total energy

$$E_{\text{ext,outside}} = -\frac{m_{\text{ext}}gh^2}{\sqrt{h^2 + a^2}}. \quad (155)$$

When the radius of the ring is small compared to the distance from the gravitational source, one can perform a Taylor expansion about  $a = 0$  to find that

$$E_{\text{ext,outside}} = -\left[ m_{\text{ext}}gh + \frac{m_{\text{ext}}ga^2}{2h} + O(a^4) \right]. \quad (156)$$

Thus, for short free fall distances near the surface of the Earth,

$$E_{\text{ext,outside}} \approx -\left( m_{\text{ext}}g_{\text{E}}R_{\text{E}} + \frac{m_{\text{ext}}g_{\text{E}}a^2}{2R_{\text{E}}} \right), \quad (157)$$

which, again, has the form of a point mass energy plus an additional term due to the extended mass distribution. An analysis similar to that done in equations (151)–(153) can be done to show that the total energy for the circular Rydberg atom is given by

$$E_{\text{tot,outside}} = -\left( Mg_{\text{E}}R_{\text{E}} + \frac{m_e g_{\text{E}} a_n^2}{2R_{\text{E}}} \right), \quad (158)$$

where the second term arises from the energy shift due to the Parker interaction Hamiltonian. Note that in both the classical and quantum cases here, the additional energy term causes the extended system to become a low gravitational field seeker, and thus both the classical ring and the circular

Rydberg atom will fall more slowly than a nearby, point-like test mass.

However, unlike the case for free fall inside the RH, here there is a non-zero, time-dependent energy shift due to the DeWitt interaction Hamiltonian given by

$$\Delta E_{\mathbf{h}\cdot\mathbf{h}} \approx \frac{m_e g_E^2 t^2 a_n^2}{2R_E^2}. \quad (159)$$

Thus, as the atom undergoes free fall, there is an additional energy shift not seen in classical systems, or even in the same atom undergoing free fall through the RH. As mentioned before, this is a positive-definite energy shift that causes the atom to experience a gravitational diamagnetism force, in addition to the gravitational diamagnetism force experienced by extended systems in tidal fields. This phenomenon will result in an atom falling more slowly than the classical rigid ring with the same radius (i.e.  $a_n$ ), which in turn falls more slowly than a point mass, though the effect would be extremely difficult to measure experimentally during free fall in the Earth's gravitational field. Nevertheless, this is a novel, quantum-mechanical effect that cannot be explained classically.

## 5.8 Gravitational Potential Inside and Outside the Rabbit Hole

An astute reader may notice that the two expressions for the total gravitational energy inside and outside the RH are not equal at the opening of the RH. Specifically, when  $h = R_E$ , the energy in (149) is only half the energy in (154). Thus, there is a discontinuity at the opening of the RH. This is not a physical discontinuity, however. Recall that the gravitational potential  $\Phi$  was set to zero at the center of Earth for the case of the RH, and set to zero at infinity for free fall above the surface of the Earth. This is appropriate when considering free fall that occurs entirely above or below the surface, since the gravitational acceleration is proportional to the gradient of  $\Phi$ , so adding an arbitrary constant potential does not change the physical results. In other words, it is only the difference in potential between two points that leads to physical effects, not the values of the individual potentials themselves. However, these two expressions for the gravitational potential are incompatible when the free fall of a massive system crosses the threshold of the RH. Though this scenario will not be considered in detail here, a gravitational potential that is valid both inside and outside the RH will be derived.

Recall from (119) that the solution to Poisson's equation for a point mass in free fall within the RH is given by

$$\Phi_{\text{in}}(r) = \frac{2}{3}\pi\rho Gr^2 + \Phi_{0,\text{in}} = \frac{g_E}{2R_E}r^2 + \Phi_{0,\text{in}}. \quad (160)$$

The solution to Laplace's equation for a point mass in free fall outside the RH is given by

$$\Phi_{\text{out}}(r) = \frac{c_1}{r} + \Phi_{0,\text{out}}. \quad (161)$$

One can arbitrarily choose a point of zero potential, which will be at infinity here, so  $\Phi_{0,\text{out}} = 0$ .

Since the two expressions and their first derivatives must be equal at the opening of the RH,

$$\Phi_{\text{in}}(R_E) = \frac{1}{2}g_E R_E + \Phi_{0,\text{in}} = \frac{c_1}{R_E} = \Phi_{\text{out}}(R_E) \quad (162)$$

$$\left. \frac{d\Phi_{\text{in}}}{dr} \right|_{r=R_E} = g_E = -\frac{c_1}{R_E^2} = \left. \frac{d\Phi_{\text{out}}}{dr} \right|_{r=R_E}. \quad (163)$$



From (163), it is clear that  $c_1 = -g_E R_E^2$ , and thus the full expression for the gravitational potential outside the RH is given by

$$\Phi_{\text{out}}(r) = -\frac{g_E R_E^2}{r}. \quad (164)$$

Substituting  $c_1$  into (162) yields

$$\frac{1}{2}g_E R_E + \Phi_{0,\text{in}} = -g_E R_E, \quad (165)$$

and thus

$$\Phi_{0,\text{in}} = -\frac{3}{2}g_E R_E, \quad (166)$$

and the full expression for the gravitational potential inside the RH is given by

$$\Phi_{\text{in}}(r) = \frac{g_E}{2R_E} r^2 - \frac{3}{2}g_E R_E. \quad (167)$$

For the purposes of graphical depiction of the gravitational potential  $\Phi$  and the gravitational acceleration  $g = -\frac{d\Phi}{dr}$ , the dimensionless variables  $\mathfrak{R} = \frac{r}{R_E}$ ,  $\Omega = \frac{\Phi}{g_E R_E}$ , and  $G = \frac{g}{g_E}$  are introduced.

The dimensionless expressions for the gravitational potentials as are given by

$$\Omega_{\text{in}}(\mathfrak{R}) = \frac{1}{2}(\mathfrak{R}^2 - 3) \quad (168)$$

$$\Omega_{\text{out}}(\mathfrak{R}) = -\frac{1}{\mathfrak{R}}, \quad (169)$$

and the dimensionless gravitational accelerations are given by

$$G_{\text{in}}(\mathfrak{R}) = \mathfrak{R} \quad (170)$$

$$G_{\text{out}}(\mathfrak{R}) = \frac{1}{\mathfrak{R}^2}. \quad (171)$$

A plot of the dimensionless potentials and accelerations are shown in Figure 6.

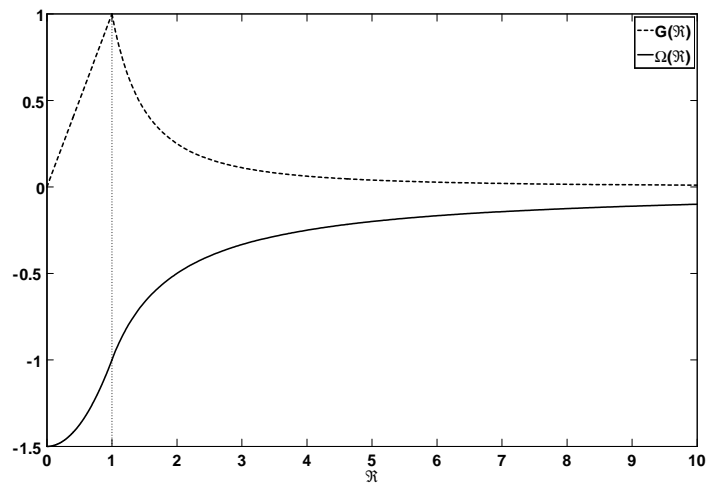


Figure 6: Plot of dimensionless gravitational acceleration and potential functions that are valid for regions both inside and outside the RH.

## 5.9 Conclusions

Though it was shown by way comparison of (150) and (153), and the fact that the DeWitt energy shift was shown to be zero in (146), that a circular Rydberg atom freely falling through the RH will behave similarly to a classical rigid ring with the same radius in the limit  $n \rightarrow \infty$ , it is noted that there exists a non-zero, negative-definite shift for all finite energy states that arises from the kinetic energy term in the full Hamiltonian (61). Recall that the large- $n$  limit is an approximation, and that a negative energy shift, given by (144), occurs for any finite value of  $n$ , even in the stretched state. This will cause the atom to become a high-field seeker, suggested by the analysis appearing in (85), and thus fall at a higher rate than that of a classical system, regardless of the mass distribution of the classical system. This is, again, a novel quantum-mechanical effect that cannot be explained classically, since it can be seen from the analysis presented in equations (7)–(11) that no classical object should fall faster than a point mass in the Earth’s gravitational field. Furthermore, since the energy shift is negative, the tidal gravitational field acts to force the electron wavefunction into a lower energy state, though as mentioned in Section 5.4, only in highly unusual circumstances will such a quantum transition take place in the Earth’s gravitational field. The analysis of the quantum transition was performed for the time-independent energy shift, but a similar conclusion is reached for the time-dependent energy shifts in the Earth’s gravitational field and short free fall times.

It was also shown that a positive-definite energy shift arises from the kinetic energy term of the full Hamiltonian operator when the atom is freely-falling outside the RH, i.e. above the Earth’s surface. It becomes clear that this energy shift is positive definite when one varies azimuthal angle  $\theta$  in (83). The fact that the shift is positive causes the atom in a circular Rydberg state to fall at a slower rate than a classical rigid ring with the same radius as the atom, and an even slower rate compared to that of a point mass. Note that for free fall above the Earth’s surface, the fact that the time-dependent energy shift is positive suggests that as the atom falls, the tidal gravitational field acts to force the electron wavefunction into a higher energy state, though again, such a transition is extremely unlikely in the gravitational field of the Earth. This result suggests

that the tidal gravitational field of the Earth acts to compress a classical ring such that its radius becomes smaller, whereas the same field acts to increase the atomic radius of a circular Rydberg atom. Though this result is somewhat counter-intuitive, it suggests that a hydrogen atom in the ground state will eventually be ionized, i.e. “torn apart,” as it falls into a black hole, as expected. Note that the time-independent energy shift from the potential energy term of the full Hamiltonian operator is zero for the ground state, or any state with angular momentum quantum number equal to zero, further suggesting that this energy shift is an incomplete analysis. This energy shift can be positive, negative, or zero, depending on the initial state of the hydrogen atom.

Energy shifts corresponding to various initial wavefunction states are presented in Table 1 below.

$n, l,  m_\ell $	$\Delta E_{P,\text{outside}}(\text{eV})$	$\Delta E_{P,\text{inside}}(\text{eV})$	$\frac{1}{r^2} \cdot \Delta E_{\mathbf{h}\cdot\mathbf{h},\text{outside}}(\frac{\text{eV}}{\text{s}^2})$	$\Delta E_{\mathbf{h}\cdot\mathbf{h},\text{inside}}(\text{eV})$
1, 0, 0	0	$3.7 \times 10^{-38}$	$1.1 \times 10^{-43}$	$-2.4 \times 10^{-38}$
2, 0, 0	0	$5.1 \times 10^{-37}$	$1.6 \times 10^{-42}$	$-4.6 \times 10^{-37}$
2, 1, 0	$-2.9 \times 10^{-37}$	$3.7 \times 10^{-37}$	$1.6 \times 10^{-42}$	$-3.2 \times 10^{-37}$
2, 1, 1	$1.5 \times 10^{-37}$	$3.7 \times 10^{-37}$	$9.0 \times 10^{-43}$	$-3.2 \times 10^{-37}$
10, 9, 9	$1.2 \times 10^{-34}$	$1.4 \times 10^{-34}$	$1.9 \times 10^{-40}$	$-1.9 \times 10^{-35}$
100, 99, 99	$1.2 \times 10^{-30}$	$1.2 \times 10^{-30}$	$1.9 \times 10^{-36}$	$-1.8 \times 10^{-32}$
1000, 999, 999	$1.2 \times 10^{-26}$	$1.2 \times 10^{-26}$	$1.9 \times 10^{-32}$	$-1.8 \times 10^{-29}$

Table 1: Energy shifts for various wavefunction states

## 6 Reflection of Gravitational Microwaves from Thin Superconducting Films

### 6.1 Abstract

Thin superconducting films are predicted to be highly reflective mirrors for gravitational waves at microwave frequencies. The quantum mechanical *delocalization* of the negatively charged Cooper pairs causes them to undergo *non-geodesic* motion in the presence of a gravitational wave, whereas the decoherence-induced *localization* of the positively charged ions in the lattice causes them to undergo *geodesic* motion in the presence of the same wave. The resulting charge separation leads to a virtual plasma excitation within the superconductor that enormously enhances its interaction with a gravitational wave, relative to that of a neutral superfluid and all normal matter. This enhancement, dubbed the “Heisenberg–Coulomb effect,” implies the specular reflection of a gravitational microwave even from a very thin superconducting film. The argument is presented using the BCS theory of superconductivity and a superconducting plasma model.

## 6.2 Introduction

One consequence of the relative motion between the lattice ions and the electron superfluid is that it predicts thin superconducting films to be highly reflective mirrors for gravitational waves at microwave frequencies. The quantum mechanical non-localizability of the negatively charged Cooper pairs, which is protected from the localizing effect of decoherence by an energy gap, causes the pairs to undergo non-picturable, non-geodesic motion in the presence of a gravitational wave. This non-geodesic motion, which is accelerated motion *through* space, leads to the existence of mass and charge supercurrents inside the superconducting film. On the other hand, the decoherence-induced localizability of the positively charged ions in the lattice causes them to undergo picturable, geodesic motion as they are carried along *with* space in the presence of the same gravitational wave. The resulting separation of charges leads to a virtual plasma excitation within the film that substantially enhances its interaction with the wave, relative to that of a neutral superfluid or any normal matter. The existence of strong mass supercurrents within a superconducting film in the presence of a gravitational wave, dubbed the “Heisenberg-Coulomb effect,” implies the specular reflection of a gravitational microwave from a film whose thickness is much less than the London penetration depth of the material, in close analogy with the electromagnetic case. The argument is developed by allowing classical gravitational fields, which obey Maxwell-like equations, to interact with quantum matter, which is described using the BCS and Ginzburg-Landau theories of superconductivity, as well as a collisionless plasma model. Several possible experimental tests of these ideas, including mesoscopic ones, are presented alongside comments on the broader theoretical implications of the central hypothesis.

Not enough effort has been made to investigate the ramifications of the gravitational Maxwell-like equations for the interaction of GR waves with matter, perhaps because the so-called “electromagnetic analogy” has been so hotly contested over the years [20]. In any case, these equations may provide a helpful framework for thinking about the response of non-relativistic matter to weak,

time-varying gravitational fields, especially that of macroscopically coherent quantum charge and mass carriers, namely, the Cooper pairs of conventional, type I superconductors. It is argued here that the electromagnetic analogy manifested in the Maxwell-like equations implies that type I superconductors can be surprisingly efficient mirrors for GR waves at microwave frequencies.

In Section 6.3, two basic claims are introduced upon which the larger argument rests. Together, these two claims open the door to an enormously enhanced interaction between a GR microwave and a type I superconductor, relative to what one would expect in the case of a neutral superfluid or, indeed, any normal metal or other classical matter. The first claim is that a GR microwave will generate quantum probability supercurrents, and thus mass and electrical supercurrents, inside a type I superconductor, due to the quantum mechanical non-localizability of the Cooper pairs within the material.

The non-localizability of Cooper pairs, which is ultimately due to the Uncertainty Principle (UP), causes them to undergo non-picturable, non-geodesic motion in the presence of a GR wave. This non-geodesic motion, which is accelerated motion through space, leads to the existence of mass and charge supercurrents inside a superconductor. By contrast, the localizability of the ions within the superconductor's lattice causes them to undergo picturable, geodesic motion, i.e., free fall, in the presence of the same wave. The resulting relative motion between the Cooper pairs and the ionic lattice causes the electrical polarization of the superconductor in the presence of a GR wave, since its Cooper pairs and ions carry not only mass but oppositely signed charge as well.

Furthermore, the non-localizability of the Cooper pairs is “protected” from the normal process of localization, i.e., from decoherence, by the characteristic energy gap of the Bardeen-Cooper-Schrieffer (BCS) theory of superconductivity. The decoherence of entangled quantum systems such as Cooper pairs (which are in the spin-singlet state) is the fundamental cause of the localizability of all normal matter [21]. Indeed, this “classicalizing” process must occur within any spatially extended system before the idea of the “universality of free fall” [22] can be meaningfully applied to its parts. After all, the classical principle behind the universality of free fall, the Equivalence Principle (EP), is a

strictly *local* principle [23].

The second of the two claims presented in Section 6.3 is that the mass supercurrents induced by a GR wave are much stronger than what one would expect in the case of a neutral superfluid or any normal matter, due to the electrical polarization of the superconductor caused by the wave. This is referred to as the “Heisenberg-Coulomb (H-C) effect.” The magnitude of the enhancement due to the H-C effect (derived in Section 6.8) is given by the ratio of the electrical force to the gravitational force between two electrons,

$$\frac{e^2}{4\pi\epsilon_0 G m_e^2} = 4.2 \times 10^{42}, \quad (172)$$

where  $e$  is the electron charge,  $m_e$  is the electron mass,  $\epsilon_0$  is the permittivity of free space, and  $G$  is Newton’s constant. The enormity of (172) implies the possibility of an enormous back-action of a superconductor upon an incident GR wave, leading to its reflection.

Of the four fundamental forces of nature, viz., the gravitational, the electromagnetic, the weak, and the strong forces, only gravity and electricity have long range, inverse square laws. The pure number obtained in (172) by taking the ratio of these two inverse-square laws is therefore just as fundamental as the fine structure constant. Because this number is so large, the gravitational force is typically ignored in treatments of the relevant quantum physics. But as shown below, a semi-classical treatment of the interaction of a superconductor with a GR wave must account for both the electrodynamics and the gravito-electrodynamics of the superconductor, since both play an important role in its overall response to a GR wave.

In Section 6.4, the interaction between an EM wave and a thin metallic film, having an arbitrary, frequency-dependent complex conductivity, is considered. The relevant boundary conditions are determined using Faraday’s and Ampere’s laws in order to derive general expressions for the transmissivity and reflectivity of a thin film. In Section 6.5, it is shown that, in the case of a superconducting film, the BCS theory implies that EM waves at microwave frequencies will be specularly reflected even from films whose thickness is less than the London penetration depth of the material, or, equivalently (at sufficiently low frequencies), less than the material’s plasma skin depth, as has



been experimentally observed [24, 25]. It is shown, furthermore, that the frequency at which reflectivity drops to 50%, what is referred to as the “roll-off frequency”  $\omega_r$ , depends only on the ratio of the speed of light  $c$  to a single parameter, the length scale  $l_k$  associated with the kinetic inductance  $L_k$  of the film’s Cooper pairs [26], which in turn depends on the plasma skin depth  $\delta_p$ . In the electromagnetic case, the microscopic size of  $\delta_p$  leads to a microscopic value for  $l_k$  and thus to the possibility of specular reflection over a wide range of frequencies (including microwave frequencies) in the EM case.

In Section 6.6, the Maxwell-like equations for linearized Einsteinian gravity are reviewed and highlight the fact that any normal matter, with its inherently high levels of dissipation, will necessarily be an inefficient reflector of GR waves because of its high impedance relative to the extremely low “gravitational characteristic impedance of free space”  $Z_G$  ( $2.8 \times 10^{-18}$  in SI units). Superconductors, on the other hand, are effectively dissipationless at temperatures near absolute zero because of their quantum mechanical nature [25]. The fact that a superconductor’s effectively zero impedance can be much smaller than the very small quantity  $Z_G$  allows it to reflect an incoming GR wave, much as a low-impedance connection or “short” at the end of a transmission line can reflect an incoming EM wave.

In Section 6.7, we appeal to the Maxwell-like equations introduced in Section 6.6, to the identity of the boundary conditions that follow from them, and to the linearity of weak GR-wave optics, in order to introduce GR analogs of the earlier EM expressions for the reflectivity and roll-off frequency. As in the EM case, the GR roll-off frequency  $\omega_{r,G}$  can be expressed as the ratio of the speed of light  $c$  to a single parameter. In this case, however, the relevant parameter is the length scale  $l_{k,G}$  associated with the gravitational kinetic inductance  $L_{k,G}$  of the Cooper pairs. In this section we treat the superconductor as if it were a neutral superfluid, i.e., as if its Cooper pairs were electrically neutral particles interacting with one another and the with ionic lattice exclusively through their mass. Although this assumption is unphysical, it leads to a result in agreement with conventional wisdom, namely, that the gravitational plasma skin depth  $\delta_{p,G}$  and the kinetic inductance length

scale  $l_{k,G}$  will be astronomical in size ( $\sim 10^{13}$  m and  $\sim 10^{36}$  m, respectively). Such enormous values imply that  $\omega_{r,G}$  will be effectively zero, and thus that superconductors cannot function as mirrors for GR microwaves in laboratory-scale experiments.

In Section 6.8, we show why the approach taken at the end of the previous section, in accord with conventional wisdom, may be wrong. It might be possible for superconductors to function as laboratory-scale mirrors for GR microwaves because of the H-C effect. When one takes into account the electrical charge separation induced within a superconductor by a GR wave (due to the BCS-gap-protected non-localizability of its Cooper pairs), the ratio given in (172) enters into the analysis in such a way as to keep  $l_{k,G}$  microscopic and to raise  $\omega_{r,G}$  to the level of  $\omega_r$ . Thus the H-C effect greatly enhances the reflection of a GR wave from the surface of a superconductor – by 42 orders of magnitude! – relative to what one would expect from a neutral superfluid, a normal metal, or any normal matter.

Because both charge supercurrents and mass supercurrents are generated by an incoming GR wave (and by an incoming EM wave), it is also necessary to consider whether superconducting films are not mirrors but rather transducers, i.e., converters, of GR radiation into EM radiation (in the case of an incident GR wave), or vice versa (in the case of an incident EM wave). In Section 6.9, we take up this particular question and show that transduction in both directions is too weak to decrease reflection by any appreciable amount. In section 6.10, however, we show that energy is conserved only when transduction is included in the overall analysis as an effective absorption mechanism.

Finally, in Section 6.11 we indicate several possible experimental tests of the basic claims advanced in the paper and offer brief comments on the broader theoretical implications of our central hypothesis. Whereas present GR-wave experiments aim to passively detect GR waves originating from astrophysical sources, our argument implies the possibility of several new types of laboratory-scale experiment involving GR waves. One type would test the physics behind the Heisenberg-Coulomb effect by looking for a departure from geodesic motion in the case of two coherently connected superconducting bodies that are allowed to fall freely through a distance large enough to

observe tidal effects. A second type would investigate the existence and strength of any gravitational Casimir-like effect between two type I superconductors. Yet a third type, involving an electrically charged pair of superconductors, would allow for more direct investigation of the existence and properties of GR-waves, the results of which would bear significantly on the search for a quantized theory of gravity.

Three appendices address ancillary issues: (6A) the relationship between the magnetic and kinetic inductances of a thin film, (6B) the kinetic inductance length scale according to a collisionless plasma model, and (6C) the relationship between the impedance argument given in Section 6.6 and Weinberg's argument regarding the scattering cross-section of a Weber-style resonant bar antenna, including an application of the Kramers-Kronig relations to the sum rule for the strength of the interaction between a GR wave and a superconductor.

### 6.3 The Uncertainty Principle Limits the Applicability of the Equivalence Principle

It is helpful to begin the analysis with a simple model of the interaction between a weak GR wave and a normal metallic film. For the sake of eventually considering the possibility of mirrors (i.e., the possibility of “ray” optics), we will assume here and throughout that the lateral dimensions of the film are very large when compared to the wavelength of the incident wave. Focusing on waves with very high frequencies, i.e., microwaves, will allow us to treat the ions and normal electrons of a laboratory-scale film as though they were freely floating, non-interacting “dust” or point particles undergoing free fall along classical trajectories, i.e., traveling along geodesics.

Although it would be possible in principle, in this approximation, to detect the passage of a GR wave over the film by observing the geodesic deviation among its different components (the principle underlying LIGO), the film cannot, in this approximation, interact energetically with a very high frequency GR wave. It cannot absorb or scatter any of the wave’s energy because each of its localized particles must, according to the EP, travel along a geodesic, i.e., each particle must remain at rest with respect to its local, co-moving, and freely-falling inertial frame [27]. And since there can be no energetic interaction with the wave, mass currents cannot be generated locally within the film without violating the conservation of energy.

It is true that a distant inertial observer will see the “dust” particles undergo quadrupolar motion, and will thus expect the film to emit GR radiation. But this apparent paradox can be resolved by noting that the wave causes the film’s ions and normal electrons (which are to be treated as test particles whose masses and gravitational fields are negligible) to be carried along with space rather than accelerated through space. Only the latter kind of motion, in which the wave does work on the particles, and hence transfers kinetic energy to them, leads to the time-varying mass quadrupole moment that enters into Einstein’s quadrupole formula for the emission of GR radiation (see Figure 7).

The classical concept of a “geodesic” depends fundamentally upon the localizability, or spatial

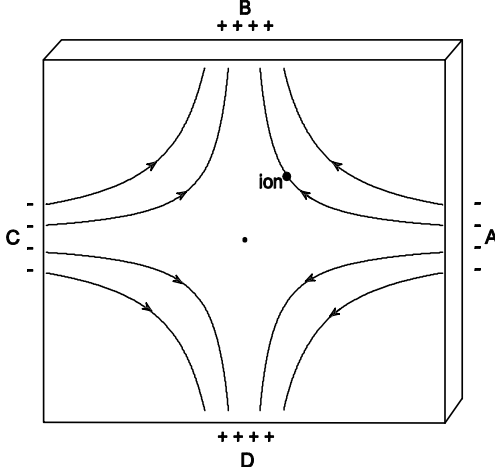


Figure 7: A snapshot of a square metallic plate with a very high frequency GR wave incident upon it at the moment when the gravitational tidal “forces” on the plate are those indicated by the hyperbolae, as seen by a distant observer. All ions, being approximately in free fall, are carried along *with* space rather than accelerated *through* space. No work is done on them, and thus no kinetic energy is transferred to them, by the wave. When the metal in the plate is normal, all ions and all normal electrons locally co-move together along the same geodesics in approximate free fall, so that the plate remains neutral and electrically unpolarized. However, when the plate becomes superconducting, the Cooper pairs, being in non-local *entangled* states, remain at rest with respect to the center of mass according to the distant observer, and do not undergo free fall along with the ions and any residual normal electrons. This non-picturable, non-geodesic, *accelerated* motion of the Cooper pairs *through* space leads to *picturable* quantum probability supercurrents, which follow the same hyperbolae as the incident tidal GR wave fields (see Eqs. (233)-(240)). Since the Cooper pairs carry not only mass but also charge, both mass and electrical supercurrents are generated, and both types of current carry energy extracted from the gravitational wave. In the snapshot shown, this leads to the accumulation of positive charge at B and D, and to the accumulation of negative charge at A and C, i.e., to a quadrupolar-patterned electrical polarization of the superconductor. The resulting enormous Coulomb forces strongly oppose the effect of the incoming tidal gravitational fields, resulting in the mirror-like reflection of the incoming GR wave.

separability, of particles. From a quantum mechanical point of view, localizability arises ultimately from the decoherence of entangled states, i.e., from the “collapse” of nonfactorizable superpositions of product wavefunctions of two or more particles located at two or more spatially well-separated points in space, into spatially separable, factorizable, product wavefunctions, upon the interaction of the particles with their environment. Decoherence typically occurs on extremely short time-scales due to the slightest interaction with the environment [21]. Whenever it does occur, one can speak classically of point particles having trajectories or traveling along geodesics. Only after decoherence has occurred does the Equivalence Principle become a well-defined principle, for only then does a

particle's geodesic become well defined. In other words, only through decoherence does the law of the "universality of free fall," i.e., the experimentally well-established claim that "the gravitational acceleration of a point body is independent of its composition" [22], become meaningful.

Entangled quantum states imply the nonlocalizability of particles, in the sense that such states lead to experimentally well-confirmed violations of Bell's inequalities [28, Chapters 6 and 19]. We claim here that Cooper pairs are completely non-localizable within a superconductor, not only in the sense of Heisenberg's Uncertainty Principle, but also because each electron in a given Cooper pair in the BCS ground state is in an entangled state, since each pair is in a superposition state of the product of two electron wavefunctions with opposite momenta, and also simultaneously in a superposition state of the product of two opposite electron spin-1/2 states (i.e., a spin-singlet state). The violation of Bell's inequalities by these entangled states in the BCS ground state means that this state is *non-local*, in the sense that instantaneous correlations-at-a-distance between the two electrons of a given Cooper pair must occur in the superconductor upon remote measurements within a long, single continuous piece of superconductor (the distance between these remote measurements can be arbitrarily large). Although these instantaneous correlations-at-a-distance cannot be used to send signals faster than light [28], they also cannot be accounted for in any local, realistic theory of quantum phenomena, including those which satisfy the completeness conditions demanded by Einstein, Podolsky, and Rosen (EPR) [29].

The localizability or spatial separability of all particles, as envisioned by EPR, would of necessity lead to the universal validity of the Equivalence Principle, and thus to the idea that even Cooper pairs must undergo geodesic motion (i.e., free-fall) within a superconductor in response to an incident GR wave. There could be no relative motion between the Cooper pairs and the ions, no spatial separation of charges inside the superconductor, and no enhancement, even in principle, of the superconductor's interaction with a GR wave relative to that of a normal metal interacting with the same wave. But Cooper pairs are manifestly not localizable within the superconductor, since they are fully quantum mechanical, non-local systems. For this reason the "dust-particles-following-geodesics"

model introduced earlier must fail in the case of a superconductor, even as a first approximation [30].

When a conventional, type I superconductor is in the BCS ground state, each of its Cooper pairs is in a zero-momentum eigenstate relative to the center of mass of the system. According to Heisenberg’s Uncertainty Principle (UP), the fact that the Cooper pairs’ momenta are perfectly definite entails that their positions within the superconductor are completely uncertain, i.e., that the pairs are non-localizable. The motion of a given Cooper pair within the superconductor is irreducibly quantum mechanical in nature, being related to the pair’s wavefunction. Such motion cannot be pictured in terms of a well-defined trajectory or geodesic [31]. Indeed, at a conceptual level, the ascription of a “trajectory” or “geodesic” to a given Cooper pair within a superconductor becomes meaningless in the BCS ground state. This is similar to what Bohr taught us concerning the meaninglessness of the concept of “orbit” in the ground state of the hydrogen atom during its interaction with radiation fields [32, pp. 113ff].

The robustness of the BCS ground state in the face of perturbations is guaranteed by the BCS energy gap, which “protects” the Cooper pairs from making quantum transitions into excited states, such as happens in pair-breaking (as long as the material is kept well below its transition temperature and the frequency of the incident radiation is below the BCS gap frequency [33]). The energy gap prevents the pairs from decohering, and from becoming localized like the superconductor’s ions and any residual, normal conduction electrons [34]. If the Cooper pairs cannot be thought of as localizable point bodies, then the “universality” of free fall cannot be meaningfully applied to them. In short, an application of the EP to the motion of Cooper pairs within a superconductor is fundamentally precluded by the UP. This is not to make the well-known point that quantum field theories may lead to measurable “quantum violations of the EP” due to possible “fifth-force” effects that produce slight corrections to particle geodesics (see, for example, Adelberger [22] and Ahluwalia [35]), but rather to observe that the non-localizability of quantum objects places a fundamental limit on the *applicability* of the EP (a point previously raised by Chiao [36, esp. Section V]).

In contrast to a superconductor’s non-localizable Cooper pairs, its ions (and, at finite temperatures, any residual background of normal electrons) are unaffected by the energy gap, and are thus fully localized by the decohering effect of their interactions with the environment. Thus, unlike Cooper pairs, the ionic lattice possesses no coherent quantum phase anywhere. The geodesic motion of the ions will therefore differ from the non-geodesic motion of the Cooper pairs. The latter, which is accelerated motion through space, implies the existence of quantum probability supercurrents, and thus of mass and electrical supercurrents, inside the superconductor (see Figure 7). These supercurrents will carry energy extracted from the GR wave. The possibility of a non-negligible energetic interaction between a GR wave and a superconductor depends crucially upon this initial claim, which is implied by the absence of the localizing effect of decoherence upon the Cooper pairs.

Before we turn to the second claim, it is worth noting that the non-geodesic motion of a superconductor’s Cooper pairs also follows from what London called the “rigidity of the wavefunction” [37]. The phase of the wavefunction of each Cooper pair must be constant in the BCS ground state prior to the arrival of a GR wave. This implies that the gradient of its phase is initially zero. Since an incoming GR wave whose frequency is less than the BCS gap frequency cannot alter this phase (in the lowest order of time-dependent perturbation theory), and since the canonical momentum of any given pair relative to the center of mass of the superconductor is proportional to the gradient of its phase, the canonical momentum of each pair must remain zero at all times with respect to the center of mass of the system in the presence of a GR wave, as seen by the distant inertial observer.

This quantum-type rigidity implies that Cooper pairs will acquire kinetic energy from a GR wave in the form of a nonzero kinetic velocity, i.e., that they will be accelerated by the wave relative to any local inertial frame whose origin does not coincide with the center of mass of the system (for example, at the corners of a large, square superconducting film; see Section 6.8). In other words, the apparent “motionlessness” of the Cooper pairs in the presence of a GR wave, as witnessed by a distant inertial observer, in fact entails their accelerated motion through local space. Again, this behavior implies the existence of mass supercurrents inside the superconductor that carry energy



extracted from the wave.

Of course, even normal matter such as in a Weber-style resonant bar detector has some extremely small degree of rigidity arising from its very weak interatomic coupling. Thus normal matter does not, strictly speaking, behave as a collection of freely falling, noninteracting “dust particles” in the presence of a very low frequency GR wave. Instead, like the Cooper pairs, but to a much smaller degree, and at much lower frequencies than the microwave frequencies being considered here, normal matter opposes the squeezing and stretching of space going on around it (as Feynman pointed out in his well-known remarks on why GR waves must carry energy [38]). Thus, even normal matter will acquire an extremely small amount of kinetic energy as it is accelerated through space by a passing GR wave. In this case, though, high levels of dissipation inside the material will cause whatever small amount of energy is extracted from the GR wave to be overwhelmingly converted into heat instead of being predominantly re-radiated as a scattered GR wave (as Weinberg has pointed out [39]). A key feature of the mass supercurrents carried by Cooper pairs is that they are dissipationless. We shall return to this particular point in Section 6.6.

The second basic claim underlying the paper’s larger argument follows from the dual nature of the supercurrents generated by a GR wave within a superconductor. Since a GR wave will generate both mass and charge supercurrents, it will electrically polarize the superconductor. This important observation implicates the Coulomb force of attraction between the oppositely signed charges that must accumulate at the edges of the superconductor, if there is to be no violation of charge conservation (see Figure 7). These oppositely signed charges will consist of negatively charged Cooper pairs, on the one hand, and corresponding, positively charged Cooper-pair holes (hereafter, “holes”), on the other. An incoming GR wave with a frequency well below the superconductor’s plasma frequency will thus generate a virtual plasma excitation inside the superconductor. The resulting Coulomb force between the Cooper pairs and holes, which acts as a Hooke’s law restoring force, strongly opposes the effect of the incident wave. The enormous back-action of this force on the motion of the Cooper pairs greatly enhances their mass conductivity (see Section 6.8), to the point

where specular reflection of an incident GR wave from a superconducting film becomes possible. The existence of strengthened mass supercurrents within a superconductor, which is due to the combined effect of the quantum non-localizability of the Cooper pairs and the Coulomb attraction between the pairs and holes, is what we refer to as the “Heisenberg-Coulomb effect.”

Consider, by way of contrast, what happens when a GR wave impinges on a superfluid, whose constituent particles are electrically neutral. Mass supercurrents will again be induced by the wave, due to quantum non-localizability, but in this case there will be no enhancement effect because the mass carriers within a superfluid are its electrically neutral atoms. Thus no appreciable fraction of incident GR-wave power can be reflected from the surface of a neutral superfluid. On the other hand, one might worry that the size of the H-C effect in a superconductor would drive its mass supercurrents above the critical level, thereby undermining the possibility of specular reflection. But it should always be possible to arbitrarily reduce the amplitude of the driving radiation field until the superconductor responds linearly to the field (see the related discussion of superluminality at the end of Section 6.8). The existence of a linear-response regime guarantees the possibility of fabricating linear GR-wave optical elements, including mirrors.

## 6.4 The Interaction of an EM Wave with a Thin Metallic Film

The question of the interaction of an EM wave with a metallic film whose thickness  $d$  is small compared to the wavelength can be addressed using “lumped-circuit” concepts such as resistance, reactance, inductance, etc., of an infinitesimal square element of the film. (As before, we assume, for the sake of considering mirror-like behavior, that the lateral dimensions of the film are at least on par with the wavelength of the incident wave.) In this section we derive a formula for the transmissivity  $\mathcal{T}$  as well as the reflectivity  $\mathcal{R}$  of a thin metallic film with an arbitrary, frequency-dependent complex conductivity. In the next section we apply this analysis to the case of a superconducting film.

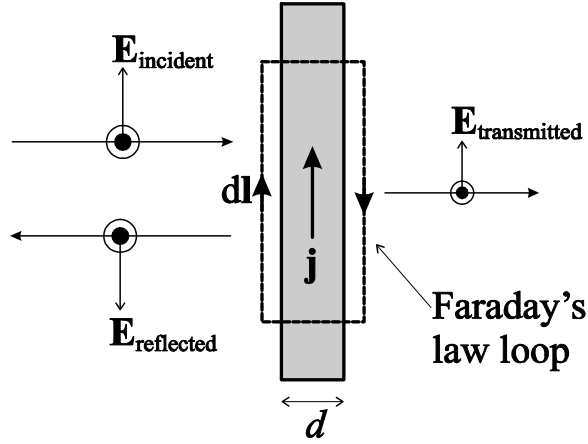


Figure 8: A thin metallic film of thickness  $d$  is straddled by a rectangular loop (dashed lines) for applying Faraday’s law to it. An incident EM wave is partially transmitted and partially reflected by the film. The EM wave generates an electrical current density  $\mathbf{j}$ , which flows uniformly inside the film. A similar rectangular loop (not shown) lying in a plane parallel to the magnetic fields (denoted by the circles with central dots) is for applying Ampere’s law.

The complex amplitude reflection coefficient  $r$  corresponding to the proportion of incident EM radiation at frequency  $\omega$  reflected from a thin film and the complex amplitude transmission coefficient  $t$  corresponding to the proportion of the same radiation transmitted through the film can be defined as follows:

$$\mathbf{E}_{\text{reflected}} = r\mathbf{E}_{\text{incident}} \quad (173a)$$

$$\mathbf{E}_{\text{transmitted}} = t\mathbf{E}_{\text{incident}} . \quad (173b)$$

By convention,  $r$ , if it is real, is defined to be *positive* when the reflected electric field  $\mathbf{E}_{\text{reflected}}$  is *oppositely* directed to the incident electric field  $\mathbf{E}_{\text{incident}}$ . On the other hand,  $t$ , if it is real, is defined to be *positive* when the transmitted electric field  $\mathbf{E}_{\text{transmitted}}$  points in the *same* direction as the incident electric field  $\mathbf{E}_{\text{incident}}$ . In general,  $r$  and  $t$  are complex quantities whose values depend on the frequency  $\omega$  of the incident wave, but all radiation fields will be treated classically.

Since the tangential components of the electric fields must be continuous across the vacuum-film interface, the electric field inside the film  $\mathbf{E}_{\text{inside}}$  drives a current density  $\mathbf{j}$  inside the film that is linearly related to this driving electric field, for the general case of a linear-response theory of the interaction of matter with weak driving fields. This linear relationship is given by

$$\mathbf{j}(\omega) = \boldsymbol{\sigma}(\omega)\mathbf{E}_{\text{inside}}(\omega), \text{ where} \quad (174)$$

$$\mathbf{E}_{\text{inside}} = (1 - r)\mathbf{E}_{\text{incident}} \text{ at frequency } \omega. \quad (175)$$

In general, the conductivity  $\boldsymbol{\sigma}(\omega)$  associated with the current generated within the film at a given driving frequency  $\omega$  will be a complex quantity:

$$\sigma(\omega) = \sigma_1(\omega) + i\sigma_2(\omega), \quad (176)$$

where  $\sigma_1(\omega)$  represents the current's in-phase, dissipative response at frequency  $\omega$  to the driving field at frequency  $\omega$ , and  $\sigma_2(\omega)$  represents the current's out-of-phase, non-dissipative response at the same frequency [40].

If the thickness of the film  $d$  is much less than a wavelength of the incident radiation, then the right-hand side of Faraday's law applied to the loop shown in Figure 8 encloses a negligible amount of magnetic flux  $\Phi_B$ , so that

$$\oint \mathbf{E} \cdot d\mathbf{l} = -\frac{d\Phi_B}{dt} \rightarrow 0. \quad (177)$$

Using the sign conventions introduced above, one finds that

$$1 - r - t = 0 . \tag{178}$$

Now let us apply Ampere’s law [41]

$$\oint \mathbf{H} \cdot d\mathbf{l} = I \tag{179}$$

to the “Amperian” loop (not shown in Figure 8) whose plane is parallel to the magnetic fields of the incident, reflected, and transmitted EM waves, and perpendicular to the Faraday’s law loop shown in Figure 8. Let this Amperian loop span the entire width  $w$  of the film in the direction of the magnetic field. For a plane EM wave propagating in free space,

$$|\mathbf{H}| = \frac{|\mathbf{B}|}{\mu_0} = \frac{|\mathbf{E}|}{Z_0} , \tag{180}$$

where  $Z_0$  is the characteristic impedance of free space and  $\mu_0$  is the magnetic permeability of free space. It then follows that

$$w(1 + r - t) \frac{E_{\text{incident}}}{Z_0} = I , \tag{181}$$

where

$$I = Aj = \sigma wd(1 - r)E_{\text{incident}} \tag{182}$$

is the total enclosed current being driven inside the film by the applied electric field inside the film (175), which leads to

$$\frac{1}{Z_0} (1 + r - t) = \sigma d(1 - r) . \tag{183}$$

From (178) and (183) we have two equations in the two unknowns  $r$  and  $t$ , which can be rewritten

as

$$1 - r - t = 0 , \text{ and} \quad (184a)$$

$$1 + r - t = x(1 - r) , \quad (184b)$$

where  $x \equiv \sigma Z_0 d$ . Solving for  $1/t$  and  $1/r$ , one obtains

$$\frac{1}{t} = 1 + \frac{1}{2}x, \text{ and} \quad (185a)$$

$$\frac{1}{r} = 1 + 2\frac{1}{x}. \quad (185b)$$

Using the definition  $\mathcal{T} = tt^* = |t|^2$ , one then obtains for the reciprocal of the transmissivity

$$\begin{aligned} \frac{1}{\mathcal{T}} &= \frac{1}{tt^*} = \left(1 + \frac{1}{2}x\right) \left(1 + \frac{1}{2}x^*\right) \\ &= 1 + \frac{1}{2}(x + x^*) + \frac{1}{4}xx^* \\ &= 1 + \operatorname{Re} x + \frac{1}{4}\left\{(\operatorname{Re} x)^2 + (\operatorname{Im} x)^2\right\} \\ &= \left(1 + \frac{1}{2}\operatorname{Re} x\right)^2 + \frac{1}{4}(\operatorname{Im} x)^2 . \end{aligned} \quad (186)$$

Substituting  $x = \sigma Z_0 d = (\sigma_1 + i\sigma_2)Z_0 d$  into this expression, one finds that

$$\mathcal{T} = \left\{ \left(1 + \frac{1}{2}\sigma_1 Z_0 d\right)^2 + \left(\frac{1}{2}\sigma_2 Z_0 d\right)^2 \right\}^{-1} . \quad (187)$$

This general result, which applies to any thin metallic film with a complex conductivity, agrees with Tinkham's expression for  $\mathcal{T}$  [25, Eq. (3.128)] in the case of a superconducting film when the index of refraction of the film's substrate in his expression is set equal to unity (i.e., when the film is surrounded on both sides by free space).

Similarly, using the definition  $\mathcal{R} = rr^* = |r|^2$ , one obtains for the reciprocal of the reflectivity

$$\begin{aligned}
\frac{1}{\mathcal{R}} &= \frac{1}{rr^*} = (1 + 2y)(1 + 2y^*) & (188) \\
&= 1 + 2(y + y^*) + 4yy^* \\
&= 1 + 4 \operatorname{Re} y + 4 \left\{ (\operatorname{Re} y)^2 + (\operatorname{Im} y)^2 \right\} \\
&= (1 + 2 \operatorname{Re} y)^2 + 4 (\operatorname{Im} y)^2 ,
\end{aligned}$$

where

$$y \equiv \frac{1}{x} = \frac{1}{\sigma Z_0 d} = \frac{\rho}{Z_0 d} \quad (189)$$

and  $\rho$  is the complex resistivity of the film (again at frequency  $\omega$ ). In general,  $\rho$  and  $\sigma$  are related by

$$\rho \equiv \frac{1}{\sigma} = \frac{1}{\sigma_1 + i\sigma_2} = \frac{\sigma_1 - i\sigma_2}{\sigma_1^2 + \sigma_2^2} = \rho_1 + i\rho_2 , \quad (190)$$

where

$$\rho_1 = \frac{\sigma_1}{\sigma_1^2 + \sigma_2^2} \quad (191a)$$

$$\rho_2 = -\frac{\sigma_2}{\sigma_1^2 + \sigma_2^2} . \quad (191b)$$

The reflectivity of any thin metallic film with complex conductivity is therefore

$$\begin{aligned}
\mathcal{R} &= \left\{ \left( 1 + 2 \frac{\sigma_1}{\sigma_1^2 + \sigma_2^2} \frac{1}{Z_0 d} \right)^2 \right. \\
&\quad \left. + \left( 2 \frac{\sigma_2}{\sigma_1^2 + \sigma_2^2} \frac{1}{Z_0 d} \right)^2 \right\}^{-1} . & (192)
\end{aligned}$$

Although the precise degree of reflection for a film of given thickness  $d$  will depend on the specific character of the film's conductivity, the presence of the sum inside the first squared term of (192) indicates that the dissipative component of the conductivity  $\sigma_1$  will inhibit reflection more strongly

than the non-dissipative component  $\sigma_2$ . With this clear hint of the importance of dissipationlessness for achieving specular reflection, we turn our attention to superconducting films.



## 6.5 A Criterion for the Specular Reflection of EM Waves from Superconducting Films

The BCS theory of superconductivity has been confirmed by many experiments. Here we review the application of this well-established theory to the problem of mirror-like reflection of EM waves from a superconducting film. We consider once again a film whose thickness  $d$  is small enough to make the use of “lumped-circuit” concepts legitimate, but which is now also much smaller than the coherence length  $\xi_0$  and the London penetration depth  $\lambda_L$  of the material (i.e., the so-called “local” or “dirty” limit).

As Tinkham has noted [25, p. 39], the dissipative part of the conductivity of such a film  $\sigma_{1s}$  goes exponentially to zero as  $T \rightarrow 0$  in response to a driving wave whose frequency is less than

$$\omega_{\text{gap}} = \frac{2\Delta(0)}{\hbar} \cong \frac{3.5k_B T_c}{\hbar}, \quad (193)$$

where  $\Delta(0)$  (henceforward abbreviated as  $\Delta$ ) is the gap energy per electron of the BCS theory at  $T = 0$ ,  $k_B$  is Boltzmann’s constant, and  $T_c$  is critical temperature for the superconducting transition. The exponential suppression of the film’s dissipative response is due to the “freezing out” of its normal electrons through the Boltzmann factor  $\exp(-\Delta/k_B T)$  as  $T \rightarrow 0$ .

On the other hand, the film’s non-dissipative conductivity  $\sigma_{2s}$  rises asymptotically to some finite value in the same limit [25, Eq. (3.125)]. The behavior of  $\sigma_{2s}$ , which can be calculated using the BCS theory, is due to the film’s inductive reactance  $X_L$ , which in turn arises from its inductance (per square element of the film)  $L$ . These three parameters are related to one another by

$$\frac{1}{\sigma_{2s}d} = X_L = \omega L. \quad (194)$$

For a superconducting film at temperatures sufficiently near  $T = 0$  (e.g., in the milli-Kelvin range for a Pb film) and for frequencies lower than  $\omega_{\text{gap}}$ , the ohmic dissipation of the film will be exponentially suppressed by the Boltzmann factor, so that one can, to a good approximation, set  $\sigma_{1s} = 0$  and

rewrite (192) as [42]:

$$\mathcal{R}_s = \left\{ 1 + \left( 2 \frac{X_L}{Z_0} \right)^2 \right\}^{-1}. \quad (195)$$

The two previous expressions allow us to define an “upper roll-off frequency”  $\omega_r$  for the reflection of EM waves from a superconducting film, i.e., the frequency at which reflectivity drops to 50% (when the film is kept at nearly  $T = 0$  and when  $\omega < \omega_{\text{gap}}$ ):

$$\omega_r = \pm \frac{Z_0}{2L}, \quad (196)$$

where we discard the negative solution as being unphysical. The film’s lower roll-off frequency is simply determined by its lateral dimensions, which for mirror-like behavior to occur must be, as noted before, much larger than the wavelength  $\lambda = (2\pi c) / \omega$  of the incident EM wave. Because the upper roll-off frequency is our primary concern, we refer to it throughout as *the* roll-off frequency. Unlike the lower roll-off frequency, it depends on the intrinsic properties of the material and cannot be adjusted at will by altering the lateral dimensions of the film.

The physical meaning of the expression for  $\omega_r$  given in (196) is that a superconducting film whose dissipative conductivity has been exponentially frozen out can “short out” and thus specularly reflect an incoming EM wave whose frequency is below  $\omega_{\text{gap}}$ , as long as the film’s inductance is sufficiently small to allow non-dissipative supercurrents to flow at frequencies less than  $\omega_{\text{gap}}$ . As happens with an RF choke, a large inductance will prevent supercurrents from being established inside the film. Thus, the roll-off frequency and reflectivity will be lowered to levels on par with those of a normal metal.

From (196) it is clear that the possibility of specular reflection of EM waves by a superconducting film at low temperatures and frequencies depends crucially on the film’s inductance  $L$ . The inductance will have two components: a magnetic inductance  $L_m$  due to the magnetic fields created by the charge supercurrents carried by the Cooper pairs, and a kinetic inductance  $L_k$  due to the inertial mass of the same Cooper pairs, which causes them to oppose the accelerating force of the

external electric field [25, pp. 88, 99][26]. As it happens,  $L_m$  is numerically negligible compared to  $L_k$  for a thin film (see Appendix 6A), so that we can proceed under the assumption that  $L \cong L_k$ .

When  $T \ll T_c$  and  $\omega \ll \omega_{\text{gap}}$ , the BCS theory yields the following relation between the imaginary part of a superconducting film's complex conductivity  $\sigma_{2s}$  and its normal conductivity  $\sigma_n$  [25, Eq. (3.125a)]:

$$\sigma_{2s} = \frac{\pi\Delta}{\hbar\omega} \sigma_n . \quad (197)$$

From the Drude model of metallic conductivity, it follows [43] that a film of thickness  $d$  will have a normal conductivity  $\sigma_n$  given by

$$\sigma_n = \frac{n_e e^2 d}{m_e v_F} , \quad (198)$$

where  $e$  is the charge of the electron,  $m_e$  is its mass,  $v_F$  is its Fermi velocity, and  $n_e$  is the number density of conduction electrons. Then  $\sigma_{2s}$  becomes

$$\sigma_{2s} = \frac{\pi\Delta}{\hbar\omega} \cdot \frac{n_e e^2 d}{m_e v_F} , \quad (199)$$

from which it follows that the kinetic inductance can be expressed as

$$L_k = \frac{1}{\omega \sigma_{2s} d} = \frac{1}{d^2} \cdot \frac{\hbar v_F}{\pi\Delta} \cdot \frac{m_e}{n_e e^2} . \quad (200)$$

The  $1/d^2$  term in (200) indicates a dependence on the film's thickness, whereas the presence of  $\hbar v_F / \pi\Delta$  implies an additional dependence on the coherence length  $\xi_0$ , since according to the BCS theory

$$\xi_0 = \frac{\hbar v_F}{\pi\Delta} . \quad (201)$$

The  $m_e/n_e e^2$  term could be interpreted as the London penetration depth  $\lambda_L$ , since

$$\mu_0 \lambda_L^2 = \frac{m_e}{n_e e^2} . \quad (202)$$

However, in the present context it is more appropriate to relate this term to the plasma frequency  $\omega_p$  by

$$\mu_0 \frac{c^2}{\omega_p^2} = \frac{m_e}{n_e e^2} , \quad (203)$$

since the Cooper pairs within a superconductor can be regarded as a type of quantum mechanical, collisionless plasma [44]. We are, after all, concerned not with the screening of DC magnetic fields through the Meissner effect, but with the reflection of EM radiation – with an electrodynamic effect rather than a magnetostatic one. In the limit of  $\omega \ll \omega_p$ , the plasma skin depth  $\delta_p$  (the depth to which an EM wave with a frequency  $\omega$  can penetrate into a plasma) is simply

$$\delta_p = \frac{c}{\omega_p} , \quad (204)$$

so that in this limit

$$\mu_0 \delta_p^2 = \frac{m_e}{n_e e^2} . \quad (205)$$

Comparing (205) with (202), we see that the electrodynamic concept of the plasma skin depth and the magnetostatic limit given by the London penetration depth coincide not just in the stronger limit of  $\omega \rightarrow 0$  but also in the weaker limit of  $\omega \ll \omega_p$ .

In light of these considerations, we can re-express the kinetic inductance  $L_k$  (200) in terms of the permeability of free space  $\mu_0$ , the coherence length  $\xi_0$ , the plasma skin depth  $\delta_p$ , and the thickness of the film  $d$ :

$$L_k = \mu_0 \xi_0 \left( \frac{\delta_p}{d} \right)^2 . \quad (206)$$

It is then possible to express  $L_k$  in more familiar form, i.e., as the product of the magnetic permeability of free space and the kinetic inductance length scale  $l_k$ :

$$L_k = \mu_0 l_k , \quad (207)$$

where  $l_k$  is

$$l_k = \xi_0 \left( \frac{\delta_p}{d} \right)^2 . \quad (208)$$

(For a comparison of this BCS-based derivation of  $l_k$  with one based on plasma concepts, see Appendix 6B.)

We can now rewrite the film's inductive reactance  $X_L$  in terms of the frequency of the incident EM wave  $\omega$ , the permeability of free space  $\mu_0$ , and the kinetic inductance length scale  $l_k$ :

$$X_L = \omega L_k = \omega \mu_0 l_k . \quad (209)$$

Returning to the crucial ratio of the inductive reactance to the characteristic impedance of free space given earlier in (196), we see that the roll-off frequency becomes

$$\omega_r = \frac{Z_0}{2L_k} = \frac{\mu_0 c}{2\mu_0 l_k} = \frac{c}{2l_k} . \quad (210)$$

Notice that  $\mu_0$  cancels out of the numerator and denominator of this expression, so that the specular reflection of an EM wave with frequency  $\omega$  from a superconducting film at temperatures sufficiently near  $T = 0$  depends only on the ratio of the speed of light  $c$  to the kinetic inductance length scale  $l_k$ .

To make this claim concrete, let us consider here (and in subsequent examples) the case of a thin lead (Pb) film with a thickness of  $d = 2$  nm and an angular frequency for the incident radiation of  $\omega = 2\pi \times (6 \text{ GHz})$ . The known values for the coherence length and the London penetration depth of Pb are  $\xi_0 = 83$  nm and  $\delta_p = \lambda_L = 37$  nm, respectively [45, p. 24]. Inserting these values into (208), we see that  $l_k \approx 30 \mu\text{m}$  and, from (210), that  $\omega_r \approx 2\pi \times (800 \text{ GHz})$ . When we recall that the theoretically calculated gap frequency for superconducting Pb at  $T = 0$  is approximately  $2\pi \times (500 \text{ GHz})$ , we see that our estimate of  $\omega_r$  is roughly equivalent to the claim that  $\omega < \omega_{\text{gap}}$  for specular reflection to occur, which is consistent with previously stated assumptions (and with the requirement that  $\omega \ll \omega_p$ , since  $\omega_p \approx 2\pi \times (1.3 \text{ PHz})$  for Pb).

The analysis presented in this section is in basic agreement with the experiments of Glover and Tinkham [24], and it belies the commonly held misconception that specular reflection can occur only when the thickness of the material  $d$  is greater than its skin depth  $\delta_p$  (or penetration depth  $\lambda_L$ ). Reflection from a superconducting film is due not to the gradual diminishment of the radiation field as it enters the film but to the destructive interference between the incident radiation and the radiation emitted in the forward scattering direction by the sheet supercurrents set up within the film. In fact, a closer examination of (208) and (210) reveals that appreciable reflection of a 6 GHz EM wave can occur from a Pb film – a type I superconductor – even when the film’s thickness is as much as 2 orders of magnitude smaller than its characteristic penetration depth. A type II superconductor, on the other hand, will generate considerable losses, due to the ohmic or dissipative flux-flow motion of Abrikosov vortices at microwave frequencies, and will therefore exhibit much poorer reflectivities in the microwave region.

What does the foregoing analysis imply about the ability of a superconducting film to reflect a GR microwave? In order to answer this question we must determine the magnitude of the kinetic inductance length scale in the GR case. First, however, we will take a moment to motivate the idea of the “characteristic gravitational impedance of free space” and to consider why objects made of normal matter are such poor reflectors of GR waves.

## 6.6 The Gravitational Characteristic Impedance of Free Space

Wald [46, Section 4.4] has introduced an approximation scheme that leads to a useful Maxwell-like representation of the Einstein equations of general relativity. The resulting equations describe the coupling of weak GR fields to slowly moving matter. In the asymptotically flat spacetime coordinate system of a distant inertial observer, the four equations in SI units are

$$\nabla \cdot \mathbf{E}_G = -\frac{\rho_G}{\varepsilon_G} \quad (211a)$$

$$\nabla \times \mathbf{E}_G = -\frac{\partial \mathbf{B}_G}{\partial t} \quad (211b)$$

$$\nabla \cdot \mathbf{B}_G = 0 \quad (211c)$$

$$\nabla \times \mathbf{B}_G = \mu_G \left( -\mathbf{j}_G + \varepsilon_G \frac{\partial \mathbf{E}_G}{\partial t} \right) \quad (211d)$$

where the gravitational analog of the electric permittivity of free space is given by

$$\varepsilon_G = \frac{1}{4\pi G} = 1.2 \times 10^9 \text{ SI units} \quad (212)$$

and the gravitational analog of the magnetic permeability of free space is given by

$$\mu_G = \frac{4\pi G}{c^2} = 9.3 \times 10^{-27} \text{ SI units.} \quad (213)$$

The value of  $\varepsilon_G$  is fixed by demanding that Newton's law of gravitation be recovered from the Gauss-like law (211a), whereas the value of  $\mu_G$  is fixed by the linearization procedure from Einstein's field equations. These two constants express the strengths of the coupling between sources (i.e., of masses and mass currents, respectively) and gravitational fields, and are analogous to the two constants  $\varepsilon_0$  (the permittivity of free space) and  $\mu_0$  (the permeability of free space), which express the strengths of coupling between sources (charges and charge currents, respectively) and electromagnetic fields in Maxwell's theory.

In the above set of equations, the field  $\mathbf{E}_G$  is the gravito-electric field, which is to be identified

with the local acceleration  $\mathbf{g}$  of a test particle produced by the mass density  $\rho_G$ , in the Newtonian limit of general relativity. The field  $\mathbf{B}_G$  is the gravito-magnetic field produced by the mass current density  $\mathbf{j}_G$  and by the gravitational analog of the Maxwell displacement current density  $\varepsilon_G \partial \mathbf{E}_G / \partial t$  of the Ampere-like law (211d). The resulting magnetic-like field  $\mathbf{B}_G$  can be regarded as a generalization of the Lense-Thirring field of general relativity. Because these equations are linear, all fields will obey the superposition principle not only outside the source (i.e., in the vacuum), but also within the matter inside the source, provided the field strengths are sufficiently weak and the matter is sufficiently slowly moving. Note that the fields  $\mathbf{E}_G$  and  $\mathbf{B}_G$  in the above Maxwell-like equations will be treated as classical fields, just like the fields  $\mathbf{E}$  and  $\mathbf{B}$  in the classical Maxwell's equations.

As noted earlier, Cooper pairs cannot freely fall along with the ionic lattice in response to an incident GR wave because the UP forbids such pairs from having classical trajectories, i.e., from traveling along geodesics. An incident field  $\mathbf{E}_G$  will therefore cause the Cooper pairs to undergo non-geodesic motion, in contrast to the geodesic motion of the ions inside the lattice. This entails the existence of mass currents (as well as charge currents) from the perspective of a local, freely falling observer who is located near the surface of the superconducting film anywhere other than at its center of mass. These mass currents will be describable by a gravitational version of Ohm's law

$$\mathbf{j}_G(\omega) = \boldsymbol{\sigma}_{s,G}(\omega) \mathbf{E}_{G\text{-inside}}(\omega) , \quad (214)$$

where  $\mathbf{j}_G(\omega)$  is the mass-current density at frequency  $\omega$ ,  $\boldsymbol{\sigma}_{s,G}(\omega) = \sigma_{1s,G}(\omega) + i\sigma_{2s,G}(\omega)$  is the complex mass-current conductivity of the film at the frequency  $\omega$  in its linear response to the fields of the incident GR wave, and  $\mathbf{E}_{G\text{-inside}}(\omega)$  is the driving gravito-electric field inside the film at frequency  $\omega$ . The existence of these mass currents can also be inferred from DeWitt's minimal coupling rule for superconductors ([15]; see Section 6.8 below). The real part of the mass conductivity,  $\sigma_{1s,G}(\omega)$ , describes the superconductor's dissipative response to the incident gravito-electric field, while the imaginary part,  $\sigma_{2s,G}(\omega)$ , describes its non-dissipative response to the same field. The basic assumption behind (214) is that the mass-current density in any superconductor responds *linearly*



to a weak GR wave at the driving frequency [47]. One should view  $\sigma_{s,G}$  as a phenomenological quantity, which, like the electrical conductivity  $\sigma_s$ , must be experimentally determined. In any case, the resulting optics for weak GR waves will be *linear*, just like the linear optics for weak EM waves.

An important physical property follows from the above Maxwell-like equations, namely, the characteristic gravitational impedance of free space  $Z_G$  [36, 48, 49]:

$$Z_G = \sqrt{\frac{\mu_G}{\varepsilon_G}} = \frac{4\pi G}{c} = 2.8 \times 10^{-18} \text{ SI units.} \quad (215)$$

This quantity is a characteristic of the vacuum, i.e., it is a property of spacetime itself, and it is independent of any of the properties of matter *per se*. As with  $Z_0 = \sqrt{\mu_0/\varepsilon_0} = 377$  ohms in the EM case,  $Z_G = \sqrt{\mu_G/\varepsilon_G} = 2.8 \times 10^{-18}$  SI units will play a central role in all GR radiation coupling problems. In practice, the impedance of a material object must be much smaller than this extremely small quantity before any significant portion of the incident GR-wave power can be reflected. In other words, conditions must be highly unfavorable for dissipation into heat. Because all classical material objects have extremely high levels of dissipation compared to  $Z_G$ , even at very low temperatures, they are inevitably very poor reflectors of GR waves [39, 49]. The question of GR-wave reflection from macroscopically coherent quantum systems such as superconductors requires a separate analysis due to the effectively zero resistance associated with superconductors, i.e., the dissipationlessness exhibited by matter in this unique state, at temperatures near absolute zero.

## 6.7 A Criterion for the Specular Reflection of GR Waves from Superconducting Films

In the case of EM waves considered above in Section 6.5, the BCS framework led us to two related expressions for the behavior of a superconducting thin film, one for its EM reflectivity (195) and one for its EM roll-off frequency (196). Now, on the basis of the similarity of the Maxwell and the Maxwell-like equations, the identity of the boundary conditions that follow from these equations, and the linearity of weak GR-wave optics that follows from the gravitational version of Ohm's law for superconductors (214), we are led to the following two expressions for the reflectivity and the roll-off frequency in the GR sector, which are analogous to (195) and (196), respectively:

$$\mathcal{R}_G = \left\{ 1 + \left( 2 \frac{X_{L,G}}{Z_G} \right)^2 \right\}^{-1} \quad (216a)$$

$$\omega_{r,G} = \pm \frac{Z_G}{2L_G} . \quad (216b)$$

Once again, we exclude the negative solution in the expression for the upper roll-off frequency given in (216b) as being unphysical.

Pausing for a moment to consider the *lower* roll-off frequency, it is found that a new constraint appears. The H-C effect, which is ultimately responsible for the mirror-like behavior of the film in the GR case, can only be presumed to operate when

$$\omega \geq \frac{2\pi v_s}{a} , \quad (217)$$

where  $\omega$  is the frequency of the incident wave,  $v_s$  is the speed of sound in the medium, and  $a$  is the transverse size of a square film. The physical significance of this constraint becomes apparent when we rewrite it as

$$a \geq \frac{2\pi v_s}{\omega} . \quad (218)$$

This form of the inequality follows from the fact that neighboring ions separated by a distance less than  $(2\pi v_s)/\omega$  will be mechanically coupled to one another, since there will be sufficient time for a mechanical signal to propagate from one to the other. Only ions separated by distances greater than  $(2\pi v_s)/\omega$  can be legitimately regarded as separately undergoing free fall in the presence of a GR wave. Ultimately, however, this additional constraint is preempted by the inequality already introduced in Section 6.3,

$$a \geq \frac{2\pi c}{\omega} , \quad (219)$$

where  $(2\pi c)/\omega$  is the wavelength of the incident wave, since this more stringent requirement must be met for the film to function as a mirror at all.

Returning to the expression for the *upper* roll-off frequency given in (216b), is it conceivable that this expression could yield a non-negligible  $\omega_{r,G}$  in the case of a superconducting film? We begin by noting that the gravitational impedance of free space  $Z_G$  can be expressed as

$$Z_G = \mu_G c . \quad (220)$$

In light of (216b) and the smallness of  $\mu_G$ , as indicated earlier in (213), it would seem highly unlikely that a superconductor's GR inductance would be small enough to produce a non-negligible roll-off frequency. Any attempt to construct laboratory-scale mirrors for GR waves would appear to be doomed from the start. However, as with  $L$  for a thin film in the electromagnetic case,  $L_G$  must be expressible as the product of the permeability and a length scale. In the GR case, we must use the analogous gravitational version of each parameter. We will neglect the contribution of the gravito-magnetic inductance  $L_{m,G}$  to the overall gravitational inductance  $L_G$  on the grounds that it will be much smaller than the gravito-kinetic inductance  $L_{k,G}$  (again, see Appendix 6A), so that

$$L_G \approx L_{k,G} = \mu_G l_{k,G} . \quad (221)$$

Inserting (220) and (221) into (216b), we see that the permeability cancels out of the numerator

and denominator as before, so that  $\omega_{r,G}$  depends only on the ratio of the speed of light  $c$  to a single parameter – in this case, the gravitational kinetic inductance length scale  $l_{k,G}$ :

$$\omega_{r,G} = \frac{\mu_G c}{2\mu_G l_{k,G}} = \frac{c}{2l_{k,G}} . \quad (222)$$

In the electromagnetic case,  $l_k$  was given by

$$l_k = \xi_0 \left( \frac{\delta_p}{d} \right)^2 , \quad (223)$$

where the plasma skin depth  $\delta_p$  was given by

$$\delta_p = \sqrt{\frac{m_e}{\mu_0 n_e e^2}} . \quad (224)$$

In the present context, the coherence length  $\xi_0$  and the thickness of the film  $d$  must remain the same, since they are internal properties of the film having nothing to do with the strength of coupling to external radiation fields. By contrast, the plasma skin depth would appear to depend on the strength of coupling to external radiation fields through the presence of  $\mu_0$  and  $e^2$  in the denominator of (224). We therefore need to consider the magnitude of this parameter in the gravitational sector.

For the moment, let us assume that the coupling of Cooper pairs to a GR wave depends solely on their gravitational mass  $2m_e$ , i.e., that their electrical charge  $2e$  is irrelevant to the gravitational plasma skin depth and thus to the gravitational kinetic inductance length scale of a superconducting film. Ultimately, we will reject this approach, since the Coulomb interaction between the superconductor's Cooper pairs and the corresponding holes created in the virtual plasma excitation induced within the film is crucial for understanding how the film responds to a GR wave. Nonetheless, it is instructive to ignore all considerations of charge and to presume, for the moment, that Cooper pairs react to a GR wave solely on the basis of their mass. In fact, the criterion presented at the end of this section may well be valid for neutral superfluids (e.g., superfluid helium or a neutral atomic

Bose-Einstein condensate), but we show in the following section that it must be modified in the case of superconductors to account for the H-C effect.

To obtain the “gravitational” version of the plasma skin depth  $\delta_{p,G}$ , let us make the following substitution

$$\frac{e^2}{4\pi\epsilon_0} \rightarrow Gm_e^2 \quad (225)$$

in the expression for the plasma skin depth  $\delta_p$  (224). Note that for this substitution to be valid, we must treat the electrons as if they were electrically neutral. The “gravitational” kinetic inductance length scale then becomes

$$l_{k,G} = \xi_0 \left( \frac{\delta_{p,G}}{d} \right)^2, \quad (226)$$

where, in this spurious approach,  $\delta_{p,G}$  is given by

$$\delta_{p,G} = \sqrt{\frac{1}{\mu_G n_e m_e}}. \quad (227)$$

Assuming here and in subsequent calculations an estimate of  $n = n_e/2 \approx 10^{30} \text{ m}^{-3}$  for the number density of Cooper pairs, one finds that  $\delta_{p,G}$  is on the order of  $10^{13} \text{ m}$ , which leads to a value for  $l_{k,G}$  on the order of  $10^{36} \text{ m}$ . Inserting this enormous value for  $l_{k,G}$  into (222) yields a roll-off frequency  $\omega_{r,G}$  of effectively zero, which of course undermines any practical possibility of GR-wave reflection.

On the grounds that one must eliminate dissipation into heat for the GR-wave scattering cross-section to become comparable to a square wavelength, Weinberg has suggested in his discussion of Weber-style resonant bar detectors that superfluids might function effectively as mirrors for GR waves [39]. The analysis presented here, however, suggests that neutral superfluids cannot substantially reflect GR waves because of the electrical neutrality of their mass carriers. (See Appendix 6C for a brief account of the relation between the “impedance” argument of the previous section and Weinberg’s analysis of the dissipation problem.) As we shall see, the fact that a superconductor’s mass carriers are not electrically neutral utterly changes the dynamics of the interaction.

## 6.8 The Specular Reflection of GR Waves

In Section 6.3, we argued that the Uncertainty Principle delocalizes a superconductor's Cooper pairs within the material, so that they must exhibit non-geodesic motion rather than the decoherence-induced geodesic motion exhibited by all localized particles, such as freely floating "dust particles" or the ions in the lattice of a superconductor. The non-localizability of the Cooper pairs within a superconducting film leads to charge supercurrents inside the film, which, by charge conservation and the accumulation of charge at its edges, must produce a Coulomb electric field inside the film in a virtual plasma excitation of the material. As a result, enormous Coulomb forces will be created between the film's negatively charged Cooper pairs and its corresponding, positively charged holes.

In the GR case, one might think to replace the Coulomb force with the much weaker Newtonian gravitational force – as we did in the previous section – but this amounts to treating the Cooper pairs and holes as if they were electrically neutral, which is patently unphysical. There can be no H-C effect in the case of a neutral superfluid, but the situation is entirely different for a superconductor. This effect, which can appear inside a superconductor, causes a superconducting film to respond extremely "stiffly" to an incident GR wave and leads to hard-wall boundary conditions for the wave. To put the point differently, the stiffness of a superconducting film in its response to an incoming GR wave is governed by the strength of the Coulomb interaction between the Cooper pairs and the corresponding holes, and not by their much weaker gravitational interaction. This fact is reflected in the appearance of the electromagnetic plasma frequency in the formulas derived below.

Let us begin our analysis of the magnitude of the H-C effect by examining the quantum probability current density  $\mathbf{j}$ . This quantity is more basic than the charge current density  $\mathbf{j}_e = nq\mathbf{v}$  or the mass current density  $\mathbf{j}_G = nm\mathbf{v}$ , since one can derive  $\mathbf{j}$  directly from quantum mechanics. It should be regarded as the cause of the charge and mass currents, whereas  $\mathbf{j}_e$  and  $\mathbf{j}_G$  should be regarded as the effects of  $\mathbf{j}$ .

Recall that in non-relativistic quantum mechanics  $\mathbf{j}$  is given by

$$\mathbf{j} = \frac{\hbar}{2mi}(\psi^*\nabla\psi - \psi\nabla\psi^*) , \quad (228)$$

where  $m$  is the mass of the non-relativistic particle whose current is being calculated (here  $m = 2m_e$ ) and  $\psi$  is the wavefunction of the system (here the Cooper pair’s “condensate wavefunction”, or London’s “macroscopic wavefunction”, or Ginzburg and Landau’s “complex order parameter”). This quantum mechanical quantity satisfies the continuity equation

$$\nabla \cdot \mathbf{j} + \frac{\partial \rho}{\partial t} = 0 , \quad (229)$$

where  $\rho = \psi^*\psi$  is the quantum probability density of the Cooper pairs. The meaning of (229) is that probability is conserved.

Now let us adopt DeWitt’s minimal coupling rule [15] and make the following substitution for the momentum operator:

$$\mathbf{p} \rightarrow \mathbf{p} - q\mathbf{A} - m\mathbf{h} \text{ or} \quad (230a)$$

$$\frac{\hbar}{i}\nabla \rightarrow \frac{\hbar}{i}\nabla - q\mathbf{A} - m\mathbf{h} , \quad (230b)$$

where  $q = 2e$ ,  $m = 2m_e$ ,  $\mathbf{A}$  is the electromagnetic vector potential, and  $\mathbf{h}$  is DeWitt’s gravitational vector potential [50] (here and henceforth the dependence on space and time  $(\mathbf{r}, t)$  of all field quantities will be suppressed as understood). In what follows, both  $\mathbf{A}$  and  $\mathbf{h}$  fields will be treated as classical fields, whereas  $\mathbf{j}$  and  $\rho$  will be treated as time-dependent quantum operators, in a semi-classical treatment of the interaction of radiation with matter.

We shall also follow DeWitt in adopting the radiation gauge conditions for both  $\mathbf{A}$  and  $\mathbf{h}$ , namely, that

$$\nabla \cdot \mathbf{A} = 0 \text{ and } \nabla \cdot \mathbf{h} = 0 , \quad (231)$$

and that the scalar potentials for both the EM and GR fields vanish identically everywhere. This choice of gauge means that the coordinate system being employed is that of an inertial observer located at infinity.

Since it is the case that

$$\frac{\hbar}{2mi}(\psi^*\nabla\psi - \psi\nabla\psi^*) = \frac{1}{m} \operatorname{Re} \left( \psi^* \frac{\hbar}{i} \nabla \psi \right) , \quad (232)$$

we can apply DeWitt's minimal coupling rule to (232) to obtain

$$\mathbf{j} = \frac{1}{m} \operatorname{Re} \left( \psi^* \left\{ \frac{\hbar}{i} \nabla - q\mathbf{A} - m\mathbf{h} \right\} \psi \right) . \quad (233)$$

The continuity equation (229) is still satisfied by (233), provided that one also applies the same minimal coupling rule to the time-dependent Schrödinger equation, in which the Hamiltonian becomes

$$H = \frac{(\mathbf{p} - q\mathbf{A} - m\mathbf{h})^2}{2m} + V , \quad (234)$$

where the first term on the right-hand side represents the kinetic energy operator, and  $V$  is the potential energy operator.

In the special case of electrically-neutral, classical “dust particles” in the presence of a GR wave,  $q = 0$  and thus  $q\mathbf{A} = 0$  (as well as  $V = 0$ ). The classical Hamilton's function  $H(\mathbf{p}, \mathbf{q})$  then becomes

$$H(\mathbf{p}, \mathbf{q}) = \frac{(\mathbf{p} - m\mathbf{h})^2}{2m} . \quad (235)$$

Defining the canonical momentum classically as  $\mathbf{p} = m\mathbf{v}_{\text{can}}$ , where  $\mathbf{v}_{\text{can}}$  is the canonical velocity, it will be the case for neutral, classical dust particles that

$$H = \frac{1}{2}m(\mathbf{v}_{\text{can}} - \mathbf{h})^2 = 0 \quad \text{or} \quad \mathbf{v}_{\text{can}} = \mathbf{h} , \quad (236)$$



as seen by a distant inertial observer, since a passing GR wave cannot impart any kinetic energy to noninteracting, freely-falling particles. The dust particles will be carried along *with* space, which follows directly from the EP.

On the other hand, when (235) is viewed as a quantum Hamiltonian operator, it implies that neutral, quantum-mechanical particles will acquire a kinetic energy equal to  $\frac{1}{2}m\mathbf{h}^2$  when they are in a nonlocalizable, gap-protected, zero-momentum eigenstate ( $\mathbf{p} = \mathbf{0}$ , where  $\mathbf{p}$  is the canonical momentum). In accord with first-order time-dependent perturbation theory, such particles must remain in their ground state in the presence of a GR wave whose frequency is less than the BCS gap frequency. They will therefore rigidly resist the stretching and squeezing of space caused by such a wave. In other words, they will be locally accelerated through space, acquiring kinetic energy in the process. In the case of superfluid helium, for example, in which the basic components of the material are both electrically neutral and quantum-mechanically protected from excitations by the roton gap, mass supercurrents will be created that carry kinetic energy extracted from the wave.

Now let us consider the case of a type I superconductor. Before the arrival of a GR wave, the superconductor's Cooper pairs will be in a zero-momentum eigenstate:

$$\psi = C \exp(i \frac{\mathbf{p}_0 \cdot \mathbf{r}}{\hbar}) \text{ where } \mathbf{p}_0 = \mathbf{0} . \quad (237)$$

Again, in accord with first-order time-dependent perturbation theory, this initial wavefunction must remain unchanged to lowest order by the radiative perturbations arising from either  $\mathbf{A}$  or  $\mathbf{h}$  after the arrival of a wave whose frequency is less than the BCS gap frequency of the material. If one evaluates (233) using the unperturbed state (237), one finds that

$$\begin{aligned} \mathbf{j} &= \frac{1}{m} \text{Re} \left( \psi^* \left\{ \frac{\hbar}{i} \nabla - q\mathbf{A} - m\mathbf{h} \right\} \psi \right) \\ &= \frac{1}{m} (-q\mathbf{A} - m\mathbf{h}) \psi^* \psi . \end{aligned} \quad (238)$$

From this one can define the “quantum velocity field”  $\mathbf{v}$ ,

$$\mathbf{v} = \frac{\mathbf{j}}{\rho} = \frac{\mathbf{j}}{\psi^* \psi}, \quad (239)$$

whose local expectation value is the local group velocity of a Cooper pair [51]. It thus follows that

$$\mathbf{v} = -\frac{q}{m} \mathbf{A} - \mathbf{h} \quad (240)$$

inside a superconducting film after the arrival of a GR wave. This velocity is the kinetic velocity of the quantum supercurrent, and not the canonical velocity of a classical dust particle given in (236), in the sense that  $\frac{1}{2}m\mathbf{v}^2$  is the local kinetic energy of the quantum supercurrent.

The generation of mass supercurrents inside a superconductor by the GR wave will also produce charge supercurrents inside the superconductor, since  $q$  is not zero for Cooper pairs. These supercurrents will electrically polarize the superconductor, which will set up an internal  $\mathbf{A}$  field – even in the absence of any incident EM wave. Thus, the term  $(-q/m)\mathbf{A}$  on the right-hand side of (240) will not be zero inside a superconductor in the presence of a GR wave. Herein lies the possibility of mirror-like reflection of GR waves from superconducting thin films.

Taking the partial derivative of (240) with respect to time, and defining the meaning of this derivative in the sense of Heisenberg’s equation of motion for the kinetic velocity operator  $\mathbf{v}$ , one obtains an operator equation of motion that has the same form as Newton’s 2nd law of motion, namely,

$$m \frac{\partial}{\partial t} \mathbf{v} = m \frac{\partial^2}{\partial t^2} \mathbf{x} = m \mathbf{a} = q \mathbf{E} + m \mathbf{E}_G, \quad (241)$$

where, by our gauge choice,  $\mathbf{E}$  and  $\mathbf{E}_G$  inside the superconductor are related to the vector potentials  $\mathbf{A}$  and  $\mathbf{h}$ , respectively, by

$$\mathbf{E} = -\frac{\partial}{\partial t} \mathbf{A} \text{ and } \mathbf{E}_G = -\frac{\partial}{\partial t} \mathbf{h}. \quad (242)$$

Both  $\mathbf{E}$  and  $\mathbf{E}_G$  will be treated here as classical fields. Following the presentation in Section 6.6,

$\mathbf{E}_G$  is the gravito-electric field that appears in the Maxwell-like equations, which is equivalent to the acceleration  $\mathbf{g}$  of a local, classical test particle due to gravity, in accord with the EP. The physical interpretation of the Newton-like equation of motion (241) is that the internal  $\mathbf{E}$  and  $\mathbf{E}_G$  fields act upon the charge  $q$  and the mass  $m$ , respectively, of the Cooper pairs, to produce an acceleration field  $\mathbf{a}$  of these pairs (in the sense of Ehrenfest's theorem) inside a superconducting film.

For all fields that vary sinusoidally with the same exponential phase factor  $\exp(-i\omega t)$ , (241) leads to the following linear-response equation at the frequency  $\omega$ :

$$\mathbf{x} = -\frac{1}{\omega^2} \left( \frac{q}{m} \mathbf{E} + \mathbf{E}_G \right) . \quad (243)$$

The mass current density source term in the Ampere-like law (211d) of the Maxwell-like equations is then given by

$$\begin{aligned} \mathbf{j}_G &= nm\mathbf{v} = nm \frac{\partial}{\partial t} \mathbf{x} \\ &= nm(-i\omega)\mathbf{x} \\ &= i \frac{n}{\omega} (q\mathbf{E} + m\mathbf{E}_G) . \end{aligned} \quad (244)$$

The total force acting on a given Cooper pair under such circumstances is thus [52]

$$\mathbf{F}_{\text{tot}} = q\mathbf{E} + m\mathbf{E}_G , \quad (245)$$

which is to say that  $\mathbf{F}_{\text{tot}}$  depends on a linear combination of the internal  $\mathbf{E}$  and  $\mathbf{E}_G$  fields, or, equivalently, that a superconductor will respond linearly to a sufficiently weak incident GR wave.

When a superconductor is operating in its linear response regime in the presence of a weak incident GR wave, the following direct proportionalities will hold:

$$\mathbf{F}_{\text{tot}} \propto \mathbf{E} \propto \mathbf{E}_G . \quad (246)$$

Let us therefore define a proportionality constant  $\Xi$ , such that

$$\mathbf{F}_{\text{tot}} = \Xi q \mathbf{E} . \quad (247)$$

We shall call this dimensionless proportionality constant the “fractional correction factor” of the total force acting upon a given Cooper pair, relative to a purely electrical force acting on the same pair.

At this point, it would be customary to ignore the extremely weak gravitational forces generated internally within the superconducting film. That is to say, one would normally set the gravitational field  $\mathbf{E}_G$  inside the film identically equal to zero everywhere by declaring that  $\Xi = 1$ , exactly. One could then solve the essentially electromagnetic problem of virtual plasma excitations produced inside the film in its linear response to a weak incident EM or GR wave.

But this simplification will not suffice in the present context, since we want to understand the dynamics of the system when one takes into account the combined effect of the internal electric field  $\mathbf{E}$  and internal gravito-electric field  $\mathbf{E}_G$ , both of which will be produced in association with the electrical polarization of the superconductor induced by an incident EM or GR wave. Although the impact on the electrodynamics of the system will be negligible, the impact on its gravito-electrodynamics will be enormous. Let us then use (245) and (247) to express the relationship between the  $\mathbf{E}$  and  $\mathbf{E}_G$  fields inside a superconducting film when  $\Xi \neq 1$ , i.e., when the gravitational forces within the film, however tiny, are explicitly taken into account:

$$\mathbf{E} = \frac{1}{\Xi - 1} \frac{m}{q} \mathbf{E}_G . \quad (248)$$

Substituting this expression into (244), we obtain [53]

$$\mathbf{j}_G = i \frac{\Xi}{\Xi - 1} \frac{nm}{\omega} \mathbf{E}_G , \quad (249)$$

from which it follows that the mass conductivity of the film  $\sigma_G$  is given by

$$\sigma_G = i \left( \frac{\Xi}{\Xi - 1} \right) \frac{nm}{\omega} \propto \frac{1}{\omega} , \quad (250)$$

implying an inductive response to internal fields on the part of the mass currents  $\mathbf{j}_G$  within the film. Note that  $\sigma_G$  can in principle become extremely large when  $\Xi \rightarrow 1$ , and therefore that  $\mathbf{j}_G$  can become extremely large.

Let us consider first the effect of the gravitational force between the Cooper pairs and holes on the plasma frequency. We start from (241) in the form

$$m \frac{\partial^2}{\partial t^2} \mathbf{x} = -m\omega^2 \mathbf{x} = q\mathbf{E} + m\mathbf{E}_G = \Xi q\mathbf{E} , \quad (251)$$

so that

$$\mathbf{x} = -\Xi \frac{q}{m\omega^2} \mathbf{E} . \quad (252)$$

The electric polarization of the superconductor will then be

$$\mathbf{P} = nq\mathbf{x} = -\Xi \frac{nq^2}{m\omega^2} \mathbf{E} = \chi'_p \varepsilon_0 \mathbf{E} , \quad (253)$$

where  $\chi'_p$  is the modified plasma susceptibility. Since this susceptibility can be expressed as

$$\chi'_p = -\frac{\omega_p'^2}{\omega^2} , \quad (254)$$

it follows that the square of the modified plasma frequency is given by

$$\omega_p'^2 = \Xi \frac{nq^2}{m\varepsilon_0} . \quad (255)$$

We thus expect that the fractional correction factor  $\Xi$ , which takes into account the gravitational forces between the Cooper pairs and holes, will lead to an extremely small correction to the standard

formula for the plasma frequency.

To determine the magnitude of  $\Xi$ , we begin with the quantum form of Newton's second law (241), rewritten as

$$\frac{\partial}{\partial t} \mathbf{v} = \frac{q}{m} \mathbf{E} + \mathbf{E}_G . \quad (256)$$

Multiplying both sides by  $nq$ , one obtains a current-density form of the same equation:

$$\frac{\partial(nq\mathbf{v})}{\partial t} = \frac{\partial}{\partial t} \mathbf{j}_e = \frac{nq^2 \mathbf{E}}{m} + nq \mathbf{E}_G . \quad (257)$$

Let us evaluate all quantities in this equation at a point  $P$  along the edge of the superconducting film where the ionic lattice abruptly ends and the vacuum begins:

$$\left. \frac{\partial}{\partial t} \mathbf{j}_e \right|_P = \left. \frac{nq^2 \mathbf{E}}{m} \right|_P + nq \mathbf{E}_G|_P . \quad (258)$$

We will assume that the incident radiation fields that excite the Cooper-pair plasma are tightly focused onto a diffraction-limited Gaussian-beam spot size located at the center of the square film. We will also assume that the radiative excitation is impulsive in nature, so that the plasma can oscillate freely after the radiation is abruptly turned off. Thus the point  $P$  at the edge of the film at which all quantities in (258) are to be evaluated, is far away from the center of the film, where the incident radiation fields can impulsively excite the film into free plasma oscillations.

Taking the divergence of both sides of (258), we obtain at point  $P$

$$\left. \frac{\partial}{\partial t} (\nabla \cdot \mathbf{j}_e) \right|_P = \left. \frac{nq^2}{m} (\nabla \cdot \mathbf{E}) \right|_P + nq (\nabla \cdot \mathbf{E}_G)|_P . \quad (259)$$

But with the help of the continuity equation

$$\nabla \cdot \mathbf{j}_e + \frac{\partial}{\partial t} \rho_e = 0 \quad (260)$$

and the 1st Maxwell and 1st Maxwell-like equations

$$\nabla \cdot \mathbf{E} = \frac{\rho_e}{\varepsilon_0} \text{ and } \nabla \cdot \mathbf{E}_G = -\frac{\rho_G}{\varepsilon_G} , \quad (261)$$

we can rewrite (259) as a differential equation for the charge and mass densities at point  $P$  [54]:

$$-\frac{\partial^2}{\partial t^2} \rho_e = \frac{nq^2}{m\varepsilon_0} \rho_e - \frac{nq}{\varepsilon_G} \rho_G . \quad (262)$$

These densities will oscillate freely in time at point  $P$  at the edge of the film, where both charge and mass can accumulate, after the impulsive excitation at the center of the film has been turned off. We then use the fact that the accumulated Cooper-pair mass density at point  $P$  must be related to the accumulated Cooper-pair charge density at point  $P$  by

$$\rho_G = \frac{m}{q} \rho_e , \quad (263)$$

since each Cooper pair accumulating at the edge of the film carries with it both a charge  $q$  and a mass  $m$ . Then at point  $P$  (262) becomes

$$-\frac{\partial^2}{\partial t^2} \rho_e = \frac{nq^2}{m\varepsilon_0} \rho_e - \frac{nm}{\varepsilon_G} \rho_e , \quad (264)$$

which leads to the simple harmonic equation of motion

$$\frac{\partial^2}{\partial t^2} \rho_e + \frac{nq^2}{m\varepsilon_0} \rho_e - \frac{nm}{\varepsilon_G} \rho_e = \frac{\partial^2}{\partial t^2} \rho_e + \omega_p'^2 \rho_e = 0 , \quad (265)$$

where the square of the modified plasma frequency  $\omega_p'$  is given by

$$\omega_p'^2 = \left( 1 - \frac{m^2 Z_G}{q^2 Z_0} \right) \frac{nq^2}{m\varepsilon_0} . \quad (266)$$

Here we have made use of the fact that  $Z_0 = (c\varepsilon_0)^{-1}$  and that  $Z_G = (c\varepsilon_G)^{-1} = 4\pi G/c$ . Comparing (266) with (255), we arrive at the following expression for  $\Xi$ :

$$\begin{aligned}\Xi &= 1 - \frac{m^2 Z_G}{q^2 Z_0} \\ &= 1 - \frac{4\pi\varepsilon_0 G m_e^2}{e^2} \\ &\approx 1 - \frac{1}{4.2 \times 10^{42}}.\end{aligned}\tag{267}$$

The fractional correction factor  $\Xi$  does indeed differ from unity by an extremely small amount, equal to the reciprocal of the ratio of the electrostatic force to the gravitational force between two electrons given by (172).

The implication of (267) for the electrodynamics of a superconductor is that the size of the modified plasma frequency given by (255) will be smaller than the standard value, albeit by a mere 4 parts in  $10^{42}$ . Although this difference is extremely small, the fact that the modified plasma frequency is smaller rather than larger points to a surprising fact: the Cooper-pair holes created inside a superconducting film by an incident EM or GR microwave must be gravitationally repelled by, rather than attracted to, the corresponding Cooper pairs in the film, i.e., the holes must have the equivalent of negative mass and must therefore behave analogously to buoyant bubbles inside a fluid in the Earth's gravity. This would be a troubling result, were it not for the fact that the holes, like bubbles, cannot exist independently in the vacuum. The existence of negative-mass pseudo-particles (i.e., holes) within the film does not imply the possibility of shielding static, longitudinal gravito-electric fields, which requires the existence of real particles with negative mass in the vacuum. That is to say, the existence of these pseudo-particles does not imply the possibility of anti-gravity devices [47].

The real significance of  $\Xi$  lies in its impact on the gravito-electrodynamics of a superconducting film. In particular, the result given in (267) leads to an enhancement of the film's mass conductivity  $\sigma_G$  by the enormous factor of  $4.2 \times 10^{42}$ , which is what we have been calling the Heisenberg-Coulomb



effect. Specifically, the expression for the mass conductivity given in (250) can now be reduced to

$$\sigma_G = -i \frac{nq^2 \Xi Z_0}{m\omega Z_G} , \quad (268)$$

or, equivalently [55],

$$\sigma_{1,G} = 0 \quad \text{and} \quad \sigma_{2,G} = -\frac{nq^2 \Xi Z_0}{m\omega Z_G} . \quad (269)$$

Let us use this result to calculate the GR reflectivity of a superconducting film.

Recall the relationship given earlier in (194) between the inductance of the film and its nondissipative conductivity. Let us assume, once again, that the gravito-magnetic inductance is negligible when compared to the gravitational kinetic inductance (which is justified in Appendix 6A). We can then equate the gravitational inductance of the film  $L_G$  with  $L_{k,G}$  and use (224), (227), (269) to express the latter as

$$\begin{aligned} L_{k,G} &= \frac{1}{\omega \sigma_{2,G} d} = -\frac{m}{nq^2 \Xi} \frac{1}{d} \frac{Z_G}{Z_0} \\ &\approx -\mu_G d \left( \frac{\delta_{p,G}}{d} \right)^2 \frac{m^2 Z_G}{q^2 Z_0} \\ &= -\mu_G d \left( \frac{\delta_p}{d} \right)^2 \\ &= -\mu_G l'_{k,G} , \end{aligned} \quad (270)$$

where the corrected gravitational kinetic inductance length scale  $l'_{k,G}$  is given by

$$l'_{k,G} = d \left( \frac{\delta_p}{d} \right)^2 . \quad (271)$$

But this is just the EM kinetic inductance length scale  $l_{k,p}$  that appears in the collisionless plasma model presented in Appendix 6B. Notice that this expression differs from the BCS expression given in (208) in Section 6.5 by a factor on the order of unity, i.e.,  $d/\xi_0$ , which is due to the fact that the plasma model knows nothing of the BCS coherence length scale. Nonetheless, the appearance of  $\delta_p$

in (271) highlights the importance of plasma concepts for correcting the approach adopted at the end of Section 6.7. The H-C effect reduces the GR kinetic inductance length scale  $l_{k,G}$  by 42 orders of magnitude, to the level of the EM kinetic inductance length scale  $l_{k,p}$  ( $\approx l_k$ ), thereby increasing the magnitude of the GR roll-off frequency  $\omega_{r,G}$  by the same factor, to the level of the EM roll-off frequency  $\omega_r$ .

Two possible criticisms of this analysis immediately come to mind. First, the group velocity of a Cooper pair given by (240) is predicted to be superluminal, even for extremely small values of the dimensionless strain  $h_+$  of an incident GR wave [50]. Using (242), (244), and (249) to solve for  $|\mathbf{v}/c|$ , one finds that

$$\left| \frac{\mathbf{v}}{c} \right| = \frac{1}{c} \frac{\Xi}{\Xi - 1} |\mathbf{h}| = \frac{1}{2} \frac{\Xi}{\Xi - 1} |h_+| . \quad (272)$$

Even for an arbitrarily chosen, extremely small value of  $|h_+| \approx 10^{-40}$  (which, for a 6 GHz GR wave, corresponds to an incident power flux on the order of  $10^{-16} \text{ W m}^{-2}$ ), the value given in (267) leads to a velocity roughly one hundred times the speed of light. This apparent violation of special relativity suggests that the response of a superconductor to a GR-wave field will in general be nonlinear, invalidating our assumption of linearity in (246).

However, group velocities much larger than  $c$  (infinite, even) have been experimentally demonstrated [56]. In particular, photon tunneling-time measurements confirm the “Wigner” transfer time, which is a measure of an effective group velocity broadly applicable to quantum scattering processes. Wigner’s analysis [57] assumes a linear relation between the initial and final states of a quantum system, and yields a transfer time that is proportional to the derivative of the phase of the system’s transfer function with respect to the energy of the incident particle. In the present context, this implies that the Wigner time will be zero, since the phase of the Cooper-pair condensate remains constant everywhere, and stays unchanged with time and energy, due to first-order time-dependent perturbation theory (i.e., assuming that no pair-breaking or any other quantum excitation is allowed [33]). Returning to Figure 7, the Wigner time implies that an observer located at the center of mass of the superconductor who spots a Cooper pair at point B during the passage of the wave will see

the pair disappear and then instantaneously re-appear at point A. This kind of simultaneity (as seen by the observer at the center of mass of the system) is a remarkable consequence of quantum theory, but it does not violate special relativity, nor does it invalidate the assumption of linearity.

We have already touched on the second criticism, namely, that the analysis presented here is defective because it does not register the BCS gap frequency. In particular, ohmic dissipation will occur at frequencies above the material's BCS gap frequency [25] and will damp out the free plasma oscillations that are otherwise predicted to occur in (266). In response, we note that these dissipative effects cannot alter the ratio given by (172) that appears in the nondissipative factor  $\Xi$  given in (267). Fundamentally, it is the strength of the Coulomb force, and not the strength of the gravitational force, that dictates the strength of a superconducting film's response to an incident GR wave.

## 6.9 The Negligibility of Single-Bounce Transduction

It is important to address the concern that an incoming GR wave will be partially or completely transduced into an outgoing EM wave by a superconducting film instead of being specularly reflected by the film. Recall that the Cooper pairs within the film cannot undergo free fall along with its lattice in the presence of an incident GR wave, contrary to a naive application of the EP to all particles. Instead, Cooper pairs must undergo non-geodesic motion, in contrast to the geodesic motion of the ions in the film's lattice. This leads to a non-zero quantum current density, one that carries mass and charge. Therefore, time-varying mass currents and time-varying charge currents will be generated by an incident GR wave. The latter will cause at least some of the incoming GR-wave energy to be transduced into an outgoing EM wave. More succinctly, the film will behave like an EM antenna. Appreciable transduction would be an interesting result in its own right, but it turns out to be negligible. The transduction effect is necessarily present in the interaction of a superconducting film with a GR wave, but it does not undermine the film's ability to specularly reflect the wave.

The size of the transduction effect can be determined from a consideration of the charge supercurrent density generated within a superconducting film by an incident GR wave. Let us examine the case of a GR plane wave normally incident upon a superconducting film located at the plane  $x = 0$ , in the absence of any incident EM radiation. In this situation, the charge supercurrent generated by a GR wave will be generated as a current sheet. If a GR wave is incident upon the film only from the left, say, the charge supercurrent generated in the film will nonetheless radiate EM radiation symmetrically, i.e., in both the  $+x$  and  $-x$  directions. This follows from the bilateral symmetry of the current sheet, which takes the form

$$\mathbf{j}_e = \mathbf{j}_0 \delta(x) \exp(-i\omega t) \tag{273}$$

around  $x = 0$  (here and henceforth we suppress the polarization vectors of the currents and fields

because they are all transverse to the  $x$  axis). The current sheet will radiate by coupling, via the Cooper pairs' charge  $q = 2e$ , to an electric field  $\mathbf{E} = -\partial\mathbf{A}/\partial t$  (in the radiation gauge) and to a magnetic field  $\mathbf{B} = \nabla \times \mathbf{A}$ .

Having chosen the radiation gauge, in which  $\nabla \cdot \mathbf{A} = 0$  and in which the scalar potential is identically zero everywhere, we can begin with the EM wave equation in terms of  $\mathbf{A}$  and  $\mathbf{j}_e$ :

$$\nabla^2 \mathbf{A} - \frac{1}{c^2} \frac{\partial^2 \mathbf{A}}{\partial t^2} = -\mu_0 \mathbf{j}_e . \quad (274)$$

Let us assume once again that all time variations are sinusoidal at an angular frequency  $\omega$ , so that we can make the replacements

$$\mathbf{A} \rightarrow \mathbf{A} \exp(-i\omega t) \text{ and } \mathbf{j}_e \rightarrow \mathbf{j}_e \exp(-i\omega t) . \quad (275)$$

Let us also take advantage of the symmetry inherent in the problem, so that we can reduce (274) to a Helmholtz equation in a single dimension for the transverse amplitudes  $A$  and  $j_e$ :

$$\frac{\partial^2 A}{\partial x^2} + k^2 A = -\mu_0 j_e = -\mu_0 j_0 \delta(x) . \quad (276)$$

The delta function in (276) vanishes everywhere except at the origin  $x = 0$ , so that for all  $x \neq 0$  this equation becomes a 1D homogeneous Helmholtz equation

$$\frac{\partial^2 A}{\partial x^2} + k^2 A = 0 . \quad (277)$$

By the principle of causality and the bilateral symmetry of the film, we can then restrict the possible solutions of this equation to *outgoing* plane waves symmetrically emitted from the film, so that

$$A = \alpha \exp(+ikx) \text{ for } x > 0 \quad (278a)$$

$$A = \alpha \exp(-ikx) \text{ for } x < 0 \quad (278b)$$

for the same value of  $\alpha$ , which is determined by the strength of the delta function as follows:

$$\begin{aligned} \lim_{\varepsilon \rightarrow 0} \int_{-\varepsilon}^{+\varepsilon} dx \left( \frac{\partial^2 A}{\partial x^2} + k^2 A \right) &= \lim_{\varepsilon \rightarrow 0} \left. \frac{\partial A}{\partial x} \right|_{-\varepsilon}^{+\varepsilon} \\ &= -\mu_0 j_0 \lim_{\varepsilon \rightarrow 0} \int_{-\varepsilon}^{+\varepsilon} dx \delta(x) = -\mu_0 j_0 . \end{aligned}$$

For  $\varepsilon > 0$ , the derivatives of  $A$  are

$$\lim_{\varepsilon \rightarrow 0} \left. \frac{\partial A}{\partial x} \right|_{-\varepsilon}^{+\varepsilon} = \lim_{\varepsilon \rightarrow 0} (+ik\alpha \exp(+ik\varepsilon)) = +ik\alpha \quad (279)$$

and

$$\lim_{\varepsilon \rightarrow 0} \left. \frac{\partial A}{\partial x} \right|_{-\varepsilon} = \lim_{\varepsilon \rightarrow 0} (-ik\alpha \exp(-ik\varepsilon)) = -ik\alpha . \quad (280)$$

Hence

$$\lim_{\varepsilon \rightarrow 0} \left. \frac{\partial A}{\partial x} \right|_{-\varepsilon}^{+\varepsilon} = +2ik\alpha . \quad (281)$$

Therefore, the amplitude  $\alpha$  of the radiation field  $A$  emitted from the charge current sheet of strength  $j_0$  generated by an incident GR wave is given by

$$\alpha = i \frac{1}{2} \frac{\mu_0 j_0}{k} . \quad (282)$$

For a very thin film of thickness  $d$ , the delta function  $\delta(x)$  is approximately

$$\delta(x) \approx \frac{1}{d} \quad (283)$$

inside the film and zero outside, since then

$$\int_{-d/2}^{d/2} \delta(x) dx = 1 , \quad (284)$$

which implies that

$$\alpha = i \frac{1}{2} \frac{Z_0 d}{\omega} j_e . \quad (285)$$

As we saw in the previous section, an incident GR wave generates within a superconducting film not only an  $E_G$  field but an internal  $E$  field as well. In each case, the tangential component of the field must be continuous across the superconductor-vacuum interface. Since there is no incoming  $E$  field, this continuity condition requires the appearance of an outgoing  $E$  field, which is to say that the charge supercurrent generated by the GR wave will cause the film to behave like an antenna and radiate EM waves. For the same sinusoidal time dependence  $\exp(-i\omega t)$  of all fields and currents, and ignoring spatial dependence, we know that

$$E = -\frac{\partial}{\partial t} A = i\omega A = i\omega\alpha . \quad (286)$$

Inserting (285) into this expression, we see that the relationship between the charge supercurrent  $j_e$  in the current sheet and the  $E$  field both outside and inside the film will be given by

$$j_e = nqv = -\frac{2}{Z_0 d} E . \quad (287)$$

The charge conductivity of the film stemming from its behavior as an EM antenna in the presence of a GR wave is thus given by

$$\sigma_e = -\frac{2}{Z_0 d} . \quad (288)$$

Now, it must be possible to re-express this charge conductivity as the real part of the complex mass conductivity. The justification for this step is that the EM radiation produced in transduction from the incident GR wave leads to power loss from the wave that escapes to infinity, never to return. Hence the transduction effect is a lossy process in the GR wave sector, which is no different from any other irreversible, ohmic process, and can therefore be characterized as the real part of the mass conductivity. Multiplying each side of (287) by  $m/q$  and using the relationship between  $E$  and

$E_G$  given earlier in (248), one finds that the lossy component of the mass current density  $\mathbf{j}_G$  arising from the transduction of the incident GR wave into an EM wave is given by

$$j_{\text{loss,G}} = -\frac{2}{Z_0 d} \frac{m^2}{q^2} \frac{1}{\Xi - 1} E_G . \quad (289)$$

The real part of the mass conductivity  $\sigma_{1,G}$  of the film due to the dissipative loss by transduction into the escaping EM radiation is therefore given by

$$\sigma_{1,G} = -\frac{2}{Z_0 d} \frac{m^2}{q^2} \frac{1}{\Xi - 1} = \frac{2}{Z_G d} , \quad (290)$$

where we have taken advantage of the fact that

$$\Xi - 1 = \left( 1 - \frac{m^2 Z_G}{q^2 Z_0} \right) - 1 = -\frac{m^2 Z_G}{q^2 Z_0} . \quad (291)$$

We can now use (290) in conjunction with the nondissipative conductivity  $\sigma_{2,G}$  given in (269)

$$\sigma_{2,G} = -\Xi \frac{nq^2}{m\omega} \frac{Z_0}{Z_G} \quad (292)$$

to determine whether loss into EM radiation will undermine the possibility of GR-wave reflection.

We begin by recalling that the full version of the GR-reflection formula is given by

$$\mathcal{R}_G = \left\{ \left( 1 + 2 \frac{\sigma_{1,G}}{\sigma_{1,G}^2 + \sigma_{2,G}^2} \frac{1}{Z_G d} \right)^2 + \left( 2 \frac{\sigma_{2,G}}{\sigma_{1,G}^2 + \sigma_{2,G}^2} \frac{1}{Z_G d} \right)^2 \right\}^{-1} . \quad (293)$$

Now let us define the parameter  $\Sigma$ , which is the dimensionless ratio of the squares of the two mass



conductivities given in (290) and (292)

$$\begin{aligned}\Sigma &\equiv \left(\frac{\sigma_{1,G}}{\sigma_{2,G}}\right)^2 = \left(\frac{2m\omega}{\Xi n q^2 Z_0 d}\right)^2 \\ &= \left(\frac{2}{\pi} \frac{\omega_d}{\omega_p'^2} \omega\right)^2,\end{aligned}\tag{294}$$

where  $\omega_p'$  is the modified plasma frequency (255) and  $\omega_d = \pi c/d$  is a characteristic frequency associated with the thickness of the film  $d$  (i.e., the resonance frequency for its lowest standing-wave mode). In general, it will be the case that  $\Sigma$  is much less than unity when the frequency of the incident wave is

$$\omega \ll \frac{\pi \omega_p'^2}{2 \omega_d} = 1.1 \times 10^{16} \text{ rad s}^{-1}.\tag{295}$$

The microwave frequencies of interest fall well below this limit, so we can simplify (293) to

$$\begin{aligned}\mathcal{R}_G &= \left\{ \left( 1 + 2 \frac{\sigma_{1,G}}{\sigma_{2,G}} \frac{1}{Z_G d} \right)^2 \right. \\ &\quad \left. + \left( 2 \frac{1}{\sigma_{2,G}} \frac{1}{Z_G d} \right)^2 \right\}^{-1}.\end{aligned}\tag{296}$$

We can then substitute (290) and (292) into (296) to obtain

$$\mathcal{R}_G = \{(1 + \Sigma)^2 + \Sigma\}^{-1}.\tag{297}$$

For  $\omega = 2\pi \times (6 \text{ GHz})$ , we see from (294) that

$$\Sigma = 1.3 \times 10^{-11}\tag{298}$$

and thus that

$$\mathcal{R}_G \approx (1 + 3\Sigma)^{-1} = (1 + 3.8 \times 10^{-11})^{-1},\tag{299}$$

which implies a reflectivity very close to unity. Thus the dissipation (i.e., transduction) of an incident

GR wave in the form of outgoing EM radiation will not interfere with the film's ability to specularly reflect GR waves.

As a check on this conclusion, let us examine the ratio  $\eta$  of the power lost in the form of outgoing EM radiation to the power reflected in the form of outgoing GR radiation, using the reasonable assumption that the film acts as a current source in both sectors. Thus,

$$\begin{aligned} \eta &= \frac{\langle \mathcal{P}_{\text{EM}} \rangle}{\langle \mathcal{P}_{\text{GR}} \rangle} = \frac{\langle I_e^2 \rangle Z_0}{\langle I_G^2 \rangle Z_G} = \frac{\langle I_{\text{loss,G}}^2 \rangle Z_G}{\langle I_G^2 \rangle Z_G} \\ &= \frac{\langle I_{\text{loss,G}}^2 \rangle}{\langle I_G^2 \rangle} = \frac{\langle j_{\text{loss,G}}^2 \rangle}{\langle j_G^2 \rangle} = \frac{\sigma_{1,G}^2}{\sigma_{2,G}^2} = \Sigma . \end{aligned} \quad (300)$$

The value for  $\Sigma$  given in (298) implies that a negligible fraction of the power of the incoming GR microwave will be lost through transduction into an outgoing EM wave. A superconducting film at temperatures sufficiently near  $T = 0$  will indeed be a highly reflective mirror for GR microwaves but a highly inefficient transducer of GR microwaves into EM microwaves.

In the parallel case of EM-wave reflection, we can once again take into account the possibility of transduction by introducing a real term into the EM conductivity that corresponds to loss into the GR sector (i.e., into an outgoing GR wave). The resulting real and imaginary parts of the complex charge conductivity of the film can then be shown to be

$$\sigma_1 = \frac{2}{Z_0 d} \quad \text{and} \quad \sigma_2 = \Xi \frac{nq^2}{m\omega} , \quad (301)$$

where  $\sigma_1$  is the dissipative part of the complex charge conductivity corresponding to loss by transduction into outgoing GR radiation. The film will radiate as a GR antenna because of the appearance of a quadrupolar pattern of mass supercurrents (when driven by a  $\text{TEM}_{11}$  incident EM plane-wave mode) that couples, via the Cooper pairs' mass  $m = 2m_e$ , to a gravito-electric field  $\mathbf{E}_G = -\partial\mathbf{h}/\partial t$  (in the radiation gauge) and to a gravito-magnetic field  $\mathbf{B}_G = \nabla \times \mathbf{h}$ , where  $\mathbf{h}$  is the gravitational analog of the electromagnetic vector potential  $\mathbf{A}$ .

In fact, (301) leads to an expression for  $\Sigma$  identical to the one given in (294). The subsequent

analysis then proceeds unaltered, confirming that the model developed here is also consistent with the prediction that at temperatures sufficiently near  $T = 0$  a superconducting film will be a highly reflective mirror for EM microwaves but a highly inefficient transducer of EM microwaves into GR microwaves. Importantly, this prediction is consistent with the experimental results of Glover and Tinkham [24].

## 6.10 Conservation of Energy in the Reflection Process

Having shown that a superconducting film can specularly reflect a GR wave and that transduction will not substantially impede this behavior, we turn finally to the question of whether the expressions for  $\sigma_{1,G}$  and  $\sigma_{2,G}$  given above in (290) and (292) are consistent with the conservation of energy. This basic physical principle requires that the absorptivity, reflectivity, and transmissivity of the film sum to unity:

$$\begin{aligned} \mathcal{A}_G + \mathcal{R}_G + \mathcal{T}_G &= 1 \\ &= \mathcal{A}_G \mathcal{R}_G \mathcal{T}_G \times \left( \frac{1}{\mathcal{A}_G \mathcal{R}_G} + \frac{1}{\mathcal{A}_G \mathcal{T}_G} + \frac{1}{\mathcal{R}_G \mathcal{T}_G} \right). \end{aligned} \quad (302)$$

From the analysis presented in Sections 6.4–6.7, we know that the reciprocal of the GR transmissivity is given by

$$\frac{1}{\mathcal{T}_G} = \left( 1 + \frac{1}{2} \sigma_{1,G} Z_G d \right)^2 + \left( \frac{1}{2} \sigma_{2,G} Z_G d \right)^2 \quad (303)$$

and that the reciprocal of the GR reflectivity is given by

$$\begin{aligned} \frac{1}{\mathcal{R}_G} &= \left( 1 + 2 \frac{\sigma_{1,G}}{\sigma_{1,G}^2 + \sigma_{2,G}^2} \frac{1}{Z_G d} \right)^2 \\ &\quad + \left( 2 \frac{\sigma_{2,G}}{\sigma_{1,G}^2 + \sigma_{2,G}^2} \frac{1}{Z_G d} \right)^2. \end{aligned} \quad (304)$$

We can determine the reciprocal of the GR absorptivity  $\mathcal{A}_G$  by considering the work done by a gravito-electric field  $\mathbf{E}_G$  to move a mass  $m$  by an infinitesimal displacement  $d\mathbf{x}$ :

$$dW = \mathbf{F} \cdot d\mathbf{x} = m \mathbf{E}_G \cdot d\mathbf{x}. \quad (305)$$

The rate of work being done, i.e., the instantaneous power  $P$  delivered by the field to the mass, is

$$\mathbf{P} = \mathbf{F} \cdot \frac{d\mathbf{x}}{dt} = m \mathbf{E}_G \cdot \frac{d\mathbf{x}}{dt}. \quad (306)$$

Let  $n$  be the number density of mass carriers moving with velocity

$$\mathbf{v} = \frac{d\mathbf{x}}{dt} , \quad (307)$$

so that the mass current density  $\mathbf{j}_G$  is

$$\mathbf{j}_G = nm\mathbf{v} . \quad (308)$$

Then the instantaneous power delivered by the field to the mass carriers per unit volume moving in a small volume  $V$  is

$$\mathcal{P} = \frac{P}{V} = nm\mathbf{E}_G \cdot \frac{d\mathbf{x}}{dt} = \mathbf{j}_G \cdot \mathbf{E}_G , \quad (309)$$

where  $\mathbf{j}_G$  and  $\mathbf{E}_G$  are real quantities. Let us, however, generalize this expression and represent the current and field by the complex quantities

$$\mathbf{j}_G = \mathbf{j}_{0,G} \exp(-i\omega t) \text{ and} \quad (310a)$$

$$\mathbf{E}_G = \mathbf{E}_{0,G} \exp(-i\omega t) . \quad (310b)$$

Then

$$\text{Re } \mathbf{j}_G = \frac{1}{2} [\mathbf{j}_{0,G} \exp(-i\omega t) + \mathbf{j}_{0,G}^* \exp(i\omega t)] \quad (311)$$

and

$$\text{Re } \mathbf{E}_G = \frac{1}{2} [\mathbf{E}_{0,G} \exp(-i\omega t) + \mathbf{E}_{0,G}^* \exp(i\omega t)] . \quad (312)$$

The *real* instantaneous power per unit volume expressed in terms of this complex current and field is given by

$$\begin{aligned} \mathcal{P} &= \text{Re } \mathbf{j}_G \cdot \text{Re } \mathbf{E}_G \quad (313) \\ &= \frac{1}{2} [\mathbf{j}_{0,G} \exp(-i\omega t) + \mathbf{j}_{0,G}^* \exp(i\omega t)] \cdot \\ &\quad \frac{1}{2} [\mathbf{E}_{0,G} \exp(-i\omega t) + \mathbf{E}_{0,G}^* \exp(i\omega t)] . \end{aligned}$$

But the time average over one wave-period  $T = 2\pi/\omega$  of each second harmonic term in this expression vanishes because

$$\frac{1}{T} \int_0^T dt [\mathbf{j}_{0,G} \cdot \mathbf{E}_{0,G} \exp(-2i\omega t)] = 0 \quad (314a)$$

$$\frac{1}{T} \int_0^T dt [\mathbf{j}_{0,G}^* \cdot \mathbf{E}_{0,G}^* \exp(+2i\omega t)] = 0 , \quad (314b)$$

leaving only the DC cross terms

$$\langle \mathcal{P} \rangle = \frac{1}{4} (\mathbf{j}_{0,G} \cdot \mathbf{E}_{0,G}^* + \mathbf{j}_{0,G}^* \cdot \mathbf{E}_{0,G}) , \quad (315)$$

which can be re-expressed as

$$\langle \mathcal{P} \rangle = \frac{1}{2} \text{Re}(\mathbf{j}_G^* \cdot \mathbf{E}_G) . \quad (316)$$

Let us apply this result for the time-averaged power density to a superconducting film by recalling that the relevant gravito-electric field is the field *inside* the film, so that

$$\langle \mathcal{P} \rangle = \frac{1}{2} \text{Re}(\mathbf{j}_G^* \cdot \mathbf{E}_{G\text{-inside}}) , \quad (317)$$

where the gravitational analog of Ohm's law is

$$\mathbf{j}_G = \sigma_G \mathbf{E}_{G\text{-inside}} . \quad (318)$$

Therefore,

$$\begin{aligned} \langle \mathcal{P} \rangle &= \frac{1}{2} (\text{Re } \sigma_G^*) (\mathbf{E}_{G\text{-inside}}^* \cdot \mathbf{E}_{G\text{-inside}}) \\ &= \frac{1}{2} \text{Re}(\sigma_{1,G} - i\sigma_{2,G}) |\mathbf{E}_{G\text{-inside}}|^2 \\ &= \frac{1}{2} \sigma_{1,G} |\mathbf{E}_{G\text{-inside}}|^2 . \end{aligned} \quad (319)$$

As in the electromagnetic case discussed in Section 6.4, the gravito-electric field inside the film will be related to the incident gravito-electric field as follows:

$$\begin{aligned}
\mathbf{E}_{\text{G-inside}} &= (1 - r_{\text{G}})\mathbf{E}_{\text{G-incident}} \\
&= t_{\text{G}}\mathbf{E}_{\text{G-incident}} \\
&= \mathbf{E}_{\text{G-transmitted}} ,
\end{aligned} \tag{320}$$

where  $r_{\text{G}}$  is the amplitude reflection coefficient and  $t_{\text{G}}$  is the amplitude transmission coefficient. Thus the time-averaged power dissipated inside the entire volume  $Ad$  of the film, where  $A$  is its area (an arbitrarily large quantity) and  $d$  is its thickness, is given by

$$\begin{aligned}
\langle \mathcal{P} \rangle Ad &= \frac{1}{2} \sigma_{1,\text{G}} t_{\text{G}}^* t_{\text{G}} |\mathbf{E}_{\text{G-incident}}|^2 Ad \\
&= \frac{A \sigma_{1,\text{G}} d}{2} \mathcal{T}_{\text{G}} |\mathbf{E}_{\text{G-incident}}|^2 ,
\end{aligned} \tag{321}$$

where  $\mathcal{T}_{\text{G}} = t_{\text{G}}^* t_{\text{G}}$  is the transmittivity of the film.

The magnitude of the time-averaged Poynting vector of the incident wave traveling in the direction  $\hat{\mathbf{k}}$  is given by an expression similar to (316), viz.,

$$\begin{aligned}
\langle S \rangle &= \frac{1}{2} \hat{\mathbf{k}} \cdot \text{Re}(\mathbf{E}_{\text{G-incident}}^* \times \mathbf{H}_{\text{G-incident}}) \\
&= \frac{1}{2} \frac{1}{Z_{\text{G}}} \text{Re}(\mathbf{E}_{\text{G-incident}}^* \cdot \mathbf{E}_{\text{G-incident}}) \\
&= \frac{1}{2Z_{\text{G}}} |\mathbf{E}_{\text{G-incident}}|^2 ,
\end{aligned} \tag{322}$$

from which it follows that the power incident on the area  $A$  of the film is

$$\langle S \rangle A = \frac{1}{2Z_{\text{G}}} |\mathbf{E}_{\text{G-incident}}|^2 A . \tag{323}$$

Thus the absorptivity  $\mathcal{A}_{\text{G}}$ , which is the ratio of the time-averaged power dissipated inside the film

to the time-averaged power incident on the film, is given by

$$\mathcal{A}_G = \frac{\langle \mathcal{P} \rangle Ad}{\langle S \rangle A} = \mathcal{T}_G \sigma_{1,G} Z_G d. \quad (324)$$

Inserting the reciprocal of (303) for  $\mathcal{T}_G$  into (324) and taking the reciprocal of the new expression, we find that

$$\frac{1}{\mathcal{A}_G} = \frac{(1 + \frac{1}{2}\sigma_{1,G} Z_G d)^2 + (\frac{1}{2}\sigma_{2,G} Z_G d)^2}{\sigma_{1,G} Z_G d}. \quad (325)$$

A calculation confirms that the expressions given in (303), (304), and (325) are in fact consistent with the requirement that the absorptivity, reflectivity, and transmissivity sum to unity. When we insert (303), (304), and (325) into the right-hand side of (302), we obtain a single equation with two variables,  $\sigma_{1,G}$  and  $\sigma_{2,G}$ . Thus the conservation of energy in the case of the interaction between a GR wave and a superconducting film depends solely on the relation between  $\sigma_{1,G}$  and  $\sigma_{2,G}$ .

Recalling the parameter  $\Sigma$  introduced in (294), which characterizes the relation between  $\sigma_{1,G}$  and  $\sigma_{2,G}$ , we can re-express the reciprocals of  $\mathcal{A}_G$ ,  $\mathcal{R}_G$ , and  $\mathcal{T}_G$  as

$$\frac{1}{\mathcal{A}_G} = 2 + \frac{1}{2\Sigma} \quad (326a)$$

$$\frac{1}{\mathcal{R}_G} = \frac{2\Sigma^2 + 10\Sigma^3 + 8\Sigma^4}{2\Sigma^2 + 4\Sigma^3 + 2\Sigma^4} \quad (326b)$$

$$\frac{1}{\mathcal{T}_G} = 4 + \frac{1}{\Sigma}. \quad (326c)$$

One then finds that

$$\mathcal{A}_G \mathcal{R}_G \mathcal{T}_G = \frac{2\Sigma^2 + 4\Sigma^3 + 2\Sigma^4}{1 + 13\Sigma + 60\Sigma^2 + 112\Sigma^3 + 64\Sigma^4} \quad (327)$$

and that

$$\left( \frac{1}{\mathcal{A}_G \mathcal{R}_G} + \frac{1}{\mathcal{A}_G \mathcal{T}_G} + \frac{1}{\mathcal{R}_G \mathcal{T}_G} \right) = \frac{1 + 13\Sigma + 60\Sigma^2 + 112\Sigma^3 + 64\Sigma^4}{2\Sigma^2 + 4\Sigma^3 + 2\Sigma^4}. \quad (328)$$



But these two expressions are just the reciprocals of one another, confirming (302) in the GR case.

In the EM case, the corresponding real and imaginary parts of the complex charge conductivity are given by

$$\sigma_1 = \frac{2}{Z_0 d} \tag{329}$$

$$\sigma_2 = \Xi \frac{nq^2}{m\omega} . \tag{330}$$

The fact that the ratio of the squares of these two conductivities is once again

$$\left( \frac{\sigma_1}{\sigma_2} \right)^2 = \frac{4m^2\omega^2}{\Xi^2 n^2 q^4 Z_0^2 d^2} = \Sigma \tag{331}$$

is a strong hint that (302) will be similarly satisfied in the EM case. In fact, the expressions given above for  $1/\mathcal{A}_G$ ,  $1/\mathcal{R}_G$ , and  $1/\mathcal{T}_G$  in (326) carry over without alteration into the EM case, so that the subsequent steps of the derivation proceed exactly as above. Consequently, we can say that the formalism presented here obeys energy conservation both in the case of GR reflection with EM loss and in the case of EM reflection with GR loss. This is a strong self-consistency check of the entire calculation.

## 6.11 Experimental and Theoretical Implications

Most of the experiments presently being conducted on gravitational radiation aim to passively detect GR waves originating from astrophysical sources. The specular reflection of GR waves at microwave frequencies from superconducting thin films due to the Heisenberg-Coulomb effect would allow for a variety of new experiments, all of which could be performed in a laboratory setting and some of which would involve mesoscopic quantum objects. Here we identify several such experiments that should be technologically feasible, commenting briefly on their interrelations and broader theoretical implications.

Consider first a conceptually simple test of the physics behind the Heisenberg-Coulomb effect itself. In this experiment, two horizontally well-separated, noninteracting superconducting bodies are allowed to fall freely in the non-uniform gravitational field of the Earth. The tidal forces acting on the two bodies, which are like the tidal forces caused by a low-frequency GR wave, cause them to converge as they fall freely toward the center of the Earth. Although the gap-protected, global quantum mechanical phase of the Cooper pairs forces each pair to remain motionless with respect to the center of mass of its own body, this does nothing to prevent the two bodies from converging during free fall. The trajectories of these two superconducting bodies – recall that they have decohered due to interactions with their environment and are therefore spatially well separated – must be identical to those of *any* two noninteracting, freely falling massive bodies, in accord with the EP.

Now connect the two bodies by a thin, slack, arbitrarily long, superconducting wire, so that they become a single, simply-connected, coherent superconducting system. From a mechanical point of view, the negligible Hooke's constant of the wire allows each body to move freely, one relative to the other. In this case, the characteristic frequency of the interaction between the bodies and the gravitational field, which is given by the inverse of the free-fall time, is far below the BCS gap frequency and far above the simple harmonic resonance frequency of the two-bodies-plus-wire system. According to first-order time-dependent perturbation theory, then, the nonlocalizable Cooper pairs of the two coherently connected bodies must remain motionless with respect to the center of mass of

the entire system, as seen by a distant inertial observer. This follows, as we have argued in Section 6.3, from the gap-protected, global, quantum mechanical phase of the Cooper pairs, which is at root a consequence of the UP. On the other hand, the ions of the two coherently connected bodies will attempt to converge toward each other during free fall, since they want to follow geodesics in accord with the EP.

In this experimental “tug-of-war” between the Uncertainty Principle and the Equivalence Principle, which principle prevails? When the temperature is low enough to justify ignoring the effect of any residual normal electrons (i.e., when the temperature is less than roughly half the critical temperature, so that the BCS gap is sufficiently close to its value at absolute zero [25]), we believe the EP will be completely overcome by the UP. This must be the case because the charge separation that would otherwise result as the ions converged while the Cooper pairs remained motionless (with respect to a distant inertial observer) would generate an unfavorable, higher-energy configuration of the system. The quantum mechanical Cooper pairs must drag the classical ionic lattice into co-motion with them, so that the coherently connected bodies depart from geodesic motion. That is to say, the bodies must maintain a constant distance from one another as they fall. If two coherently connected superconducting bodies were to converge like any two noninteracting bodies, one would have to conclude that the UP had failed with respect to the EP, i.e., that the EP is more universal and fundamental in its application to all objects than the UP. We do not believe this to be the case.

Theories that propose an “intrinsic collapse of the wavefunction” or “objective state reduction,” through some decoherence mechanism, whether by means of a stochastic process that leverages the entanglement of object and environment (as originally proposed by Ghirardi, Rimini, and Weber [58]), or by means of a sufficiently large change in the gravitational self-energy associated with different mass configurations of a system (as proposed by Penrose [59]), would imply the failure of the Superposition Principle, and thus of the Uncertainty Principle, in the experiment outlined above. The existence of any such mechanism would destroy the Heisenberg-Coulomb effect, but it would also pose a serious problem for any quantum theory of gravity.

A straightforward geometrical calculation for the free-fall experiment outlined above shows that the convergence of two noninteracting massive bodies initially separated by several centimeters would be on the order of microns for free-fall distances presently attainable in aircraft-based zero-gravity experiments. Though small, this degree of convergence is readily measurable by means of laser interferometry. The exact decrease, if any, in the convergence measured for two coherently connected superconducting bodies, relative to the decrease measured for the same two bodies when the coherent connection is broken, would allow one to measure the strength of the Heisenberg-Coulomb effect, with null convergence corresponding to maximal deflection from free fall.

The specular reflection of GR waves from superconducting films, which we have argued follows from the Heisenberg-Coulomb effect (see Section 6.8), might also allow for the detection of a gravitational Casimir-like force (we thank Dirk Bouwmeester for this important suggestion). In the EM case, an attractive force between two nearby metallic plates is created by radiation pressure due to quantum fluctuations in the EM vacuum energy. If the two plates were made of a type I superconducting material, it should be possible to detect a change in the attractive force between them, due to the additional coupling of the plates to quantum fluctuations in the GR vacuum energy, as the plates were lowered through their superconducting transition temperature. Observation of the gravitational analog of the Casimir force could be interpreted as evidence for the existence of quantum fluctuations in gravitational fields, and hence as evidence for the need to quantize gravity. If no analog of the Casimir force were observed despite confirmation of the Heisenberg-Coulomb effect in free-fall experiments, one would be forced to conclude either that gravitational fields are not quantizable or that something other than the Heisenberg-Coulomb effect is wrong with our “mirrors” argument.

In Sections 6.9 and 6.10, we discussed the transduction of GR waves to EM waves and vice-versa. Although we showed that transduction in either direction will be highly inefficient in the case of a single superconducting film, experimentally significant efficiencies in both directions may be attainable in the case of a pair of charged superconductors [60]. This would lead to a number of ex-

perimental possibilities, all of which employ the same basic apparatus: two levitated (or suspended) and electrically charged superconducting bodies that repel one another electrostatically even as they attract one another gravitationally. For small bodies, it is experimentally feasible to charge the bodies to “criticality,” i.e., to the point at which the forces of repulsion and attraction cancel [60]. At criticality, the apparatus should become an effective transducer of incoming GR radiation, i.e., it should enable 50% GR-to-EM transduction efficiency. By time-reversal symmetry, it should also become an effective transducer of incoming EM radiation, i.e., it should also enable 50% EM-to-GR transduction efficiency. Chiao has previously labeled this type of apparatus a “quantum transducer” [60].

Two variations on a single-transducer experiment could provide new and compelling, though still indirect, evidence for the existence of GR waves. First, an electromagnetically isolated transducer should generate an EM signal in the presence of an incoming GR wave, since the transducer should convert half the power contained in any incoming GR wave into a detectable outgoing EM wave. This might allow for the detection of the cosmic gravitational-wave background (CGB) at microwave frequencies, assuming that certain cosmological models of the extremely early Big Bang are correct [61]. If no transduced EM signal were detected despite confirmation of the H-C effect, one would be forced to conclude either that something is wrong with the “mirrors” argument or the GR-to-EM “transduction” argument, or that there is no appreciable CGB at the frequency of investigation.

A single quantum transducer should also behave anomalously below its superconducting transition temperature in the presence of an incoming EM wave (we thank Ken Tatebe for this important suggestion). By the principle of the conservation of energy, an EM receiver directed at the transducer should register a significant drop in reflected power when the transducer is “turned on” by lowering its temperature below the transition temperature of the material, since energy would then be escaping from the system in the form of invisible (transduced) GR waves. If no drop in reflected power were observed despite confirmation of GR-to-EM transduction in the experiment outlined in the previous paragraph, one would need to reconsider the validity of the principle of time-reversal

symmetry in the argument for EM-to-GR transduction.

Finally, if an efficient quantum transducer were to prove experimentally feasible, two transducers operating in tandem would open up the possibility of GR-wave communication. As a start, a gravitational Hertz-like experiment should be possible. An initial transducer could be used to partially convert an incoming EM into an outgoing GR wave. A second transducer, spatially separated and electromagnetically isolated from the first, could then be used to partially back-convert the GR wave generated by the first transducer into a detectable EM wave. The same two-transducer arrangement could also be used to confirm the predicted speed and polarization of GR waves. Of course, wireless communication via GR waves would be highly desirable, since all normal matter is effectively transparent to GR radiation. Such technology would also open up the possibility of wireless power transfer over long distances. On the other hand, if a Hertz-like arrangement were to yield a null result despite the success of the previously outlined single-transducer experiments, one would infer that the success of those experiments was due to something other than the existence of GR waves.

In summary, a new class of laboratory-scale experiments at the interface of quantum mechanics and gravity follows if the argument presented here for superconducting GR-wave mirrors is correct. Such experiments could be a boon to fundamental physics. For example, one could infer from the experimental confirmation of a gravitational Casimir effect that gravitational fields are in fact quantized. Confirmation of the Heisenberg-Coulomb effect would also point to the need for a unified gravito-electrodynamical theory for weak, but quantized, gravitational and electromagnetic fields interacting with nonrelativistic quantum mechanical matter. As with the Rydberg atom analysis explored in Section 5, such a theory would again fall far short of the ultimate goal of unifying all known forces of nature into a “theory of everything,” but it would nonetheless be a very useful theory to have.

## 6.12 Appendix 6A: The Magnetic and Kinetic Inductances of a Thin Metallic Film

The EM inductance  $L$  of the superconducting film is composed of two parts: the magnetic inductance  $L_m$ , which arises from the magnetic fields established by the charge supercurrents, carried by the Cooper pairs, and the kinetic inductance  $L_k$ , which arises from the Cooper pairs' inertial mass [26]. Using (208) and the values of  $\xi_0 = 83$  nm and  $\delta_p = \lambda_L = 37$  nm for Pb at microwave frequencies, one finds for our superconducting film that  $l_k$  is on the order of  $10^{-5}$  m and that  $L_k$  is on the order of  $10^{-11}$  henries.

$L_m$  can be found using the magnetic potential energy relations

$$U = \int \frac{B^2}{2\mu_0} d^3x = \frac{1}{2}L_m I^2, \quad (332)$$

where  $U$  is the magnetic potential energy,  $B$  is the magnetic induction field, and  $I$  is the (uniform) current flowing through the film. Thus,

$$L_m = \int \frac{B^2}{I^2\mu_0} d^3x. \quad (333)$$

A closed-form, symbolic expression for this integral is complicated for the geometry of a film, but numerical integration shows that in the case of a Pb film with dimensions  $1 \text{ cm} \times 1 \text{ cm} \times 2 \text{ nm}$ ,  $L_m$  is on the order of at most  $10^{-15}$  henries, which is much smaller than  $L_k$ . The experiments of Glover and Tinkham [24] corroborate the validity of this approximation. Thus, we can safely neglect the magnetic inductance  $L_m$  in our consideration of  $L$ .

A comparison of this result for  $L_m$  with the result for  $L_{m,G}$  in the gravitational sector reveals that

$$\frac{L_{m,G}}{L_m} = \frac{\mu_G}{\mu_0}. \quad (334)$$

Recall now that the expression for  $l'_{k,G}$  given by (271) is

$$l'_{k,G} = d \left( \frac{\delta_p}{d} \right)^2, \quad (335)$$

which is just the expression for  $l_{k,p}$  ( $\approx l_k$ ) derived in Appendix 6B below. Thus we see that

$$\frac{L_{k,G}}{L_k} = \frac{\mu_G l'_{k,G}}{\mu_0 l_k} \approx \frac{\mu_G}{\mu_0}. \quad (336)$$

From (334) and (336), it follows that

$$\frac{L_{m,G}}{L_{k,G}} \approx \frac{L_m}{L_k}. \quad (337)$$

Thus, we can also safely neglect the gravito-magnetic inductance  $L_{m,G}$  in our consideration of  $L_G$ .



### 6.13 Appendix 6B: The Kinetic Inductance Length Scale in a Collisionless Plasma Model

In this appendix we ignore the quantum mechanical properties of superconducting films and consider the simpler, classical problem of the kinetic inductance (per square) of a thin metallic film. We begin with a physically intuitive derivation of the kinetic inductance length scale  $l_k$  due to D. Scalapino (whom we thank for pointing out this derivation to us). The current density for a thin metallic film is given by

$$j = n_e e v = \frac{I}{A} = \frac{I}{w d}, \quad (338)$$

where  $e$  is the electron charge,  $v$  is the average velocity of the electrons,  $n_e$  is the number density,  $A$  is the cross-sectional area of the film through which the current flows,  $w$  is film's width, and  $d$  is its thickness. The velocity of the electrons within the film can then be expressed as

$$v = \frac{I}{w} \frac{1}{n_e e d} = \frac{I_w}{n_e e d}, \quad (339)$$

where  $I_w$  is the current per width. Now, by conservation of energy it must be the case that

$$\frac{L_k I_w^2}{2} = \frac{m_e v^2}{2} n_e d. \quad (340)$$

The left-hand side of (340) gives the energy per square meter carried by the film's electrons in terms of the film's kinetic inductance per square and the square of the current per width, whereas the right-hand side gives the same quantity in terms of the kinetic energy per electron multiplied by the number of electrons per square meter of the film. Substituting (339) into (340) and recalling the expression for the plasma skin depth given in (205), one finds that

$$L_k = \frac{m_e}{n_e e^2 d} = \mu_0 \frac{\delta_p^2}{d}, \quad (341)$$

which implies that the kinetic inductance length scale of the film is given by

$$l_k = \frac{L_k}{\mu_0} = d \left( \frac{\delta_p}{d} \right)^2. \quad (342)$$

Now let us derive the kinetic inductance length scale of a thin superconducting film by treating the film as though it were a neutral, collisionless plasma consisting of Cooper-paired electrons moving dissipationlessly through a background of a positive ionic lattice. We assume that the film is at absolute zero temperature and that the mass of each nucleus in the lattice is so heavy that, to a good first approximation, the motion of the lattice in response to an incident EM wave can be neglected when compared to the motion of the electrons. If one then analyzes the film's response to the incident EM wave using the concepts of polarization and susceptibility, it is possible to show for all non-zero frequencies that

$$\sigma_1 = 0 \quad \text{and} \quad \sigma_2 = \varepsilon_0 \frac{\omega_p^2}{\omega}. \quad (343)$$

Recalling the basic relationship between the kinetic inductance  $L_k$  and  $\sigma_2$  given in (194), as well as the fact that  $\mu_0 = 1/\varepsilon_0 c^2$ , and that  $\delta_p = c/\omega_p$  when  $\omega \ll \omega_p$ , we see that according to this model the kinetic inductance of the superconducting film (in the limit of  $\omega \ll \omega_p$ )  $L_{k,p}$  is given by

$$L_{k,p} = \frac{1}{\varepsilon_0 \omega_p^2 d} = \mu_0 \frac{\delta_p^2}{d}, \quad (344)$$

which implies that the plasma version of the kinetic inductance length scale  $l_{k,p}$  for a superconducting film at absolute zero is

$$l_{k,p} = \frac{L_{k,p}}{\mu_0} = d \left( \frac{\delta_p}{d} \right)^2 \quad (345)$$

in agreement with (342). The discrepancy between these expressions and the one obtained in (208) in Section 6.5 on the basis of the more sophisticated BCS model,

$$l_k = \xi_0 \left( \frac{\delta_p}{d} \right)^2, \quad (346)$$

arises from the fact that the classical approaches taken here know nothing of the additional length scale of the BCS theory, namely, the coherence length  $\xi_0$ . This quantum mechanical length scale is related to the BCS energy gap  $\Delta$  through (201) and cannot enter into derivations based solely on classical concepts; hence the appearance of the prefactor  $d$  instead of  $\xi_0$  in (342) and (345).

## 6.14 Appendix 6C: Impedance and Scattering Cross-Section

The relevance of the concept of impedance to the question of scattering cross-section can be clarified by considering the case of an EM plane wave scattered by a Lorentz oscillator, which plays a role analogous to the resonant bar in Weinberg's considerations of GR-wave scattering [39]. The Poynting vector  $\mathbf{S}$  of the incident EM wave is related to the impedance of free space  $Z_0$  as follows:

$$\mathbf{S} = \mathbf{E} \times \mathbf{H} = \frac{1}{Z_0} E^2 \hat{\mathbf{k}}, \quad (347)$$

where the wave's electric field  $\mathbf{E}$  and magnetic field  $\mathbf{H}$  are related to one another by  $|\mathbf{E}| = Z_0 |\mathbf{H}|$ , where  $Z_0 = \sqrt{\mu_0/\epsilon_0} = 377$  ohms is the characteristic impedance of free space, and where  $\hat{\mathbf{k}}$  is the unit vector denoting the direction of the wave's propagation.

Multiplying the scattering cross-section  $\sigma$  (not to be confused with the conductivity) by the time-averaged magnitude of the Poynting vector  $\langle S \rangle$ , which is the average energy flux of the incident wave, we get the time-averaged power  $\langle P \rangle$  scattered by the oscillator, viz.,

$$\sigma \langle S \rangle = \langle P \rangle = \sigma \langle E^2 \rangle / Z_0, \quad (348)$$

where the angular brackets denote a time average over one cycle of the oscillator. It follows that

$$\sigma = \frac{Z_0 \langle P \rangle}{\langle E^2 \rangle}. \quad (349)$$

When driven on resonance, a Lorentz oscillator dissipates an amount of power given by

$$\langle P \rangle = \left\langle eE \frac{dx}{dt} \right\rangle = \frac{\langle E^2 \rangle}{\gamma m_e / e^2}, \quad (350)$$

where  $x$  denotes the oscillator's displacement,  $e$  is the charge of the electron,  $m_e$  is its mass, and  $\gamma$  is the oscillator's dissipation rate. The oscillator's EM scattering cross-section is thus related to  $Z_0$

as follows:

$$\sigma = \frac{Z_0}{\gamma m_e / e^2} . \quad (351)$$

Maximal scattering will occur when the dissipation rate of the oscillator  $\gamma$  and thus  $\gamma m_e / e^2$  are minimized. In general, one can minimize the dissipation rate of an oscillator by minimizing its ohmic or dissipative resistance, which is a form of impedance. Hence Weinberg suggested using dissipationless superfluids instead of aluminum for the resonant bar, and we suggest here using zero-resistance superconductors instead of superfluids. In particular, Weinberg's analysis showed that if the damping of the oscillator is sufficiently dissipationless, such that radiation damping by GR radiation becomes dominant, the cross-section of the oscillator on resonance is on the order of a square wavelength, and is independent of Newton's constant  $G$ . However, the bandwidth of the resonance is extremely narrow, and is directly proportional to  $G$ .

In this regard, an important difference between neutral superfluids and superconductors is the fact that the electrical charge of the Cooper pairs enters into the interaction of the superconductor with the incoming GR wave. This leads to an enormous enhancement of the oscillator strength of Weinberg's scattering cross-section extended to the case of a superconductor in its response to the GR wave, relative to that of a neutral superfluid or of normal matter like that of a Weber bar.

As we have seen earlier, the non-localizability of the negatively charged Cooper pairs, which follows from the Uncertainty Principle and is protected by the BCS energy gap, causes them to undergo non-geodesic motion in contrast to the decoherence-induced geodesic motion of the positively charged ions in the lattice, which follows from the Equivalence Principle. The resulting charge separation leads to a virtual plasma excitation inside the superconductor. The enormous enhancement of the conductivity that follows from this, i.e., the H-C effect, can also be seen from the infinite-frequency sum rule that follows from the Kramers-Kronig relations, which are based on causality and the linearity of the response of the superconductor to either an EM or a GR wave [25, p. 88, first equation].

In the electromagnetic sector, the Kramers-Kronig relations for the real part of the charge conduc-

tivity  $\sigma_1(\omega)$  and the imaginary part  $\sigma_2(\omega)$  (not to be confused with the above scattering cross-section  $\sigma$ ) are given by [62, p. 279]

$$\sigma_1(\omega) = \frac{2}{\pi} \int_0^{\infty} \frac{\omega' \sigma_2(\omega') d\omega'}{\omega'^2 - \omega^2} \quad (352a)$$

$$\sigma_2(\omega) = -\frac{2\omega}{\pi} \int_0^{\infty} \frac{\sigma_1(\omega') d\omega'}{\omega'^2 - \omega^2} . \quad (352b)$$

From (352b) and the fact that electrons become free particles at infinitely high frequencies, one can derive the infinite-frequency sum rule given by Kubo [62, 63]

$$\int_0^{\infty} \sigma_1(\omega) d\omega = \frac{\pi}{2} \varepsilon_0 \omega_p^2 , \text{ where } \omega_p^2 = \frac{n_e e^2}{\varepsilon_0 m_e} . \quad (353)$$

In the GR sector, making the replacement in (353),

$$\frac{e^2}{4\pi\varepsilon_0} \rightarrow Gm^2 , \quad (354)$$

where  $m$  is regarded as the mass of the neutral atom that transports the mass current within the superfluid, is relevant to the interaction between a neutral superfluid and an incident GR wave. This leads to the following infinite-frequency sum rule:

$$\int_0^{\infty} \sigma_{1,G}(\omega) d\omega = 2\pi^2 n \varepsilon_0 Gm . \quad (355)$$

Numerically, this result is extremely small relative to the result given in (353), which implies a much narrower scattering cross-section bandwidth in the GR sector.

In the case of a superconductor, the replacement given by (354) is unphysical, due to the charged nature of its mass carriers, i.e., Cooper pairs. Here, Kramers-Kronig relations similar to those given in (352) lead to a result identical to the one given in (353). Thus, using superconductors in GR-wave detectors will lead to bandwidths of scattering cross-sections that are orders of magnitude broader

than those of neutral superfluids.

One important implication of this argument concerns the GR scattering cross-section of a superconducting sphere. If the sphere's circumference is on the order of a wavelength of an incident GR wave, the wave will undergo the first resonance of Mie scattering. In the case of specular reflection from the surface of a superconducting sphere, this corresponds to a broadband, geometric-sized scattering cross-section, i.e., a scattering cross-section on the order of a square wavelength over a wide bandwidth. This implies that two charged, levitated superconducting spheres in static mechanical equilibrium, such that their electrostatic repulsion balances their gravitational attraction, should become an efficient transducer for converting EM waves into GR waves and vice versa [60]. As suggested in Section 6.11, two such transducers could be used to perform a Hertz-like experiment for GR microwaves.

## 7 Gravitationally-Induced Charge Separation in Finite Superconductors

Charge separation was discussed in detail in Section 6.6 in the context of reflection of high-frequency gravitational waves from thin superconducting films. Another potential aspect of this effect, which is perhaps more experimentally feasible, is that of direct measurement of the charge separation in a bulk superconductor in the presence of a weak, low-frequency tidal gravitational field. The ability to measure this effect may constitute a novel coupling between gravitation and electromagnetism.

### 7.1 Charge Separation During Free Fall in the Earth's Tidal Gravitational Field

Since the positively charged lattice ions and the negatively charged Cooper pairs undergo relative motion, a tidal gravitational field will electrically polarize a superconductor through charge separation. This leads to internal electric fields. Consider two superconducting cubes connected by a wire. The wire is slack so that the two cubes are completely mechanically decoupled. If the wire is not superconducting, the cubes will converge as they fall toward the center of the Earth in the Earth's inhomogeneous gravitational field, in accordance with the Weak Equivalence Principle. If the wire is superconducting, however, then the system comprised of the two cubes and the wire becomes a single, coherent superconducting system. While this coherent superconducting system is falling in the Earth's inhomogeneous gravitational field, the Cooper-pair electrons are not allowed to converge along with the lattice ions, as shown above. The relative motion between the electrons and the ions creates a charge separation and induces a measurable voltage potential across opposite faces of each cube. It will be shown that this effect can be observed in a laboratory setting.

The charge separation that ensues from the relative motion between the electrons and the ions will cause a voltage potential to appear across opposite ends of each superconducting cube. For simplicity, let each cube have sides with lengths  $L$ , and let  $L$  also be the initial distance between



each cube. Modeling the charge extrusions on each side of a single superconducting cube as thin, infinite sheets of charge, the magnitude of the electric field inside the cube will be given by

$$E = \frac{Q}{\epsilon_0 L^2}, \quad (356)$$

where  $\pm Q$  is the charge on the edges of the cubes, and  $\epsilon_0$  is the permittivity of free space. The amount of charge required to balance the tidal forces on the cubes can be found by equating the tidal force and the electrostatic force, and thus

$$F_E = \frac{Q^2}{\epsilon_0 L^2} = mg' = (\rho L^3) \left( \frac{gL}{2R_E} \right) = F_g, \quad (357)$$

where  $\rho$  is the mass density of the cube (lead is used in this case, where  $\rho_{\text{Pb}} = 11340 \frac{\text{kg}}{\text{m}^3}$ ),  $R_E$  is the radius of the Earth, and the horizontal component of the tidal gravitational acceleration  $g'$  was first discussed in Section 5.3. Thus, the charge is given by

$$Q = \sqrt{\frac{\rho g \epsilon_0}{2R_E}} L^3. \quad (358)$$

This formula uses the realistic approximation that the Earth's radius is much larger than both  $L$  and the height from which the system is dropped. The voltage potential across the faces of a single cube is

$$V = EL = \frac{Q}{\epsilon_0 L} = \sqrt{\frac{\rho g}{2\epsilon_0 R_E}} L^2. \quad (359)$$

Table 2 below shows the magnitude of the charge and of the voltage potential as a function of length  $L$  for this charge distribution model.

	$L = 1 \text{ cm}$	$L = 5 \text{ cm}$
Charge (C)	$2.8 \times 10^{-13}$	$3.5 \times 10^{-11}$
Voltage (V)	3.1	78

Table 2: Charge and voltage potential as a function of length for charged sheet model

If the charge distribution is modeled using point charges instead of infinite sheets, the system can be represented by two sub-systems, where each sub-system consists of two point charges of opposite charge, connected by a rigid, electrically-neutral rod, as in Figure 9.

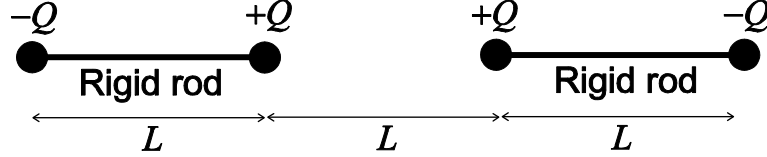


Figure 9: Point charge distribution model in the charge separation experiment

The net force between the two sub-systems can be calculated by summing the forces on each charge, recognizing that the distance between the two sub-systems can change, but that the two point charges within each sub-system cannot move with respect to each other. Since the forces on each sub-system will be symmetric, it is sufficient to calculate the force of the left sub-system in the figure on the right sub-system. The notation  $F_{-+}$ ,  $F_{--}$ ,  $F_{++}$ , and  $F_{+-}$  will be used to symbolize the force of the left point charges on the right point charges, where the first subscript denotes the charge within the left sub-system, and the second subscript denotes the charge in the right sub-system. These forces, which all act along one dimension, are given by

$$F_{-+} = -\frac{1}{4} \frac{Q^2}{4\pi\epsilon_0 L^2} \quad (360a)$$

$$F_{--} = \frac{1}{9} \frac{Q^2}{4\pi\epsilon_0 L^2} \quad (360b)$$

$$F_{++} = \frac{Q^2}{4\pi\epsilon_0 L^2} \quad (360c)$$

$$F_{+-} = -\frac{1}{4} \frac{Q^2}{4\pi\epsilon_0 L^2}. \quad (360d)$$

The sum of these forces is the total force of the left sub-system on the right sub-system, given by

$$F_Q = \frac{11}{18} \frac{Q^2}{4\pi\epsilon_0 L^2}. \quad (361)$$

Setting this force equal to the tidal gravitational force defined in (357) and solving for  $Q$  yields

$$Q = \sqrt{\frac{36\pi\epsilon_0\rho g}{11R_E}} L^3, \quad (362)$$

and thus the voltage potential is

$$V = EL = \frac{L}{Q} F_Q = \sqrt{\frac{11}{144} \frac{\rho g}{\pi\epsilon_0 R_E}} L^2. \quad (363)$$

Table 3 below shows the magnitude of the charge and of the voltage potential as a function of length  $L$  for this charge distribution model.

	$L = 1 \text{ cm}$	$L = 5 \text{ cm}$
Charge (C)	$1.3 \times 10^{-12}$	$1.6 \times 10^{-10}$
Voltage (V)	0.69	17

Table 3: Charge and voltage potential as a function of length for point-charge model

The values shown in these two tables suggest that the voltage should be experimentally detectable. However, these calculations do not take into account the amount of time, or, equivalently, the amount of free fall distance is required for this equilibrium. For experimental feasibility, the amount of free fall time/distance must be sufficiently short. Consider the situation depicted in Figure 10 showing a point mass falling a distance  $\Delta h$  near the Earth's surface, and converging a distance  $\Delta x$  as it falls. The opposite point mass that would make this figure identical to the situation depicted in Figure 1 is not shown.

Using similar triangles, the relationship between the free fall distance and the convergence distance is given by

$$\Delta x = \frac{L}{2R_E} \Delta h. \quad (364)$$

Consider now the model that the superconducting electron wavefunction exhibits quantum incompressibility, and therefore the superfluid does not follow the local geodesic, but instead falls

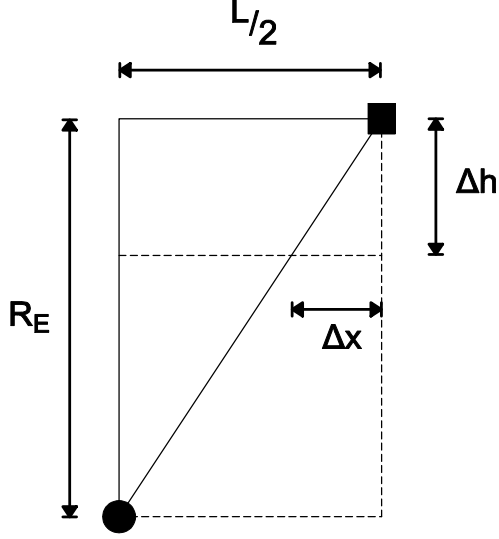


Figure 10: A point mass, shown as a square, falls near the surface of the Earth along a local geodesic (diagonal line) that points towards the center of the Earth, shown as a circle.

straight down, i.e. such that it preserves the distance between the objects during free fall. An expression for the charge accumulated on the outside faces of the samples is given in (362), but the charge can also be expressed in terms of the extrusion distance by

$$Q = n_s e L^2 \Delta x, \quad (365)$$

where  $n_s$  is the superconducting electron density, since the ions will follow the local geodesic. Equating this expression with (362) and solving for  $\Delta x$  yields

$$\Delta x_{eq} = \sqrt{\frac{36\pi\epsilon_0\rho g}{11n_s^2 e^2 R_E}} L. \quad (366)$$

Solving (363) for  $L$  and substituting into the above expression yields

$$\Delta x_{eq} = \left[ \left( \frac{18}{11} \right)^3 \frac{(4\pi\epsilon_0)^3 \rho g V^2}{2n_s^4 e^4 R_E} \right]^{1/4}. \quad (367)$$

Substituting this into (364) and solving for  $\Delta h$ , again using (363) for  $L$ , yields

$$\Delta h_{eq} = \sqrt{\frac{18 (4\pi\epsilon_0) 2\rho g R_E}{11 n_s^2 e^2}}, \quad (368)$$

which is the required free fall distance for the electrostatic and gravitational forces to reach equilibrium. Using  $\Delta h_{eq} = \frac{1}{2}gt_{eq}^2$  shows that the free fall time for these forces to reach equilibrium is given by

$$t_{eq} = \left[ \frac{18 (4\pi\epsilon_0) 8\rho R_E}{11 n_s^2 e^2 g} \right]^{1/4}. \quad (369)$$

Note that the equilibrium distance and time are independent of the sample dimensions and separation. The superconducting electron density (near absolute zero) is related to the London penetration depth of the superconducting material by [25]

$$n_s = \frac{m_e}{\mu_0 \lambda_L^2 e^2}, \quad (370)$$

which, for lead, has a value of  $n_{s,Pb} = 2.1 \times 10^{28}$  electrons per cubic meter, using the known value of the London penetration depth of lead  $\lambda_{L,Pb} = 37$  nm [64]. Thus, for equilibrium to be achieved, a free fall distance of  $\Delta h_{eq} \approx 5$  nm, corresponding to a free fall time of  $t_{eq} \approx 30$   $\mu$ s. Though this model assumes that the ions will accelerate at a constant rate until equilibrium is achieved, whereas in reality, the horizontal acceleration will decrease to zero as the sub-system approaches equilibrium, and therefore the required free fall distance and time are somewhat underestimated, these results suggest that the experiment may be able to be performed in a laboratory setting.

## 7.2 Experimental Detection of Charge Separation in the Earth's Tidal Gravitational Field

An experiment was performed in the Chiao lab in which two superconducting lead spheres were connected by a thin superconducting lead wire. Copper wires, which are not superconducting, were attached to the outer and inner faces of the spheres and connected to independent channels of a Techtronix model TDS2024B to measure the voltage potential across the faces. The samples were resting on a spring-loaded platform, which released the system into free fall and automatically triggered the oscilloscope.

The experiment was performed roughly 100 times. Though a change in the voltage potential was registered frequently, it was later determined that this was due to microphonic interference by the violent jarring of the apparatus imparted by the springs when the mechanism was triggered. This was verified when changes in the voltage potential were observed at temperatures above the critical temperature of lead. Since the charge separation effect is not predicted to occur in normal matter, it was this control experiment which suggested that the original measurements were false.

Furthermore, it was also determined that direct measurement of the charge separation through leads made of normal conducting material was not feasible, since the superconducting electrons cannot travel through the normal wire. However, if charge separation does exist, external electrical fields would be created near the inner and outer faces of the falling superconductors. If the electric fields were sufficiently large, one might be able to use these fields to induce a charge on a normal conducting plate, placed just outside the superconducting sample, such that the two are electrically isolated. The following section explores this possibility further, using time-varying tidal gravitational forces, instead of free fall in the Earth's gravitational field.

### 7.3 Charge Separation Induced by External Source Masses

Consider two large, diametrically-opposite source masses rotating around two stationary pendula. Consider each pendulum to have two support wires, so that the motion is constrained along one dimension. See Figure 11.

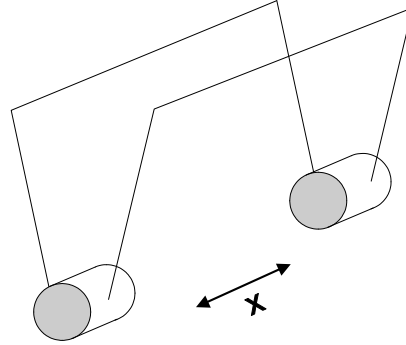


Figure 11: Pendula are supported by two wires each. This configuration causes motion along a single axis, denoted by  $x$  in the figure.

The source masses rotate around the dilution refrigerator (Oxford Instruments model DR200) containing the pendula at approximately 1 rpm, and so the angular frequency is approximately  $\omega = \frac{\pi}{30} s^{-1}$ . The gravitational forces on the pendula due to the source masses will thus be periodic in time with a period of approximately 60 seconds (a 30-second period is theoretically possible due to symmetry, but for systematic errors in the setup and design, the period will be assumed to be 60 seconds). The magnitude of the gravitational forces will vary according to Newton's inverse-square law. In each instant in time, the forces on the pendula can be calculated. Assuming that the angular frequency of the rotating source masses is sufficiently small, a quasi-static model can be implemented, in which the system is in static equilibrium at any given time.

Figure 12 shows the system at an arbitrary instant in time where  $\theta = \omega t$ . The forces  $\mathbf{F}_1$  and  $\mathbf{F}_2$  are gravitational forces exerted by the source masses.  $\mathbf{F}_3$  is the gravitational force exerted by the opposite pendulum. The separation distance between the two pendula is  $s$ . Let the vertical faces of the source masses that are (roughly) oriented radially have length  $a$ , the vertical faces facing the dilution refrigerators have length  $b$ , and the heights have dimension  $c$ .

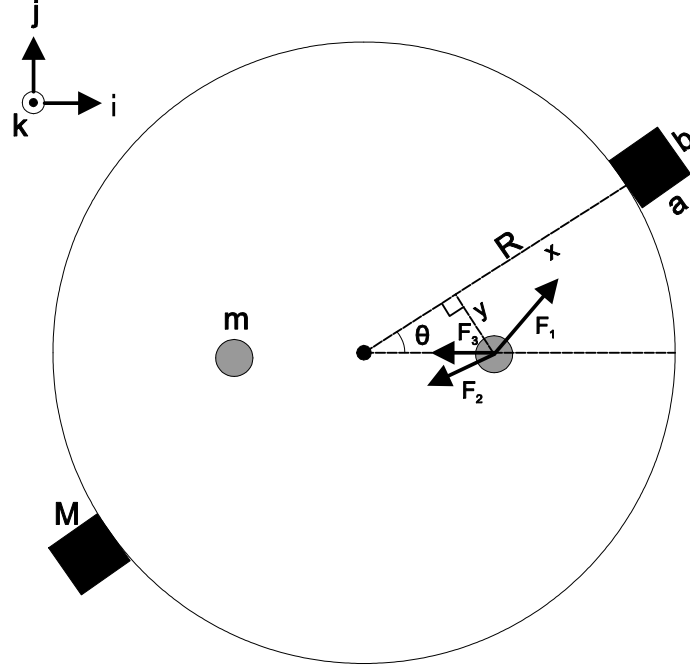


Figure 12: The experimental setup of the Cavendish-like experiment. The figure shows a snapshot of the dynamic system, where the small displacements of the pendula have, for the moment, been neglected. The coordinates  $x, y$ , and  $z$  will vary with the angle  $\theta$ , but the unit vectors  $\mathbf{i}, \mathbf{j}$ , and  $\mathbf{k}$  will remain constant as depicted in the figure. Recall that the pendula are constrained to move along the axis parallel to the unit vector  $\mathbf{i}$ .

A differential mass element  $dM$  of the upper source mass in Figure 12 exerts a differential force on the right pendulum with magnitude (direction will be considered separately) given by

$$|d\mathbf{F}_1| = \frac{Gm}{x^2 + y^2 + z^2} dM = \frac{Gm\rho}{x^2 + y^2 + z^2} dV, \quad (371)$$

where  $\rho$  is the density of the material (assumed to be uniform). Integrating this expression, we obtain the total force exerted by the upper source mass, given by

$$|\mathbf{F}_1| = Gm\rho \int_{-c/2}^{c/2} \int_{s/2 \sin \omega t - b/2}^{s/2 \sin \omega t + b/2} \int_{R-s/2 \cos \omega t}^{R-s/2 \cos \omega t + a} \frac{dx dy dz}{x^2 + y^2 + z^2}. \quad (372)$$

Similarly, the total force exerted on the right pendulum by the lower source mass in Figure 12 is



given by

$$|\mathbf{F}_2| = Gm\rho \int_{-c/2}^{c/2} \int_{s/2 \sin \omega t - b/2}^{s/2 \sin \omega t + b/2} \int_{R+s/2 \cos \omega t}^{R+s/2 \cos \omega t + a} \frac{dx dy dz}{x^2 + y^2 + z^2}. \quad (373)$$

It is stated here without proof that the angle  $\beta$  subtended by vector  $\mathbf{F}_1$  and the line joining the two pendula in Figure 12 satisfies the equations

$$\cos \beta = \sqrt{\frac{(R + a/2)^2 \cos^2 \omega t + s^2/4 - s(R + a/2) \cos \omega t}{(R + a/2)^2 + s^2/4 - s(R + a/2) \cos \omega t}} \quad (374a)$$

$$\sin \beta = \frac{(R + a/2) \sin \omega t}{\sqrt{(R + a/2)^2 + s^2/4 - s(R + a/2) \cos \omega t}} \quad (374b)$$

and that the angle  $\gamma$  subtended by  $\mathbf{F}_2$  and the line joining the two pendula in Figure 12 satisfies the equations

$$\cos \gamma = \frac{\frac{s}{2R+a} + \cos \omega t}{\sqrt{\left(\frac{s}{2R+a} + \cos \omega t\right)^2 + \sin^2 \omega t}} \quad (375a)$$

$$\sin \gamma = \frac{\sin \omega t}{\sqrt{\left(\frac{s}{2R+a} + \cos \omega t\right)^2 + \sin^2 \omega t}}, \quad (375b)$$

and thus the full expressions for the forces acting on the right pendulum in Figure 12 are given by

$$\mathbf{F}_1 = Gm\rho \int_{-c/2}^{c/2} \int_{s/2 \sin \omega t - b/2}^{s/2 \sin \omega t + b/2} \int_{R-s/2 \cos \omega t}^{R-s/2 \cos \omega t + a} \frac{dx dy dz}{x^2 + y^2 + z^2} (\cos \beta \mathbf{i} + \sin \beta \mathbf{j}) \quad (376)$$

$$\mathbf{F}_2 = Gm\rho \int_{-c/2}^{c/2} \int_{s/2 \sin \omega t - b/2}^{s/2 \sin \omega t + b/2} \int_{R+s/2 \cos \omega t}^{R+s/2 \cos \omega t + a} \frac{dx dy dz}{x^2 + y^2 + z^2} (-\cos \gamma \mathbf{i} - \sin \gamma \mathbf{j}), \quad (377)$$

assuming that the pendula and the centers of mass of the source masses are coplanar. Recalling that the pendula are constrained to move along the axis parallel to the unit vector  $\mathbf{i}$ , the unconstrained components of the forces exerted by the source masses on the right pendulum are given by

$$F_1 = Gm\rho \cos \beta \int_{-c/2}^{c/2} \int_{s/2 \sin \omega t - b/2}^{s/2 \sin \omega t + b/2} \int_{R-s/2 \cos \omega t}^{R-s/2 \cos \omega t + a} \frac{dx dy dz}{x^2 + y^2 + z^2} \quad (378)$$

$$F_2 = Gm\rho \cos \gamma \int_{-c/2}^{c/2} \int_{s/2 \sin \omega t - b/2}^{s/2 \sin \omega t + b/2} \int_{R+s/2 \cos \omega t}^{R+s/2 \cos \omega t + a} \frac{dx dy dz}{x^2 + y^2 + z^2}. \quad (379)$$

The force exerted by the left pendulum on the right pendulum is anti-parallel to  $\mathbf{i}$ , and its magnitude is given by

$$F_3 = \frac{Gm^2}{s^2}. \quad (380)$$

Viewing the right pendulum from the side, the free body diagram can be pictured as in Figure 13. Comparing the vertical and horizontal components of the vectors in Figure 13, we obtain an

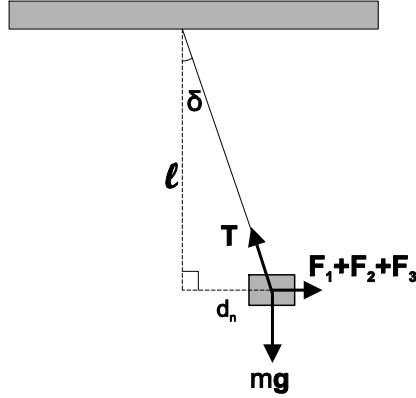


Figure 13: Free-body diagram of one pendulum acted upon by the tidal forces of the rotating source masses.

expression for the deflection magnitude  $d_n$ , given by

$$d_n \approx \frac{\ell}{mg} (F_1 - F_2 - F_3), \quad (381)$$

where we have assumed  $d_n$  to be small, so that (381) is explicit. The subscript  $n$  is used for the case that the pendula are normal, so that both the ionic lattice and the valence electron system follow the same local geodesics. It is likely that  $F_3$  can be neglected if the source masses are sufficiently large.

Let us now turn to the concept of charge separation within superconductors. Let the pendula now be superconducting, and share a continuous superconducting connection, so that the Cooper-pair wavefunction has a constant phase across both pendula. If we assume that only the ionic lattice of the pendula are subject to the gravitational forces of the source masses, a charge separation will ensue.

For the moment, let us assume that the Cooper pair wavefunction is completely rigid, and that the superfluid will therefore remain motionless with respect to the center of mass of the pendulum system, which lies approximately at the midpoint between the two pendula. This charge separation will cause Coulomb forces both between the two pendula, and within the pendula themselves. These forces must be taken into account to accurately predict the motions of the ionic lattices, and the magnitude of the charge separation.

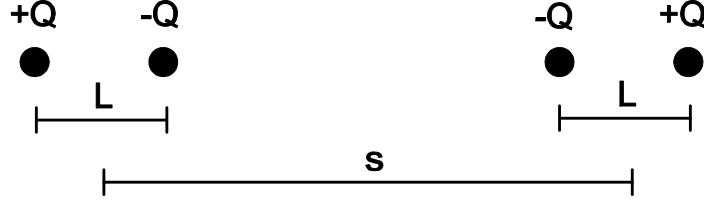


Figure 14: Superconducting pendula under the influence of tidal forces that produce charge separation. The physical dimension of the pendulum along the axis of the charge separation is given by  $L$ , and the center-to-center distance between the pendula is given by  $s$ .

Figure 14 shows the pendula at an instant in time when the ionic lattices are pulled outwards by the source masses. The charged faces of the pendula are modeled here using point charges.

Summing the Coulombic forces that the left pendulum exerts on the ionic lattice of the right pendulum in Figure 14, it can be shown that the total Coulombic force is

$$\mathbf{F}_{Q,d>0} \approx \frac{-Q^2}{4\pi\epsilon_0 s^2} \left[ \frac{L(2s+L)}{(s+L)^2} \right] \mathbf{i}, \quad (382)$$

where the charge extrusion distance  $d$  has been ignored, since  $d$  is much smaller than  $s$  and  $L$ . The Coulomb force on the ionic lattice of the right pendulum exerted by the electron superfluid within the right pendulum, due to charge separation, is

$$\mathbf{F}_{c,d>0} \approx -\frac{Q^2}{4\pi\epsilon_0 L^2} \mathbf{i}, \quad (383)$$

where the same approximation has been used. The subscript  $d > 0$  has been used since (382) and (383) are only valid when the positively-charged ionic lattice is extruded from the negatively-charged

superfluid on the outer faces of the pendula. When the signs of the charges are reversed, the forces on the ionic lattice of the right pendulum can be found by making the substitution  $L \rightarrow -L$ , so the general expression for the Coulombic forces on the right pendulum are

$$\mathbf{F}_Q \approx \frac{-Q^2}{4\pi\epsilon_0 s^2} \left\{ \frac{L \text{sgn}(d) [2s + L \text{sgn}(d)]}{[s + L \text{sgn}(d)]^2} \right\} \mathbf{i} \quad (384)$$

and

$$\mathbf{F}_c \approx -\frac{Q^2 \text{sgn}(d)}{4\pi\epsilon_0 L^2} \mathbf{i}, \quad (385)$$

where

$$\text{sgn}(d) = \begin{cases} 1, & d > 0 \\ 0, & d = 0 \\ -1, & d < 0 \end{cases} \quad (386)$$

Considering all forces on a single superconducting pendulum, we have a model that is similar to that depicted in Figure 13, but  $\mathbf{F}_Q$  and  $\mathbf{F}_c$  are considered, in addition to  $\sum_{i=1}^3 \mathbf{F}_i$ . For this case,

$$d \approx \frac{\ell}{mg} (F_1 - F_2 - F_3 - F_Q - F_c), \quad (387)$$

where  $F_Q$  and  $F_c$  are the magnitudes of the vectors defined in (384) and (385), respectively.

The extruded charge  $Q$  depends on the extrusion length. Starting with

$$Q = 2en_s V, \quad (388)$$

where  $n_s$  is the superconducting electron density,  $-2e$  is the Cooper pair charge, and  $V$  is the extrusion volume. The current experimental design involves cylindrically-shaped pendula, so (388) becomes

$$Q = 2en_s \pi r^2 d, \quad (389)$$

where  $r$  is the cylindrical radius of the sample. Thus,

$$d = \frac{Q}{2en_s\pi r^2}, \quad (390)$$

and it is noted that

$$\text{sgn}(d) = \text{sgn}(Q). \quad (391)$$

Substitution of (390) and (391) into (387), we have

$$Q = \frac{2en_s\pi r^2\ell}{mg} \left( F_1 - F_2 - F_3 - \frac{Q^2\text{sgn}(Q)}{4\pi\epsilon_0 s^2} \left\{ \frac{L[2s + L\text{sgn}(Q)]}{[s + L\text{sgn}(Q)]^2} \right\} - \frac{Q^2\text{sgn}(Q)}{4\pi\epsilon_0 L^2} \right). \quad (392)$$

The feasibility of detecting this charge in the laboratory will be discussed in Section 7.5.

## 7.4 Beyond First Order: Exploring the Zero-Momentum Approximation

In the previous sections, the approximation was made that the electron superfluid of the superconducting sample had infinite quantum rigidity. This approximation is only valid if the wavefunction is sufficiently incompressible when acted upon by weak tidal gravitational fields, as well as sufficiently incompressible when compared to the ionic lattice of the system to cause a charge separation. To show that this is the case, consider the complex order parameter  $\varphi$  in the Ginzburg-Landau theory of superconductivity. The complex order parameter for a semi-infinite superconductor (where the superconductor resides in the half-plane  $x > 0$ ) is the solution to the time-independent, non-linear Schrödinger equation

$$-\frac{\hbar^2}{4m_e}\nabla^2\varphi + \alpha\varphi + \frac{\beta}{2}|\varphi|^2\varphi = 0, \quad (393)$$

where  $\alpha$  and  $\beta$  are phenomenological parameters given by

$$\alpha = -\frac{\hbar^2}{4m_e\xi_0^2} \quad (394)$$

$$\beta = \frac{\mu_0\hbar^4}{16m_e^2\xi_0^4B_c^2}, \quad (395)$$

where  $\xi_0$  is the coherence length, and  $B_c$  is the critical magnetic field of the superconducting material.

The solution to (393) is given by [65]

$$\varphi = \varphi_0 \tanh(Cx), \quad (396)$$

where  $C \equiv \frac{1}{\sqrt{2}\xi_0}$ , and

$$\varphi_0 = \sqrt{\frac{2|\alpha|}{\beta}} = \frac{2\xi_0 B_c}{\hbar} \sqrt{\frac{2m_e}{\mu_0}}, \quad (397)$$

is the value of  $\varphi$  at positive infinity. For a finite superconductor, the complex order parameter is well approximated by

$$\varphi(x) = \varphi_0 \{ \tanh(Cx) + \tanh[C(L-x)] - 1 \}, \quad (398)$$

where  $L$  is the length of the sample in the  $x$  dimension. The form of (398) was determined by noting the qualitative similarity of the hyperbolic tangent function and the Heaviside function. Figure 15 shows the analytical solutions for two semi-infinite superconductors (where  $C = 1$  arbitrary unit of inverse length and  $L = 10$  units of length), and the approximate solution for a finite superconductor, given by (398). The approximation is valid as long as the length  $L$  of the finite superconductor is much greater than the coherence length  $\xi_0$ .

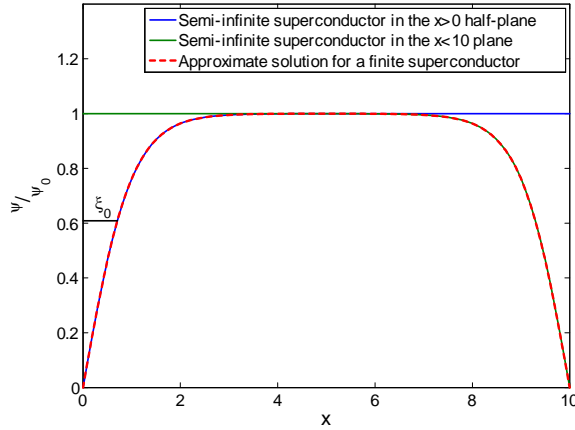


Figure 15: Plot of complex order parameters for semi-infinite superconductors, and an approximation for a finite superconductor.

The free energy density of a superconductor is given by [25]

$$f = f_{n0} + \alpha |\varphi|^2 + \frac{\beta}{2} |\varphi|^4 + \frac{1}{4m_e} \left| \left( -i\hbar \frac{d}{dx} - 2eA - 2m_e h \right) \varphi \right|^2 + \frac{B^2}{2\mu_0}, \quad (399)$$

where DeWitt's minimal coupling rule [15] has been included to account for tidal gravitational fields. The factors of 2 that appear in the minimal coupling rule in this expression are due to the fact that the mass and charge of a Cooper pair are twice that of a single electron. Near  $T = 0$ , and in the

absence of any persistent currents or external electromagnetic fields, this becomes

$$\begin{aligned}
f &= \alpha |\varphi|^2 + \frac{\beta}{2} |\varphi|^4 + \frac{1}{4m_e} \left| \left( -i\hbar \frac{d}{dx} - 2m_e h \right) \varphi \right|^2 \\
&= \alpha |\varphi|^2 + \frac{\beta}{2} |\varphi|^4 + \frac{1}{4m_e} \left| \left( -i\hbar \frac{d}{dx} - 2m_e \frac{gt}{R_E} x \right) \varphi \right|^2 \\
&= \alpha \varphi^2 + \frac{\beta}{2} \varphi^4 + \frac{1}{4m_e} \left[ \hbar^2 \left( \frac{d\varphi}{dx} \right)^2 + 4m_e^2 \left( \frac{gt}{R_E} \right)^2 x^2 \varphi^2 \right] \\
&= \left[ \alpha + m_e \left( \frac{gt}{R_E} \right)^2 x^2 \right] \varphi^2 + \frac{\beta}{2} \varphi^4 + \frac{\hbar^2}{4m_e} \left( \frac{d\varphi}{dx} \right)^2.
\end{aligned} \tag{400}$$

The derivative of  $\varphi$  is equal to

$$\frac{d\varphi}{dx} = C\varphi_0 \{ \operatorname{sech}^2(Cx) - \operatorname{sech}^2[C(L-x)] \}, \tag{401}$$

and so the free energy density is

$$\begin{aligned}
f &= \left[ \alpha + m_e \left( \frac{gt}{R_E} \right)^2 x^2 \right] \varphi_0^2 \{ \tanh(Cx) + \tanh[C(L-x)] - 1 \}^2 \\
&\quad + \frac{\beta}{2} \varphi_0^4 \{ \tanh(Cx) + \tanh[C(L-x)] - 1 \}^4 + \frac{\hbar^2}{4m_e} C^2 \varphi_0^2 \{ \operatorname{sech}^2(Cx) - \operatorname{sech}^2[C(L-x)] \}^2.
\end{aligned} \tag{402}$$

The force is equal to the derivative with respect to  $L$  of the free energy, which is equal to the integral with respect to  $x$  of the free energy density, so by the fundamental theorem of calculus,

$$F = \frac{dE}{dL} = \frac{d}{dL} \int_0^L f(x) dx = f(L), \tag{403}$$

which is equal to

$$F = f(L) = \left[ \alpha + m_e \left( \frac{gt}{R_E} \right)^2 L^2 \right] \varphi_0^2 [\tanh(CL) - 1]^2 + \frac{\beta}{2} \varphi_0^4 [\tanh(CL) - 1]^4 + \frac{\hbar^2}{4m_e} C^2 \varphi_0^2 \{ \operatorname{sech}^2(CL) - 1 \}^2. \tag{404}$$

This force is on the order of Newtons for aluminum, and kilo-Newtons for lead. Since the tidal gravitational field of the Earth will not produce these forces under ordinary circumstances (i.e.



realistic masses and separation distances), the zero-momentum approximation is valid while the entire electron superfluid remains in the BCS ground state.

## 7.5 Experimental Detection of Charge Separation Induced by External Source Masses

Two stacks of lead bricks were diametrically placed on a heavy-duty rotating platform (Synergy model 788088). Each stack has a mass of approximately 430 kg. Figure 16 shows a drawing of the experimental configuration. Since there are several ways to orient the bricks, the orientation used

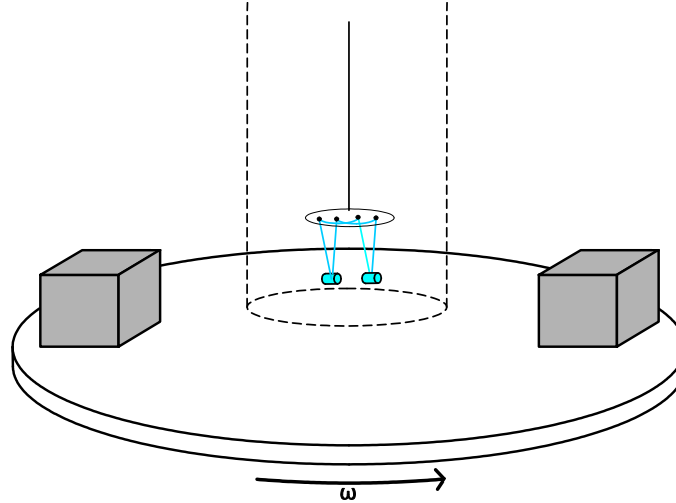


Figure 16: A drawing of the experimental setup used in the charge separation experiment. The grey blocks are lead masses of approximately 430 kg each, which are placed on a rotating turntable. The dashed line is a stationary dilution refrigerator, containing the superconducting pendula. The pendula are the only superconducting material used in the experiment.

was that which gave the largest outward deflection of the pendula when the line joining the centers of the source masses is co-linear with the line joining the axis of the pendula, found by evaluating the integral in (378) for all possible combinations of  $a$ ,  $b$ , and  $c$ . It was found that  $a=6$  in,  $b=24$  in, and  $c=16$  in led to this maximum deflection. These values (in meters) were used in calculation of the forces that appear in the expression for the charge in (392). Solving this expression explicitly for  $Q$  is non-trivial, so a numerical method was used, with fixed values determined by actual experimental constraints. The expressions for  $F_1$  and  $F_2$  were evaluated separately, using an adaptive Simpson quadrature numerical integration method. Figure 17 shows the expected charge as a function of time using realistic values for the experiment to be performed in a laboratory setting.

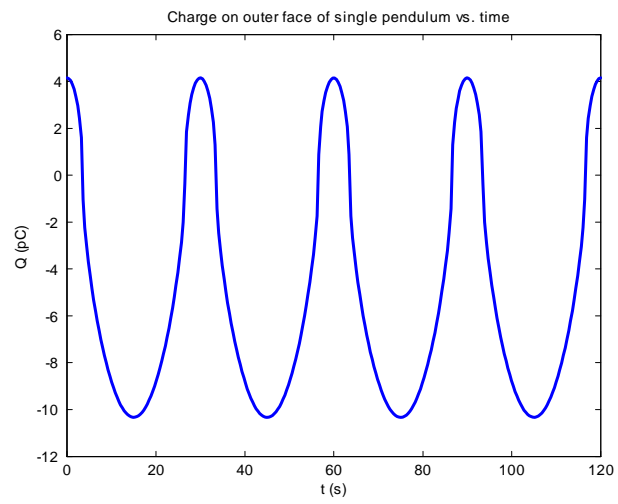


Figure 17: Charge vs. time in the charge separation experiment.

## 7.6 Experimental Results and Conclusions

The data collected from the electrometer failed to reproduce the predicted curve depicted in Figure 17. The electrometer showed a DC offset of approximately 3 pC at its most sensitive detection range. The specifications for the electrometer state that variations in charge in the femto-Coulomb range should be detectable. However, the charge signal remained flat during the rotation of the masses, with a noise floor of roughly 400 fC. Data was continuously collected and averaged while the masses were stationary, continuously collected and averaged again after rotating the masses by 90 degrees, where the largest difference was expected, and the two sets were compared to see if any difference was present. No substantial difference was observed.

However, with full credit to be given to Luis Martinez, this negative result may be able to be explained using the London equation

$$\mathbf{E} = \mu_0 \lambda_L^2 \frac{\partial \mathbf{j}}{\partial t} = 2\mu_0 \lambda_L^2 n_s e \frac{\partial \mathbf{v}}{\partial t}, \quad (405)$$

where current density  $\mathbf{j} = 2n_s e \mathbf{v}$ . This equation shows that a DC electric field within a superconductor will accelerate Cooper-pair electrons to infinite velocities, which is unphysical. Thus, only the electric field that arises due to the Schiff-Barnhill effect can be present within a superconductor.

If the charge separation predicted in the preceding experiment were to occur, charge layers would be formed that have a voltage potential between them of approximately 1 volt. Thus, kinetic energy would be imparted to the Cooper-pair electrons with a magnitude on the order of an electron volt. The BCS energy gap for temperatures  $T \ll T_c$  is well-approximated by

$$E_{\text{gap}} \approx 3.5 k_B T_c, \quad (406)$$

where  $k_B$  is Boltzmann's constant, and  $T_c$  is the critical temperature of the material. Using the known value of the critical temperature of aluminum ( $T_{c,Al} = 1.1 \text{ K}$  [64]), the gap energy is less than 1 meV, suggesting that pair-breaking within the electron superfluid is a more energetically favorable

outcome than low-frequency charge separation. It is noted that the experiments were performed at temperatures of approximately 30 mK, so the approximation in (406) is valid.

Thus, it is expected that when low-frequency relative motion exists between the ions and the electron superfluid, pair-breaking occurs so that normal electrons accumulate to oppose the electric field induced by the gravitational field. At first glance, it appears that no charge separation can exist within the superconductor, and that the arguments presented in favor of the reflection of gravitational radiation from a thin superconducting film are invalid. However, (405) only precludes low-frequency electric fields from existing within a superconductor. For sufficiently large superconducting films, and sufficiently high gravitational radiation frequencies, reflection can occur. As discussed in Section 6.8, there should always be a regime where the superconductor will respond linearly to the gravitational radiation field, thus making efficient mirrors for gravitational radiation a possibility.

These results suggest that charge separation within superconductors will not occur in the presence of low-frequency/high-amplitude gravitational radiation, but the possibility of charge separation in the presence of high-frequency/low-amplitude gravitational radiation remains.

## 8 Gravitational Wave Transducer Experiment

Section 6.11 discussed transduction between gravitational wave power and electromagnetic wave power. Experiments have been performed in the Chiao lab on using efficient conversion between the two types of waves to communicate using gravitational carrier waves. The transmitter apparatus consisted of a two-body superconducting system that would convert microwave-frequency EM input to a GR output at the same frequency. The emitted GR waves should scatter from a second two-body superconducting system in a receiver apparatus to create EM radiation that could be detected with a quadrupole antenna.

### 8.1 Brief Outline of Proposed Experiment

There is no physical principle which forbids the conversion of electromagnetic wave energy into gravitational wave energy, or vice versa. Here a method is proposed to perform this conversion efficiently using macroscopically coherent, charged quantum matter. Specifically, it is proposed that the use of pairs of charged superconducting spheres at cryogenic temperatures as efficient “quantum transducers” for this wave-to-wave conversion process. The charge on the spheres enables them to couple to electromagnetic radiation, and their mass enables them to couple to gravitational radiation. The superconductors possess a macroscopic quantum coherence that makes the wave-to-wave conversion process efficient. The spheres and their separations are designed to be comparable in size to the microwave wavelength of the radiations which are being converted from one form to the other, so that the system becomes an efficient quadrupole antenna for coupling to both kinds of radiations. Important applications to communications would immediately follow from a successful implementation of this kind of device, since the Earth is transparent to gravitational radiation.

Based upon the linearization of Einstein’s field equations, and the BCS theory of superconductivity, the Chiao group at UC Merced has recently shown it to be theoretically possible to build a high-efficiency communications transceiver that converts electromagnetic radiation to gravitational radiation and vice-versa using the above two-charged-superconducting-sphere configurations. An

impedance-matched transceiver has been shown in principle to be able to convert an input of 1 mW of electromagnetic wave power to 0.5 mW of gravitational wave power.

The interaction of charged, macroscopically coherent quantum systems, such as a pair of charged superconducting spheres, with both electromagnetic and gravitational waves, is to be studied experimentally. When the charge-to-mass ratio of a pair of identical spheres is adjusted so as to satisfy the “criticality condition”  $Q/M = \sqrt{4\pi\epsilon_0 G}$ , where  $\epsilon_0$  is the permittivity of free space, and  $G$  is Newton’s gravitational constant, the attractive gravitational force will be balanced against the repulsive electrostatic force between the two spheres. At criticality, when these two spheres undergo simple harmonic motion relative to each other, they will generate equal amounts of GR and EM radiations in an equipartition of energy. If the spheres are superconducting, they will also scatter an incoming GR or EM wave into equal amounts of GR and EM radiations.

The superconducting spheres possess an energy gap (the BCS gap) separating the ground state from all excited states. The quantum adiabatic theorem then implies that the quantum phase everywhere inside the superconductors, in their linear response to both kinds of weak incident electromagnetic and gravitational radiation fields, whose frequencies are less than the BCS gap frequency, such as at microwave frequencies, will remain single-valued at all positions and times. This linear response of these coherent quantum systems leads to hard-wall boundary conditions at the surfaces of the spheres, in which both the incident EM and GR radiation fields will undergo specular reflections at the surfaces of these superconducting spheres. Therefore the scattering cross-sections for both kinds of radiation fields will be quite large, being on the order of  $\sigma = 2\pi a^2$ , where  $a$  is the radius of the spheres, when the radii are comparable in size to the microwave wavelength. The distance separating the two spheres will also be assumed to be comparable to the microwave wavelength. Under these circumstances, the Mie scattering cross-sections of pairs of charged superconducting spheres for both EM and GR radiations at microwave frequencies will be large enough to be detected.

At sufficiently low temperatures with respect to the BCS gap, all dissipative degrees of freedom of the spheres will be frozen out by the Boltzmann factor. Then, at criticality, there will be an

equipartition of energy into both kinds of scattered radiation, so that the scattering cross-section is the same for the time-reverse process as for the time-forward process, by time-reversal symmetry. This implies that a Hertz-like experiment, i.e., a transmitter-receiver (or “transceiver”) experiment, in which GR waves are generated at the transmitter by EM microwaves incident on a pair of charged superconducting spheres at criticality, and detected at the receiver by another pair of charged superconducting (impedance-matched) spheres at criticality in a separate, EM shielded apparatus. This would enable a communication device to make use of gravitational carrier waves, which, unlike electromagnetic carrier waves, are not prone to mass-based attenuation.



## 8.2 Levitation of Gravitational Wave Scatterers

One important aspect in the early stages of the transduction experiment was the levitation of the quantum-coherent systems. Initially, charged superfluid helium drops were to be used, since they exhibit the necessary quantum mechanical properties, such as a gap-protected ground state, required for EM and GR wave transduction. Liquid helium drops can be levitated by inhomogeneous magnetic fields [66], such as those created by a pair of coaxial, current-carrying coils, with their currents oppositely oriented. In the special case that the radius of the coils is equal to the separation distance, the system is commonly called a set of anti-Helmholtz coils. The magnetic energy density of the inhomogeneous field is given by

$$U = \frac{B^2 \chi}{2\mu_0}, \quad (407)$$

where  $\chi$  is the magnetic susceptibility. Since liquid helium is diamagnetic,  $\chi$  is negative, and therefore a force given by

$$F = -\nabla U = -\frac{\chi}{2\mu_0} \nabla (B^2) \quad (408)$$

will act to accelerate the helium drop towards the point of lowest field magnitude. Thus, for levitation,

$$\frac{|\chi|}{\mu_0} \left| B \frac{\partial B}{\partial z} \right| \geq \rho g, \quad (409)$$

where  $\rho$  is the mass density of liquid helium. Using these known values [67], the required value of  $\left| B \frac{\partial B}{\partial z} \right|$  is 20.7 T<sup>2</sup> per cm. However, for the spatial constraints of the dilution refrigerator systems in the Chiao lab, this required a current density of 70 kA per square cm within the magnetic coils, which exceeded the maximum current density of 10 kA per square meter. Thus, a magnet which would generate this force was not possible to integrate into the cryogenic system.

A superconductor shares many of the same quantum mechanical properties of superfluid helium, and is a perfect diamagnet, where  $\chi = -1$ . Since the molar susceptibility of liquid helium is on the order of  $10^{-6}$  [68], much weaker levitation forces are required for superconductors, despite a larger mass density. For superconducting lead, levitation can be achieved when  $\left| B \frac{\partial B}{\partial z} \right|$  is smaller by a

factor on the order of  $10^4$  as compared to liquid helium.

The situation is slightly more complicated, however, as a pair of oppositely-oriented coils has only one stable equilibrium point, and two objects are required for efficient transduction (see Section 6.9).

The following sections describe specific levitation methods that were considered for the experiment.

### 8.2.1 Electrostatic Levitation Using a Charged Ring, and Extending Earnshaw’s Theorem to Include Neutral, Polarizable Particles

**Introduction** In this tribute in honor of the memory of Prof. Dr. Herbert Walther, we consider the possibility of extending his famous work on the trapping of an ordered lattice of ions [69] in a Paul trap [70], to the trapping of neutral atoms, and more generally, to the levitation of a macroscopic neutral polarizable object, in a purely electrostatic trap, for example, in the DC electric field configuration of a charged ring. Earnshaw’s theorem will be extended to the case of such neutral objects, and we shall show below that the stable levitation and trapping of a neutral, polarizable object, which is a high-field seeker, is generally impossible in an arbitrary electrostatic field configuration. We shall do this first for the special case of the electrostatic configuration of a simple charged ring, and then for the general case of any DC electric field configuration.

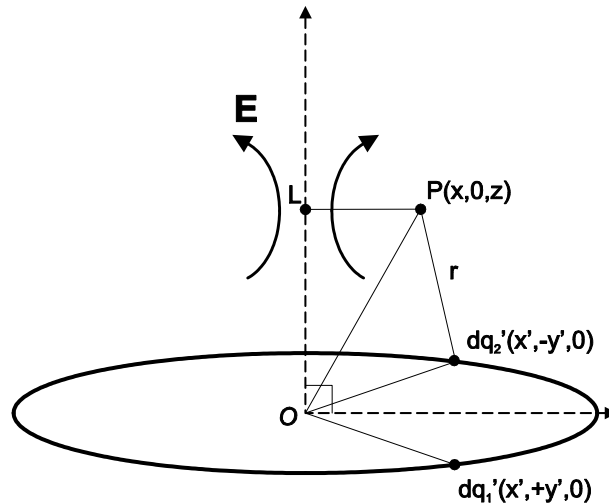


Figure 18: A uniformly charged ring with radius  $a$  lies on the horizontal  $x$ - $y$  plane, with its axis of symmetry pointing along the vertical  $z$  axis. Can levitation and trapping of a neutral particle occur stably near point  $L$ , where there is a convergence of  $\mathbf{E}$ -field lines?

Consider the charged-ring geometry shown in Figure 18. The region near the so-called “levitation” point  $L$  in this figure is akin to the focal region of a lens in optics. Just as two converging rays of light emerging from a lens in physical optics cannot truly cross at a focus, but rather will undergo an “avoided crossing” near the focal point of this lens due to diffraction, so likewise two

converging lines of the electric field cannot cross, and therefore they will also undergo an “avoided crossing” near  $L$ . There results a maximum in the  $z$  component of the electric field along the vertical  $z$  axis at point  $L$ . The resulting “avoided crossing” region of electric field lines in the vicinity of point  $L$  is therefore similar to the Gaussian beam-waist region of a focused laser beam. Ashkin and his colleagues [71] showed that small dielectric particles, which are high-field seekers, are attracted to, and can be stably trapped at, such Gaussian beam waists in “optical tweezers”. Similarly here a neutral dielectric particle, which is a high-field seeker, will also be attracted to the region of the convergence of  $\mathbf{E}$ -field lines in the neighborhood of  $L$ , where there is a local maximum in the electric field along the  $z$  axis. The question arises: Can such a high-field seeker be *stably* levitated and trapped near  $L$ ?

**Calculation of the Electric Potential and Field of a Charged Ring** The electric potential at the field point  $P$  due to a charge element  $dq'$  of the ring is given in by

$$d\Phi = \frac{dq'}{r} \quad (410)$$

where the distance  $r$  from the source point, whose coordinates are  $(x', y', 0)$ , to the field point  $P$ , whose coordinates are  $(x, 0, z)$ , is

$$r = \sqrt{(x' - x)^2 + y'^2 + z^2}. \quad (411)$$

(Primed quantities refer to the source point; unprimed ones to the field point). Since the charged ring forms a circle of radius  $a$  which lies on the horizontal  $x$ - $y$  plane,

$$x'^2 + y'^2 = a^2. \quad (412)$$

An infinitesimal charge element  $dq'$  spanning an infinitesimal azimuthal angle of  $d\phi'$  can be expressed as follows:

$$dq' = \left(\frac{Q}{2\pi a}\right) ad\phi' = -\left(\frac{Q}{2\pi a}\right) \frac{ad(x'/a)}{\sqrt{1 - (x'/a)^2}} \quad (413)$$

where  $Q$  is the total charge of the ring. Let us introduce the dimensionless variables

$$\xi' \equiv \frac{x'}{a}, \quad \eta' \equiv \frac{y'}{a}, \quad \zeta \equiv \frac{z}{a}, \quad \varepsilon \equiv \frac{x}{a}. \quad (414)$$

Thus

$$dq' = -\frac{Q}{2\pi} \frac{d\xi'}{\sqrt{1 - \xi'^2}}.$$

Due to the bilateral symmetry of the ring under the reflection  $y' \rightarrow -y'$ , it is useful to sum up in pairs the contribution to the electric potential from symmetric pairs of charge elements, such as  $dq'_1$  and  $dq'_2$  with coordinates  $(x', +y', 0)$  and  $(x', -y', 0)$ , respectively, shown in Figure 18. These

two charge elements contribute equally to the electric potential  $\Phi$  if they span the same infinitesimal azimuthal angle  $d\phi'$ . Thus one obtains

$$\Phi(\varepsilon, \zeta) = \frac{Q}{\pi a} \int_{-1}^{+1} d\xi' \frac{1}{\sqrt{1-\xi'^2}} \frac{1}{\sqrt{\varepsilon^2 - 2\varepsilon\xi' + 1 + \zeta^2}} . \quad (415)$$

Along the  $z$  axis, this reduces to the well-known result

$$\Phi(\varepsilon = 0, \zeta) = \frac{Q}{a} \frac{1}{\sqrt{1+\zeta^2}} = \frac{Q}{\sqrt{z^2 + a^2}} . \quad (416)$$

The  $z$  component of the electric field, which is the dominant  $E$ -field component in the neighborhood of point  $L$ , is given by

$$E_z = -\frac{\partial\Phi}{\partial z} = \frac{Q}{\pi a^2} \zeta \int_{-1}^{+1} d\xi' \frac{1}{\sqrt{1-\xi'^2}} \frac{1}{\left(\sqrt{\varepsilon^2 - 2\varepsilon\xi' + 1 + \zeta^2}\right)^3} . \quad (417)$$

Along the  $z$  axis, this also reduces to the well-known result

$$E_z = \frac{Qz}{(z^2 + a^2)^{3/2}} , \quad (418)$$

which has a maximum value at

$$z_0 = \frac{a}{\sqrt{2}} \text{ or } \zeta_0 = \frac{1}{\sqrt{2}} . \quad (419)$$

The “levitation” point  $L$  then has the coordinates

$$L \left( 0, 0, \frac{a}{\sqrt{2}} \right) , \quad (420)$$

neglecting for the moment the downwards displacement of a light particle due to gravity.

The potential energy  $U$  for trapping a neutral particle with polarizability  $\alpha$  in the presence of

an electric field  $(E_x, E_y, E_z)$  is given by

$$U = -\frac{1}{2}\alpha(E_x^2 + E_y^2 + E_z^2) \approx -\frac{1}{2}\alpha E_z^2, \quad (421)$$

since the contributions to  $U$  from the  $x$  and  $y$  components of the electric field, which vanish as  $\varepsilon^4$  near the  $z$  axis for small  $\varepsilon$ , can be neglected in a small neighborhood of  $L$ .

We now calculate the curvature at the bottom of the potential-energy well  $U$  along the longitudinal  $z$  axis, and also along the transverse  $x$  axis. The force on the particle is given by

$$\mathbf{F} = -\nabla U. \quad (422)$$

Therefore the  $z$  component of the force is, to a good approximation,

$$F_z = \alpha E_z \frac{\partial E_z}{\partial z}, \quad (423)$$

and the Hooke's law constant  $k_z$  in the longitudinal  $z$  direction is given by

$$k_z = -\frac{\partial F_z}{\partial z} = -\alpha \left\{ \left( \frac{\partial E_z}{\partial z} \right)^2 + E_z \frac{\partial^2 E_z}{\partial z^2} \right\}, \quad (424)$$

where all quantities are to be evaluated at  $L$  where  $\varepsilon = 0$  and  $\zeta_0 = 1/\sqrt{2}$ . Taking the indicated derivatives and evaluating them at  $L$ , one obtains

$$k_z|_L = +\frac{32}{81} \frac{\alpha Q^2}{a^6}, \quad (425)$$

where the positive sign indicates a longitudinal stability of the trap in the vertical  $z$  direction.

The  $x$  component of the force is, to the same approximation,

$$F_x = \alpha E_z \frac{\partial E_z}{\partial x}, \quad (426)$$

and the Hooke's law constant  $k_x$  in the transverse  $x$  direction is

$$k_x = -\frac{\partial F_x}{\partial x} = -\alpha \left\{ \left( \frac{\partial E_z}{\partial x} \right)^2 + E_z \frac{\partial^2 E_z}{\partial x^2} \right\}, \quad (427)$$

where again all quantities are to be evaluated at  $L$  where  $\varepsilon = 0$  and  $\zeta_0 = 1/\sqrt{2}$ . Again taking the indicated derivatives and evaluating them at  $L$ , one obtains

$$k_x|_L = -\frac{16}{81} \frac{\alpha Q^2}{a^6}, \quad (428)$$

where the negative sign indicates a transverse instability in the horizontal  $x$  direction.

Similarly, the Hooke's law constant  $k_y$  in the transverse  $y$  direction is

$$k_y|_L = -\frac{16}{81} \frac{\alpha Q^2}{a^6}, \quad (429)$$

where the negative sign indicates a transverse instability in the horizontal  $y$  direction. Note that the trap is azimuthally symmetric around the vertical axis, so that the  $x$  and  $y$  directions are equivalent to each other. Because of the negativity of two of the three Hooke's constants  $k_x$ ,  $k_y$ , and  $k_z$ , the trap will be unstable for small displacements in two of the three spatial dimensions near  $L$ , and hence  $L$  is a saddle point. Note also that the sum of the three Hooke's constants in Equations (425),(428), and (429) is zero, i.e.,

$$k_x + k_y + k_z = 0. \quad (430)$$



**Earnshaw's Theorem Revisited** We shall see that Equation (430) can be derived from Earnshaw's theorem when one generalizes this theorem from the case of a charged particle to the case of a neutral, polarizable particle in an arbitrary DC electrostatic field configuration. A quantitative consideration of the force on the particle due to the uniform gravitational field of the Earth, in conjunction with the force due to the DC electrostatic field configuration, does not change the general conclusion that the mechanical equilibrium for both charged and neutral polarizable particles is unstable.

**Charged Particle Case** We shall first briefly review here Earnshaw's theorem [72], which implies an instability of a charged particle placed into any configuration of electrostatic fields in a charge-free region of space in the absence of gravity. Suppose that there exist a point  $L$  of mechanical equilibrium of a charged particle with charge  $q$  in the presence of arbitrary DC electrostatic fields in empty space. The potential  $\Phi$  for these fields obey Laplace's equation

$$\nabla^2\Phi = \frac{\partial^2\Phi}{\partial x^2} + \frac{\partial^2\Phi}{\partial y^2} + \frac{\partial^2\Phi}{\partial z^2} = 0. \quad (431)$$

Now the force on the charged particle is given by

$$\mathbf{F} = -q\nabla\Phi = -q \left\{ \mathbf{e}_x \frac{\partial\Phi}{\partial x} + \mathbf{e}_y \frac{\partial\Phi}{\partial y} + \mathbf{e}_z \frac{\partial\Phi}{\partial z} \right\} = \langle F_x, F_y, F_z \rangle, \quad (432)$$

where  $\mathbf{e}_x, \mathbf{e}_y, \mathbf{e}_z$  are the three unit vectors in the  $x, y$ , and  $z$  directions, respectively. By hypothesis, at the point  $L$  of mechanical equilibrium

$$\left. \frac{\partial\Phi}{\partial x} \right|_L = \left. \frac{\partial\Phi}{\partial y} \right|_L = \left. \frac{\partial\Phi}{\partial z} \right|_L = 0. \quad (433)$$

*Stable* equilibrium would require all three Hooke's constants  $k_x$ ,  $k_y$ , and  $k_z$  at point  $L$  to be positive definite, i.e.,

$$k_x = - \left. \frac{\partial F_x}{\partial x} \right|_L = + \left. \frac{\partial^2 \Phi}{\partial x^2} \right|_L > 0 \quad (434)$$

$$k_y = - \left. \frac{\partial F_y}{\partial y} \right|_L = + \left. \frac{\partial^2 \Phi}{\partial y^2} \right|_L > 0 \quad (435)$$

$$k_z = - \left. \frac{\partial F_z}{\partial z} \right|_L = + \left. \frac{\partial^2 \Phi}{\partial z^2} \right|_L > 0. \quad (436)$$

However, Laplace's equation, Equation (431), can be rewritten as follows:

$$k_x + k_y + k_z = 0, \quad (437)$$

i.e., the sum of the three components of Hooke's constants for the charged particle must be exactly zero. The simultaneous positivity of all three Hooke's constants is inconsistent with this, and hence at least one of the Hooke's constants along one of the three spatial directions must be negative. Therefore the system is unstable.

The azimuthally symmetric field configurations like that of a charged ring is an important special case. Let  $z$  be the vertical symmetry axis of the ring. Suppose that there is stability in the longitudinal  $z$  direction (such as along the  $z$  axis above point  $L$ ), so that

$$k_z > 0. \quad (438)$$

By symmetry

$$k_x = k_y \equiv k_{\perp} \quad (439)$$

so that Equation (437) implies that

$$k_{\perp} = -\frac{1}{2}k_z < 0, \quad (440)$$

implying instability in the two transverse  $x$  and  $y$  directions.

Conversely, suppose there is instability in the longitudinal  $z$  direction (such as along the  $z$  axis below point  $L$ ), so that

$$k_z < 0 . \tag{441}$$

Again, by symmetry

$$k_x = k_y \equiv k_\perp \tag{442}$$

so that Equation (437) implies that

$$k_\perp = -\frac{1}{2}k_z > 0,$$

implying stability in the two transverse  $x$  and  $y$  directions.

### Adding a Uniform Gravitational Field Such as the Earth's, in the Case of a Charged

**Object** The potential energy of a charged, massive particle in a DC electrostatic field in the presence of Earth's gravitational field is

$$U_{tot} = q\Phi + mgz. \quad (443)$$

Note that the term due to gravity, i.e., the  $mgz$  term, is linear in  $z$ , and therefore will vanish upon taking the second partial derivatives of this term. Therefore the Hooke's constants  $k_x$ ,  $k_y$ , and  $k_z$  will be unaffected by Earth's gravity. The force on the particle is

$$\mathbf{F}_{tot} = -\nabla U_{tot} = -q\nabla\Phi - mg\mathbf{e}_z \quad (444)$$

where  $\mathbf{e}_z$  is the unit vector in the vertical  $z$  direction. In equilibrium,  $\mathbf{F}_{tot} = 0$ , but this equilibrium is again unstable, since upon taking another partial derivative of the term  $mg\mathbf{e}_z$  with respect to  $z$  will yield zero, and therefore all of the above Hooke's law constants are the same in the presence as in the absence of Earth's gravity.

**Generalization to the Case of a Neutral, Polarizable Particle** Now suppose that there exists a point  $L$  of mechanical equilibrium of the neutral particle with positive polarizability  $\alpha > 0$  somewhere within an arbitrary electrostatic field configuration. Such a particle is a high-field seeker, and hence point  $L$  must be a point of high field strength. Choose the coordinate system so that the  $z$  axis is aligned with respect to the local dominant electric field at point  $L$ . Thus the dominant electric field component at  $L$  is thus  $E_z$ . The potential energy  $U$  for a neutral particle with polarizability  $\alpha$  in the presence of an electric field  $(E_x, E_y, E_z)$  is given by

$$U = -\frac{1}{2}\alpha(E_x^2 + E_y^2 + E_z^2) \approx -\frac{1}{2}\alpha E_z^2, \quad (445)$$

since the contributions to  $U$  from the  $x$  and  $y$  components of the electric field, which vanish as  $\varepsilon^4$  near the  $z$  axis for small  $\varepsilon$ , can be neglected in a small neighborhood of  $L$ . The force on the particle is

$$\mathbf{F} = -\nabla U. \quad (446)$$

Therefore the  $z$  component of the force is, to a good approximation,

$$F_z = \alpha E_z \frac{\partial E_z}{\partial z}, \quad (447)$$

and the Hooke's law constant  $k_z$  in the  $z$  direction is given by

$$k_z = -\frac{\partial F_z}{\partial z} = -\alpha \left\{ \left( \frac{\partial E_z}{\partial z} \right)^2 + E_z \frac{\partial^2 E_z}{\partial z^2} \right\} \Big|_L = -\alpha E_z \frac{\partial^2 E_z}{\partial z^2} \Big|_L, \quad (448)$$

where the last equality follows from the hypothesis of mechanical equilibrium at point  $L$ .

Similarly, the  $x$  component of the force is, to the same approximation,

$$F_x = \alpha E_z \frac{\partial E_z}{\partial x}, \quad (449)$$

and the Hooke's law constant  $k_x$  in the  $x$  direction is given by

$$k_x = -\frac{\partial F_z}{\partial x} = -\alpha \left\{ \left( \frac{\partial E_z}{\partial x} \right)^2 + E_z \frac{\partial^2 E_z}{\partial x^2} \right\} \Big|_L = -\alpha E_z \frac{\partial^2 E_z}{\partial x^2} \Big|_L, \quad (450)$$

where the last equality follows from the hypothesis of mechanical equilibrium at point  $L$ .

Similarly the  $y$  component of the force is, to a good approximation,

$$F_y = \alpha E_z \frac{\partial E_z}{\partial y}, \quad (451)$$

and the Hooke's law constant  $k_y$  in the  $y$  direction is given by

$$k_y = -\frac{\partial F_z}{\partial y} = -\alpha \left\{ \left( \frac{\partial E_z}{\partial y} \right)^2 + E_z \frac{\partial^2 E_z}{\partial y^2} \right\} \Big|_L = -\alpha E_z \frac{\partial^2 E_z}{\partial y^2} \Big|_L, \quad (452)$$

where again the last equality follows from the hypothesis of mechanical equilibrium at point  $L$ .

Thus the sum of the Hooke's law constants along the  $x$ ,  $y$ , and  $z$  axes is given by

$$\begin{aligned} k_x + k_y + k_z &= -\alpha \left\{ E_z \left( \frac{\partial^2 E_z}{\partial x^2} + \frac{\partial^2 E_z}{\partial y^2} + \frac{\partial^2 E_z}{\partial z^2} \right) \right\} \Big|_L \\ &= -\alpha E_z \frac{\partial}{\partial z} \left\{ \frac{\partial^2 \Phi}{\partial x^2} + \frac{\partial^2 \Phi}{\partial y^2} + \frac{\partial^2 \Phi}{\partial z^2} \right\} \Big|_L = 0. \end{aligned} \quad (453)$$

Therefore

$$(k_x + k_y + k_z)|_L = 0, \quad (454)$$

and again, the sum of the three Hooke's law constants must be exactly zero according to Laplace's equation.

Suppose that the system possesses axial symmetry around the  $z$  axis with

$$k_z > 0, \quad (455)$$

i.e., with stability along the  $z$  axis. Then by symmetry

$$k_x = k_y \equiv k_\perp \tag{456}$$

so that Equation (454) implies that

$$k_\perp = -\frac{1}{2}k_z < 0 , \tag{457}$$

implying instability in both  $x$  and  $y$  directions. This is exactly what we found by explicit calculation for the case of a neutral, polarizable object near point  $L$  of the charged ring.

**Adding a Uniform Gravitational Field Such as the Earth's, in the Case of a Neutral, Polarizable Object** The potential energy of a neutral, polarizable, massive particle in a DC electrostatic field plus Earth's gravity is

$$U_{tot} = U + mgz. \quad (458)$$

Again, note that the term due to gravity, i.e., the  $mgz$  term, is linear in  $z$ , and therefore will vanish upon taking the second partial derivatives of this term. Therefore again the Hooke's constants  $k_x$ ,  $k_y$ , and  $k_z$  will not be affected by Earth's gravity. The force on the particle is

$$\mathbf{F}_{tot} = -\nabla U_{tot} = -q\nabla U - mg\mathbf{e}_z \quad (459)$$

where  $\mathbf{e}_z$  is the unit vector in the vertical  $z$  direction. In equilibrium,  $\mathbf{F}_{tot} = 0$ , but this equilibrium is again unstable, since upon taking another partial derivative of the term  $mg\mathbf{e}_z$  with respect to  $z$  will yield zero, and therefore again all of the above Hooke's law constants are the same in the presence as in the absence of Earth's gravity.



**The Electric Field Distributions of a Charged Ring and a Focused Laser Beam** Small dielectric particles have been stably trapped at the maximum of the square of the electric field in focused laser beams, also known as Gaussian beam waists. How is this situation different from the case of the charged ring? Figure 19 shows a depiction of the electric field distributions in each case. The electric potential for the charged ring is a harmonic function, as it solves Laplace's equation, which causes this distribution to be governed by Earnshaw's theorem. While the square of the electric field at point  $L$  is a local maximum in the vertical direction, it is a local minimum along the horizontal plane, giving rise to the previously discussed transverse instability. In a focused laser beam, however, the electric potential is a solution of the Helmholtz equation, and thus Earnshaw's theorem does not apply. The square of the electric field at the levitation point of the focused laser beam is a local maximum in all three spatial directions, and the electric field strength rapidly approaches zero outside of the beam.

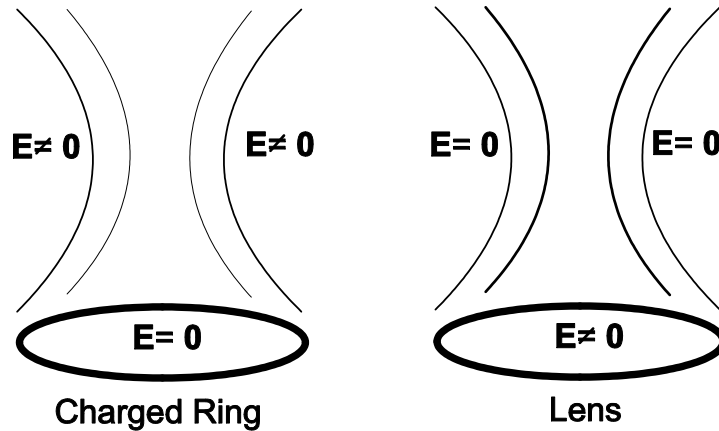


Figure 19: Comparison of the electric field distributions of a charged ring and a focused laser beam.

### 8.2.2 Ways to Evade Earnshaw's Theorem

Some known ways to evade Earnshaw's theorem and thereby to construct a truly stable trap for charged particles or for neutral particles are (1) to use non-electrostatic fields such as a DC magnetic field (e.g., the Penning trap [73]) in conjunction with DC electric fields, or (2) to use time-varying, AC electric fields, rather than DC fields (e.g., the Paul trap [70]), or (3) to use active feedback to stabilize the neutral equilibrium of a charged particle in a uniform electric field, such as was done for a charged superfluid helium drop [74], or (4) to use the low-field seeking property of neutral, diamagnetic objects to levitate them in strong, inhomogeneous magnetic fields [66]. The latter two methods may be useful for levitating the superfluid helium "Millikan oil drops" in the experiment described in [75].

**Magnetostatic Levitation** Consider a thin ring of radius  $R$  in the  $xy$ -plane with its center placed at the origin. The ring is carrying a current  $I$  with direction parallel to differential direction vector  $d\mathbf{s}$ . The magnetic field at an arbitrary field point  $(x, z)$  is given by the Biot-Savart law

$$d\mathbf{B} = \frac{\mu_0 I}{4\pi} \frac{d\mathbf{s} \times \mathbf{r}}{r^3}, \quad (460)$$

where  $\mathbf{r}$  is the vector that points from  $d\mathbf{s}$  to the field point. The axial symmetry of the problem allows for consideration of the field point to be along a single radial axis and a vertical axis only, without loss of generality. This configuration is shown in Figure 20.

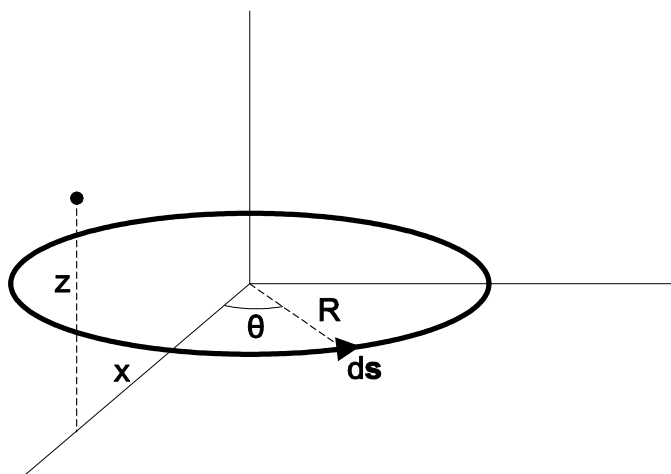


Figure 20: A thin, current-carrying ring creates a magnetic field at an arbitrary field point given by the Biot-Savart law.

The vectors  $d\mathbf{s}$  and  $\mathbf{r}$  on the right side of (460) are given by

$$d\mathbf{s} = \langle -R \sin \theta \, d\theta, R \cos \theta \, d\theta, 0 \rangle \quad (461)$$

$$\mathbf{r} = \langle x - R \cos \theta, -R \sin \theta, z \rangle, \quad (462)$$

in Cartesian coordinates, and thus the field is given by

$$\mathbf{B}_{ring} = \frac{\mu_0 I}{4\pi} \int_0^{2\pi} \frac{\langle z \cos \theta, 0, R^2 - xR \cos \theta \rangle \, d\theta}{(x^2 + z^2 + R^2 - 2xR \cos \theta)^{3/2}}. \quad (463)$$

To find the magnetic field of a thin shell of length  $L$  with its axis along the  $z$ -axis, and its ends at  $z = 0$  and  $z = L$ , (463) must be integrated with respect to  $z$  and multiplied by  $\frac{N}{L}$ , where  $N$  is the number of turns in the shell. Thus,

$$\mathbf{B}_{shell} = \frac{\mu_0 N I}{4\pi L} \int_0^L \int_0^{2\pi} \frac{\langle z \cos \theta, 0, R^2 - xR \cos \theta \rangle d\theta dz}{(x^2 + z^2 + R^2 - 2xR \cos \theta)^{3/2}}. \quad (464)$$

To find the magnetic field of a thick, finite solenoid of length  $L$  and thickness  $r_2 - r_1$ , where  $r_1$  and  $r_2$  are the inner and outer radii of the solenoid, respectively, with its axis along the  $z$ -axis, and its ends at  $z = 0$  and  $z = L$ , (464) must be integrated with respect to  $R$  and divided by  $r_2 - r_1$ . Thus,

$$\mathbf{B}_{solenoid} = \frac{\mu_0 N I}{4\pi L (r_2 - r_1)} \int_0^L \int_0^{2\pi} \int_{r_1}^{r_2} \frac{\langle z \cos \theta, 0, R^2 - xR \cos \theta \rangle dr d\theta dz}{(x^2 + z^2 + R^2 - 2xR \cos \theta)^{3/2}}. \quad (465)$$

Stable levitation can occur at minima in the total potential energy density  $u$ , which consists of a magnetic field term and a gravitational field term. The expression for this potential energy density is

$$u = u_B + u_g = \frac{B^2}{2\mu_0} + \rho g z. \quad (466)$$

There are no local extrema in the potential energy density for a single coil, but two coaxial coils, separated by distance  $d$  and oriented such that their fields are anti-parallel have zero potential energy density at  $z = L + d/2$ , which is a local minimum. The magnetic field of the second coil can be found using the replacements  $I \rightarrow -I$  and  $z \rightarrow d - z$  in (465), and the two can be added vectorially to find the total field. When the radius of two identical coils in this configuration is equal to the separation distance, the system is commonly called a set of “anti-Helmholtz coils,” or “Helmholtz coils” when the fields are parallel. A contour plot of the potential energy density, where the magnetic term is produced by a set of oppositely-oriented coils, is shown in Figure 21. The closed contour in the center of the coils contains the local minimum, where stable levitation of a perfect diamagnet (e.g. superconductor) can occur. The magnetic field was calculated numerically, using a Gaussian quadrature method.

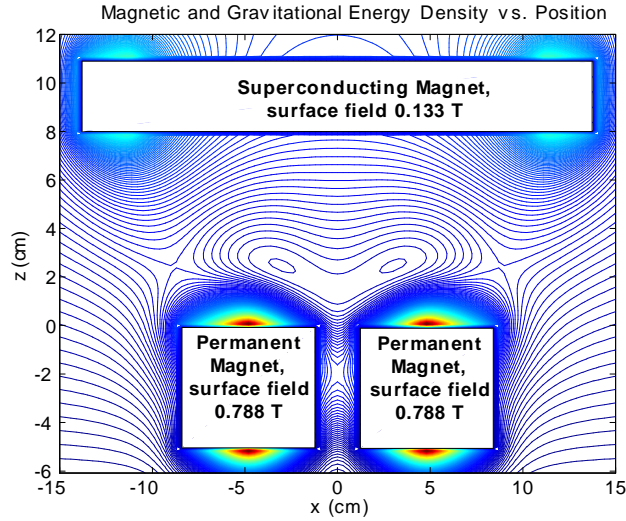


Figure 21: Contour plot of potential energy density in a DC homogeneous gravitational field and a inhomogeneous magnetostatic field for perfect diamagnets with mass density  $\rho = 1 \text{ g/cm}^3$ . The two small closed curves contain local minima at which the diamagnets can be stably levitated.

Two superconducting samples will be stably levitated at these local minima, as long as they are sufficiently small. This requirement is not due to the necessity of a small mass, since the location of the potential minima is dependent on the mass density, and not the mass itself, but due to the fact that the superconductors must remain within a region where the magnetic field is below the critical field of the superconducting material used. Though the figure depicts local minima for perfect diamagnets with a fairly low mass density, the complete expulsion of the magnetic field from the interior of the superconductor will occur as long as the superconducting portion of the sample is thicker than the London penetration depth, which tends to be on the order of tens of nanometers for Type-I superconductors. Thus, the sample need not be a solid superconductor.

Another aspect to consider is the depth of the potential energy wells. The depth must be sufficiently large for stable levitation to be maintained if the system is perturbed. In performing a Taylor expansion of the total potential around the levitation points, it was found that, for small displacements from equilibrium (around 1 mm), the oscillation frequencies are on the order of tens of Hertz in all three spatial directions, and the center of mass of the samples can be moved up to a few centimeters in any direction before they are pulled out of the potential well.

The final concern is the value of the magnetic field at points near the levitation point. If the value of the magnetic field is too high, the superconductor will be driven normal, lose its perfect diamagnetism, and will no longer be levitated by the field. The magnetic field at the levitation point is approximately 200 G. Though this is above the critical field of aluminum near absolute zero temperature (approximately 100 G), it is below the critical field of lead, which is approximately 800 G. If the levitated spheres can have a diameter of less than approximately 1.5 cm, they will remain completely within a region that is below the critical field, and thus will remain superconducting.

## 9 Conclusions

Many research possibilities, both theoretical and experimental, arising from the incompressibility of the quantum mechanical wavefunction have yet to be explored. Though difficult to perform, an experiment to detect the transition frequency shift in a Rydberg atom in curved space (such as in a highly-elliptical orbit around the Earth) may yield interesting results if and when the technology becomes available to make this endeavor more practical. Upon calculating energy shifts both in the Parker and DeWitt cases, many patterns arose, and it would be useful to construct a comprehensive mathematical model that explains these trends. Though some of those trends were explained in this work, a full model was not developed.

Successful, efficient implementation of the transduction between gravitational and electromagnetic radiation would revolutionize communications, as the attenuation by massive objects that affects electromagnetic radiation is practically invisible to gravitational radiation. Furthermore, wireless power transfer may become a possibility as well, through the generation of electrical power through time-varying gravitational fields.

Experimental detection of the behavior of quantum-mechanically coherent systems in inhomogeneous gravitational fields may lead to a better understanding of the interface between quantum mechanics and general relativity, where some inconsistencies arise. The scenarios outlined in this work are but a fraction of the total number of possibilities that would come out of different behavior between quantum and classical matter in the presence of gravitational fields.

## References

- [1] S.J. Minter, K. Wegter-McNelly, R.Y. Chiao. *Physica E* 42, 234 (2010).
- [2] S.J. Minter, K. Wegter-McNelly, R.Y. Chiao. *AIP Conf. Proc.* 1168, 1084 (2009).
- [3] S.J. Minter, R.Y. Chiao. *Laser Physics*. **17** (7), 942 (2007).

- [4] Laughlin, R.B. Phys. Rev. Lett. **50** (18), 1395 (1983).
- [5] J.J. Sakurai, *Modern Quantum Mechanics* (Addison-Wesley, 1994).
- [6] S. Haroche, J.-M. Raimond, *Exploring the Quantum*, Oxford University Press, 2006.
- [7] Parker, L. Phys. Rev. D. **22** (8), 1922 (1980).
- [8] L. Parker, Phys. Rev. Lett. **44**, 1559 (1980).
- [9] L. Parker, Phys. Rev. D. **25** (12), 1922 (1982).
- [10] J.B. Hartle, *Gravity: An Introduction to Einstein's General Relativity* (Addison-Wesley, San Francisco, 2003), p. 445 - 454.
- [11] E. Gill, et al, Class. Quantum Grav. **4**, 1031 (1987).
- [12] I.L. Beigman, V.S. Lebedev, Phys. Rep. **250**, 95 (1995).
- [13] E. Fischbach, B.S. Freeman, W.-K. Cheng, Phys. Rev. D. **23** (10), 2157 (1981).
- [14] U. Fischer, Class. Quantum Grav. **11**, 463 (1994).
- [15] B.S. DeWitt, Phys. Rev. Lett. **16** (1966) 1092.
- [16] J.I. Martin, V.M. Perez, A.F. Ranada, Anales de Fisica, Serie A. **87**, 1991.
- [17] L.D. Landau and E.M. Lifshitz, *Quantum Mechanics*, Butterworth-Heinemann, Oxford, 2003.
- [18] The proton is spatially separated from the center of mass of the system by a very small mean square distance  $r_p^2 = \left(\frac{\mu}{m_p} a_n\right)^2$ , whereas the electron is separated from the center of mass by the much larger mean square distance  $r_e^2 = a_n^2 \left(1 - \frac{\mu}{m_p}\right)^2$ . This, in addition to the difference between the particle masses, leads to the electron term being larger than the proton term by nine orders of magnitude in (69) and three orders of magnitude in (77) and (83).
- [19] V.B. Bezerra, Phys. Rev. D. **35** (6), 2031 (1987).



- [20] D. Kennefick, *Traveling at the Speed of Thought: Einstein and the Quest for Gravitational Waves* (Princeton University Press, Princeton, NJ, 2007).
- [21] W. H. Zurek, *Rev. Mod. Phys.* **75**, 715 (2003).
- [22] E.G. Adelberger, S. Baessler, J.H. Gundlach, B.R. Heckel, C.D. Hoyle, S.M. Merkowitz, G.L. Smith, H.E. Swanson, in *Physics Beyond the Standard Model*, P. Herczeg, C.M. Hoffman, H.V. Klapdor-Kleingrothaus (Eds.), World Scientific, Singapore, 1999.
- [23] By “Equivalence Principle (EP),” we shall mean throughout this paper the *Weak* Equivalence Principle (WEP), i.e., that all bodies fall with the same acceleration, when they are locally subjected to the same gravitational force (but not to any non-gravitational forces), and that their common acceleration is independent of mass, composition, thermodynamic state, quantum state, internal structure, charge, etc. This form of the EP is also known as the “Universality of Free Fall” [22]. The WEP is to be distinguished from the stronger form of the EP known as the “Einstein Equivalence Principle (EEP),” which adds Poincaré invariance to the above statement of the WEP. See C.M. Will, *Living Rev. Relativity* 9 (2006) 3.
- [24] R. E. Glover and M. Tinkham, *Phys. Rev.* **104**, 844 (1956).
- [25] M. Tinkham, *Introduction to Superconductivity*, 2nd edition (Dover Books on Physics, New York, 2004).
- [26] R. Merservey and P. M. Tedrow, *J. Appl. Phys.* **40**, 2028 (1969). E. G. Harris, *Am. J. of Phys.* **59**, 421 (1991); S. J. Clarke and R. W. Tucker, *Class. Quant. Grav.* **17**, 4125 (2000).
- [27] A free particle initially at rest will remain at rest during and after the passage of a weak (linearized) GR wave. A particle can absorb energy from a GR wave “only if (i) it is interacting with other particles, or (ii) it has nonzero energy initially, or (iii) the wave is strong so that nonlinear effects are important.” S. A. Teukolsky, *Phys. Rev. D.* **26**, 745 (1982).
- [28] J.C. Garrison, R.Y. Chiao, *Quantum Optics*, Oxford University Press, Oxford, 2008.

- [29] A. Einstein, B. Podolsky, N. Rosen, Phys. Rev. 47 (1935) 777.
- [30] An interpretation of “the universal validity of the EP” that ignores the existence of forces other than gravity, and also ignores quantum mechanics, would lead to a universal length contraction or expansion between all parts of a piece of matter in response to an incident GR wave. This would nullify the non-geodesic motion of the Cooper pairs, but it would also nullify all forms of rigidity, including those of an ordinary ruler. This interpretation of the EP is clearly false, as demonstrated by the fact that the expansion of the Universe in the Friedmann metric would accordingly become meaningless.
- [31] P.C.W. Davies, Class. Quantum Grav. 21 (2004) 2761.
- [32] N. Bohr, in Quantum Theory and Measurement, J.A. Wheeler and W.H. Zurek (Eds.), Princeton University Press, Princeton, 1983, p. 113.
- [33] As in the case of the photoelectric effect, here in the case of Cooper-pair-breaking by incident radiation with a frequency above the BCS gap frequency, it is possible to treat the quantum transition process entirely self-consistently in the semi-classical approximation, where the radiation field is treated *classically* as a wave with a well-defined frequency and only the matter is treated *quantum mechanically*. Neither the photoelectric effect nor the pair-breaking process requires the quantization of the incident radiation field [28, pp. 21-3].
- [34] It should be noted that a superconductor’s normal conduction electrons are just as localizable within the material as the ions, since no energy gap exists in their case. The behavior of normal conduction electrons is said by condensed-matter physicists to be “delocalized” with respect to a given ion within a few lattice constants, but these electrons are not “nonlocalizable” in the sense of the Cooper pairs discussed here.
- [35] G. Z. Adunas, E. Rodriguez-Milla, and D. V. Ahluwalia, Gen. Rel. Grav. **33**, 183 (2001).
- [36] R. Y. Chiao, in *Science and Ultimate Reality*, eds. J. D. Barrow, P. C. W. Davies, and C. L. Harper, Jr. (Cambridge University Press, Cambridge, 2004), page 254 (quant-ph/0303100).

- [37] F. London, *Superfluids*, vol. I (Wiley, New York, 1950).
- [38] R. P. Feynman, “An expanded version of the remarks by R. P. Feynman on the reality of gravitational waves, mentioned briefly on page 143 of the Report.” Expanded remarks from the Conference on the Role of Gravitation in Physics, held in Chapel Hill, North Carolina, January 18–23, 1957. A copy of the document can be found in the Feynman Papers at the California Institute of Technology, Box 91, Folder 2. The report to which Feynman refers was edited by Cecile M. DeWitt and published by the Wright Air Development Center as Technical Report 57-216 (United States Air Force, Wright-Patterson Air Force Base, Ohio).
- [39] S. Weinberg, *Gravitation and Cosmology: Principles and applications of the general theory of relativity* (John Wiley & Sons, New York, 1972).
- [40] Tinkham [25] uses a different convention, namely,  $\sigma_s(\omega) = \sigma_{1s}(\omega) - i\sigma_{2s}(\omega)$ , which arises from his choice for time dependence to be  $\exp(+i\omega t)$ , whereas we employ a time dependence of  $\exp(-i\omega t)$ , so that here  $\sigma_s(\omega) = \sigma_{1s}(\omega) + i\sigma_{2s}(\omega)$ .
- [41] The electron’s *negative* charge means that the charge current density  $\mathbf{j}_e$  flows in a direction *opposite* to the velocity vector  $\mathbf{v}$  of the electrons, whereas the electron’s *positive* mass means that the mass-current density  $\mathbf{j}_G$  flows in the *same* direction as  $\mathbf{v}$ . Hence the mass-current density  $\mathbf{j}_G$  flows in a direction *opposite* to the charge current density  $\mathbf{j}_e$ . But because of the negative sign in front of the mass current density source term on the right-hand side of the gravitational Ampere-like law in the Maxwell-like equations (211d),  $\nabla \times \mathbf{B}_G = -\mu_G \mathbf{j}_G$ , there is a minus sign on the right-hand side of (179) in the GR case, which cancels the former minus sign, so that on the right-hand side of (183) and in all subsequent equations for the GR case, the signs remain unchanged. The minus sign in front of the mass-current-density source term on the right-hand side of the Ampere-like law in the Maxwell-like equations (211d) stems from the fact that, when one takes the divergence of both sides of this equation, one must obtain zero, since the divergence of a curl is zero. This will indeed be the result, provided that both the continuity

equation for the mass current density and the Gauss-like law in the Maxwell-like equations (211a) are simultaneously satisfied on the right-hand side of the resulting equation. The minus sign in front of the mass-density source term in the Gauss-like law (211a) is necessitated by the experimental fact that the gravitational force between all masses is attractive, which implies that the minus sign in front of the mass-current-density source term in the Ampere-like law (211d) is also necessitated by the same experimental fact. These two minus signs also emerge naturally from the linearization of Einstein's field equations.

[42] This formula can be understood in terms of a simple transmission line model, where the line has a characteristic impedance  $Z$  and a reactive shunt element  $iX$ , where the element  $iX$  could represent the effect of the kinetic inductance of the film. We wish to calculate the power reflected from this element when an incident wave propagates down the transmission line. The equivalent circuit consists of the same transmission line terminated by means of a parallel combination of the reactive element and a resistor having a resistance  $Z$ , which is a real number. The reflectivity of this configuration is given by

$$\mathcal{R} = |\rho|^2 = \rho^* \rho = \left| \frac{Z - Z_{\text{eff}}}{Z + Z_{\text{eff}}} \right|^2$$

where

$$\rho = \frac{Z - Z_{\text{eff}}}{Z + Z_{\text{eff}}}$$

and

$$Z_{\text{eff}} = \frac{iX \cdot Z}{iX + Z}.$$

From this it follows that

$$\begin{aligned} \rho &= \left( Z - \frac{iX \cdot Z}{iX + Z} \right) \left( Z + \frac{iX \cdot Z}{iX + Z} \right)^{-1} \\ &= \frac{1}{1 + 2iX/Z} \end{aligned}$$

and that

$$\begin{aligned}\mathcal{R} &= \left( \frac{1}{1 - 2iX/Z} \right) \left( \frac{1}{1 + 2iX/Z} \right) \\ &= \left\{ 1 + \left( 2\frac{X}{Z} \right)^2 \right\}^{-1} .\end{aligned}$$

With the identifications of  $X = X_L$  and  $Z = Z_0$ , we see that the reflectivity of the reactive element has the same form as the EM reflectivity of the superconducting film given by (195).

[43] The Drude model involves an equation of motion for the expectation value of the electron velocity, namely

$$m_e \frac{d}{dt} \langle \mathbf{v}_e \rangle = \frac{-m_e}{\tau} \langle \mathbf{v}_e \rangle - e\mathbf{E} ,$$

where we use the semi-classical approach in which the electrons are treated quantum-mechanically, and the external fields classically. This Langevin-like equation follows from the Fokker-Planck equation, which models diffusion in phase-space. The mean free time  $\tau$  in the Drude model is assumed to be  $d/v_F$  where  $d$  is the thickness of the film and  $v_F$  is the Fermi velocity. The steady-state solution of this model is given by

$$\langle \mathbf{v}_e(t \rightarrow \infty) \rangle = \frac{\tau e}{m_e} \mathbf{E} .$$

If we now use the usual expression for the current density

$$\langle \mathbf{j}_e \rangle = n_e e \langle \mathbf{v}_e \rangle$$

where  $n_e$  is the number density of the electrons, we see that

$$\langle \mathbf{j}_e \rangle = \frac{n_e e^2 d}{m_e v_F} \mathbf{E} .$$

Equating  $\sigma_n$  with the prefactor on the right-hand side, we recover Ohm's law and arrive at the

expression given in (198) for the normal conductivity.

[44] Buisson et al., Phys. Rev. Lett. **73**, 3153 (1994).

[45] P. G. De Gennes, *Superconductivity of Metals and Alloys* (W. A. Benjamin, New York, 1966).

[46] R. M. Wald, *General Relativity* (University of Chicago Press, Chicago, 1984). The Maxwell-like equations are to be supplemented by the Lorentz-like force law

$$\mathbf{F}_G = m_{\text{test}} (\mathbf{E}_G + 4\mathbf{v} \times \mathbf{B}_G) ,$$

where  $m_{\text{test}}$  is the mass of a local test particle moving at a non-relativistic velocity  $\mathbf{v}$ . The Maxwell-like approach derived by Wald (as well as the approach used by DeWitt in [15]) is fully equivalent to the standard transverse-traceless approach used by the GR community for GR wave physics. A coordinate transformation based on a local Galilean transformation exists between the Wald gauge and the transverse-traceless (TT) gauge, which shows that the two coordinate systems are equivalent to one another. A transformation of our Wald-based calculations into the standard TT gauge will not change the value of the ratio given by (1). The necessarily quadrupolar nature of the mass and the mass-current sources in Wald's equations, which originates physically from the fact that there is only one sign of mass and which follows from the EP, excludes the usual, uniform, crossed electric- and magnetic-field EM plane-wave solutions. Thus the lowest-order allowed plane-wave solutions of Wald's equations in the vacuum, which are homologous to the TEM<sub>11</sub> solutions for EM plane waves propagating in the vacuum, will induce a *quadrupolar* pattern of mass supercurrents in a superconducting film at normal incidence.

[47] Our focus on mass currents should put to rest any concerns that we are claiming that static longitudinal gravito-electric fields can be shielded by matter, i.e., that anti-gravity is possible. This would require negative mass, the very existence of which would violate the EP. Our claim is rather that time-varying transverse gravito-magnetic fields can be reflected by mass currents

generated in superconductors by GR waves. Mass currents of opposite signs, i.e., mass currents flowing in opposite directions, *can* exist in nature. Time-varying mass currents can generate time-varying gravito-magnetic fields, which can in turn lead to the reflection of time-varying, transverse gravito-electric fields.

- [48] C. Kiefer and C. Weber, *Ann. der Phys. (Leipzig)* **14**, 253 (2005). The earliest mention of the concept of the characteristic gravitational impedance of free space, which was based on a dimensional analysis that resulted in an estimate of  $Z_G$  based on a ratio of Newton’s constant  $G$  to the speed of light  $c$ , was perhaps made by J. D. Krauss (private communication).
- [49] R. Y. Chiao, W. J. Fitelson, and A. D. Speliotopoulos (gr-qc/0304026); R. Y. Chiao and W. J. Fitelson (gr-qc/0303089), “Time and Matter in the Interaction between Gravity and Quantum Fluids: Are There Macroscopic Quantum Transducers between Gravitational and Electromagnetic Waves?” published in the proceedings of the ‘Time & Matter Conference’ in Venice, Italy, 11-17 August 2002, eds. Ikaros Bigi and Martin Faessler (World Scientific, Singapore, 2006), p. 85.
- [50] The relationship between the gravitational vector potential  $\mathbf{h}$  used in (230a), which has units of velocity, and the usual dimensionless strain amplitude  $h_+$  used, for example, by Saulson [76, Eq. 7] is as follows. The GR-wave flux, which follows from (322), is

$$\langle S_{\text{GR}} \rangle = \frac{1}{2Z_G} \langle E_G^2 \rangle .$$

Using the fact that  $\mathbf{E}_G = -\partial\mathbf{h}/\partial t$ , and assuming sinusoidally-varying incident radiation, this leads to

$$\langle S_{\text{GR}} \rangle = \frac{\omega^2}{2Z_G} |\mathbf{h}|^2 .$$

Comparing this with Saulson’s expression for the gravitational wave flux and using the value of

$Z_G$  given in (215), we see that

$$\langle S_{GR} \rangle = \frac{\omega^2 c^2}{8Z_G} |h_+|^2 ,$$

and thus that

$$|h_+| = 2 \frac{|\mathbf{h}|}{c} .$$

[51] In the case of a plane wave  $\psi = \sqrt{n} \exp(i\mathbf{k} \cdot \mathbf{r})$ , the probability current density given in (228)

becomes

$$\mathbf{j} = \frac{\hbar}{2mi} (\psi^*(i\mathbf{k})\psi - \psi(-i\mathbf{k})\psi^*) = n \frac{\hbar}{m} \mathbf{k} = n\mathbf{v} .$$

Thus the speed  $v$  associated with the current density  $j$  is

$$v = \frac{\hbar}{m} k .$$

Now, the dispersion relation for de-Broglie matter waves is given by

$$\omega = \frac{\hbar k^2}{2m} ,$$

which leads to

$$\begin{aligned} v_{\text{group}} &\equiv \frac{d\omega}{dk} = \frac{\hbar}{m} k \\ v_{\text{phase}} &\equiv \frac{\omega}{k} = \frac{1}{2} \frac{\hbar}{m} k . \end{aligned}$$

Hence the velocity  $\mathbf{v}$  given in (240), which is associated with the probability current density  $\mathbf{j}$  given in (228), is the *group* velocity, and not the *phase* velocity, of a Cooper pair.

[52] Note that the  $\mathbf{j}_G$  and  $\mathbf{F}_{\text{tot}}$  will be nonzero as long as the Schiff-Barnhill effect [15]

$$q\mathbf{E} + m\mathbf{g} = \mathbf{0} ,$$



which is present in a normal metal, is absent in the superconductor. The static mechanical equilibrium represented by the equation above is never achieved inside a superconductor, since the establishment of such equilibrium requires the action of dissipative processes that are present in a normal metal but absent in a superconductor. In particular, we should expect a large breakdown of the Schiff-Barnhill effect at microwave frequencies, when plasma oscillations of the superconductor can in fact be excited purely electromagnetically.

[53] Only a certain amount of current can exist in the film before it is driven normal by the resulting magnetic field. It is therefore important to take into account the critical field of the superconducting film when considering the linear response of the film to any incident radiation. In the EM sector, it can be shown using the Poynting vector that an incident wave-power flux density of 10 Watts per square meter will induce a magnetic field of 2 milli-Gauss, which is five orders of magnitude below the critical magnetic field of lead at temperatures well below  $T_c$ . Alternatively, lead will remain superconducting for incident power flux densities below tera-Watts per square meter. The critical magnetic field of a superconductor is related to the Helmholtz free energy density of the superconducting state stored in the condensate [25], which in turn is related to the BCS energy gap. This gap is related only to quantities that correspond to intrinsic properties of the superconductor, and not to any coupling to external fields. Exactly the same considerations will thus apply in the GR sector. The critical *gravito*-magnetic field of a superconductor will correspond to the same free energy density as the critical magnetic field, and a GR wave containing a power flux density of 10 Watts per square meter will produce a gravito-magnetic field that lies equally far below the critical gravito-magnetic field.

[54] One should regard (262) as a quantum-mechanical operator equation of motion for the Cooper pair's charge density operator  $\rho_e$  and mass density  $\rho_G$  operator, which are related to the quantum-mechanical density operator  $\rho = |\psi\rangle\langle\psi|$  by

$$\rho_e = q |\psi\rangle\langle\psi| \text{ and } \rho_G = m |\psi\rangle\langle\psi| ,$$

respectively. Similarly, the probability current density  $\mathbf{j}$ , the quantum velocity field  $\mathbf{v}$ , and the acceleration field  $\mathbf{a}$  of the superconductor are also quantum operators.

- [55] This applies to non-zero frequencies only, since at DC, the mass conductivity  $\sigma_{1,G}$ , like the charge conductivity, is infinite, i.e., where

$$\sigma_{1,G} = A_G \delta(\omega)$$

for some constant  $A_G$ .

- [56] R.Y. Chiao, A.M. Steinberg, in *Progress in Optics*, Vol. 37, E. Wolf (Ed.), Elsevier, Amsterdam, 1997; R.W. Boyd, D.J. Gauthier, in *Progress in Optics*, Vol. 43, E. Wolf (Ed.), Elsevier, Amsterdam, 2002.
- [57] E.P. Wigner, *Phys. Rev.* 98 (1955) 145.
- [58] G.C. Ghirardi, A. Rimini, T. Weber, *Phys. Rev. D* 34 (1986) 470.
- [59] R. Penrose, *The Road to Reality: A Complete Guide to the Laws of the Universe*, Vintage Books, New York, 2007, pp. 810-868.
- [60] R.Y. Chiao, arXiv:gr-qc/0904.3956.
- [61] R.Y. Chiao, *Int. J. Mod. Phys. D* 16 (2008) 2309; arXiv:gr-qc/0606118.
- [62] L. D. Landau, L. Pitaevskii, and E. M. Lifshitz, *Electrodynamics of Continuous Media*, 2nd edition (Elsevier Butterworth-Heinemann, Oxford, 2004), p. 279.
- [63] R. Kubo, *J. Phys. Soc. Jpn.* **12**, 570 (1957).
- [64] C. Kittel, *Solid State Physics*, 8th ed., Wiley, 2005.
- [65] J.F. Annett, *Superconductivity, Superfluids, and Condensates*, Oxford Univ. Press, 2004.

- [66] M. A. Weilert, D. L. Whitaker, H. J. Maris, and G. M. Seidel, Phys. Rev. Letters **77**, 4840 (1996); M. A. Weilert, D. L. Whitaker, H. J. Maris, and G. M. Seidel, J. Low Temp. Phys. **106**, 101 (1997).
- [67] R.J. Donnelly, Experimental Superfluidity, Univ. of Chicago Press, 1967.
- [68] R.E. Glick, J. Phys. Chem. **65**, 1552 (1961).
- [69] F. Diedrich, E. Peik, J. M. Chen, W. Quint, and H. Walther, Phys. Rev. Lett. **59**, 2931 (1987).
- [70] W. Paul, Rev. Mod. Phys. **62**, 531 (1990).
- [71] A. Ashkin, Proc. Natl. Acad. Sci. **94**, 4853 (1997); *Optical Trapping and Manipulation of Neutral Particles Using Lasers: A Reprint Volume With Commentaries* (World Scientific, Singapore, 2005).
- [72] J. A. Stratton, *Electromagnetic Theory* (McGraw Hill, New York, 1941).
- [73] F. M. Penning, Physica **3**, 873 (1936).
- [74] J. J. Niemela, J. Low Temp. Phys. **109**, 709 (1997).
- [75] R. Y. Chiao, J. Mod. Optics **53**, 2349 (2006); gr-qc/0610146.
- [76] P. R. Saulson, Class. Quantum Grav. **14**, 2435 (1997).